National Library
of Canada

Acquisitions and
Bibliographic Services Branch

395 Wellington Street
Ottawa, Ontario
K1A 0N4

Bibliothèque nationale
du Canada

Direction des acquisitions et
des services bibliographiques

395, rue Wellington
Ottawa (Ontario)
K1A 0N4

Your file Votre référence

Our file Notre référence

NOTICE

The quality of this microform is heavily dependent upon the quality of the original thesis submitted for microfilming. Every effort has been made to ensure the highest quality of reproduction possible.

If pages are missing, contact the university which granted the degree.

Some pages may have indistinct print especially if the original pages were typed with a poor typewriter ribbon or if the university sent us an inferior photocopy.

Reproduction in full or in part of this microform is governed by the Canadian Copyright Act, R.S.C. 1970, c. C-30, and subsequent amendments.

AVIS

La qualité de cette microforme dépend grandement de la qualité de la thèse soumise au microfilmage. Nous avons tout fait pour assurer une qualité supérieure de reproduction.

S'il manque des pages, veuillez communiquer avec l'université qui a conféré le grade.

La qualité d'impression de certaines pages peut laisser à désirer, surtout si les pages originales ont été dactylographiées à l'aide d'un ruban usé ou si l'université nous a fait parvenir une photocopie de qualité inférieure.

La reproduction, même partielle, de cette microforme est soumise à la Loi canadienne sur le droit d'auteur, SRC 1970, c. C-30, et ses amendements subséquents.

Canada

THE UNIVERSITY OF ALBERTA

COMPARISON OF REVERSAL DYNAMICS BETWEEN RAPID AXONALLY TRANSPORTED PROTEIN AND ORGANELLES AT A LESION

BY

XIN CHEN

A thesis submitted to the Faculty of Graduate Studies and Research in partial fulfillment of the requirements for the degree of MASTER OF SCIENCE.

DEPARTMENT OF APPLIED SCIENCES IN MEDICINE

EDMONTON, ALBERTA

SPRING, 1993

National Library
of Canada

Acquisitions and
Bibliographic Services Branch

395 Wellington Street
Ottawa, Ontario
K1A 0N4

Bibliothèque nationale
du Canada

Direction des acquisitions et
des services bibliographiques

395, rue Wellington
Ottawa (Ontario)
K1A 0N4

Your file Votre référence

Our file Notre référence

The author has granted an irrevocable non-exclusive licence allowing the National Library of Canada to reproduce, loan, distribute or sell copies of his/her thesis by any means and in any form or format, making this thesis available to interested persons.

L'auteur a accordé une licence irrévocable et non exclusive permettant à la Bibliothèque nationale du Canada de reproduire, prêter, distribuer ou vendre des copies de sa thèse de quelque manière et sous quelque forme que ce soit pour mettre des exemplaires de cette thèse à la disposition des personnes intéressées.

The author retains ownership of the copyright in his/her thesis. Neither the thesis nor substantial extracts from it may be printed or otherwise reproduced without his/her permission.

L'auteur conserve la propriété du droit d'auteur qui protège sa thèse. Ni la thèse ni des extraits substantiels de celle-ci ne doivent être imprimés ou autrement reproduits sans son autorisation.

ISBN 0-315-82185-X

Canada

University of Alberta
Edmonton

Canada T6G 2G3

Department of Applied Sciences in Medicine

10-102 Clinical Sciences Building, Telephone (403) 492-6339
Fax (403) 492-8259

15 January 1993

TO WHOM IT MAY CONCERN:

By way of this letter, and on behalf of Dr. R.S. Smith, and myself, I hereby grant permission to Dr. CHEN Xin to make use of the figure, in modified form, that appeared on page 442 of the book 'Axoplasmia Transport', edited by D.G. Weiss, Springer-Verlag, Basel, 1982. Permission is granted for the above said figure to be included in the M.Sc. thesis of Dr. Chen to be published by the University of Alberta in 1993.

R. Snyder

R.E. Snyder

RES:em

THE UNIVERSITY OF ALBERTA

RELEASE FORM

NAME OF AUTHOR:	XIN CHEN
TITLE OF THESIS:	COMPARISON OF REVERSAL DYNAMICS BETWEEN RAPID AXONALLY TRANSPORTED PROTEIN AND ORGANELLES AT A LESION
DEGREE:	MASTER OF SCIENCE
YEAR THIS DEGREE GRANTED:	SPRING 1993

Permission hereby granted to THE UNIVERSITY OF ALBERTA LIBRARY to reproduce single copies of this thesis and to lend or sell such copies for private, scholarly or scientific research purposes only.

The author reserves other publication rights, and neither the thesis nor extensive extracts from it may be printed or otherwise reproduced without the author's written permission.

(student's signature)

No. 7, 10515-85 Ave.,
Edmonton, Alberta.
(student's permanent address)

Date: January 15, 1993.

THE UNIVERSITY OF ALBERTA

FACULTY OF GRADUATE STUDIES AND RESEARCH

The undersigned certify they have read, and recommend to the Faculty of Graduate Studies and Research for acceptance, a thesis entitled COMPARISON OF REVERSAL DYNAMICS BETWEEN RAPID AXONALLY TRANSPORTED PROTEIN AND ORGANELLES AT A LESION submitted by XIN CHEN in partial fulfillment of the requirements for the degree of MASTER OF SCIENCE.

R. E. Snyder

R. S. Smith

D. Fenna

R. C. Berdan

Date: December 15, 1992

ABSTRACT

To reveal some aspects of the relationship between rapid axonally transported protein and organelles, the transport kinematics and particularly the reversal dynamics of protein at a neuronal lesion in sciatic nerve of *Xenopus laevis* were compared to those of organelles.

The transport of newly synthesized, ^{35}S-labeled proteins was studied using a position-sensitive detector of ionizing radiation. Organelle transport in single living axons was detected with video-enhanced, differential interference contrast microscopy. Experimental conditions were similar for protein and organelle transport studies. The preparations were incubated in either a physiological saline compatible with extra-axonal fluid or a potassium glutamate solution compatible with intra-axonal function after the lesion was created. Transport kinematics and reversal dynamics were determined for both organelles and proteins.

Protein transport rates were found to be generally in agreement with those of organelles. Twenty-five percent of the anterogradely moving organelles were able to reverse their transport direction adjacent to an axonal lesion to the retrograde direction within less than 10 minutes. However, protein turnaround adjacent to a lesion required about 3 hours. In addition, the amount of reversed protein was reduced in nerves bathed in the potassium glutamate solution compared to that in nerves bathed in physiological saline. But no significant difference was found in organelle-transport reversal between axons bathed in either solution.

The main conclusions are as follows. (1) The correlation in transport rates between protein and organelles supports the supposition that they transport together as an associated unit. (2) The difference in reversal time between protein

and organelles suggests that the relationship between protein molecules and membranous organelles is dynamic during reversal. During transport reversal, protein molecules, at least in some capacity, may dissociate from their original carrier organelles and reassociate with other organelles that undergo transport reversal. (3) If a dynamic relationship does exist between protein and organelles, protein-transport reversal, at least for some proteins, may be controlled by a different mechanism than that of organelles. It is likely that some Ca^{2+}-dependent process is involved in protein turnaround at a neuronal lesion, but not in organelle-transport reversal.

TABLE OF CONTENTS

Chapter			Page
1	Introduction		1
2	Background Information Related to the Problem		8
	2.1 Historical Development of Axonal Transport		8
		2.1.1 Axonal Transport of Molecules	9
		2.1.1.1 Two Components, Fast and Slow, of Axonal Transport	9
		2.1.1.2 Fast Retrograde Axonal Transport	14
		2.1.1.3 Summary	16
		2.1.2 Axonal Transport of Membranous Organelles	17
	2.2 Transport Mechanisms		21
		2.2.1 Mechanisms of Organelle Movement	21
		2.2.2 Rapidly Transported Materials are Carried by Membranous Organelles	23
	2.3 Relationship of Rapidly Transported Molecules to Membranous Organelles and Vesicles		24
		2.3.1 Protein Traffic via Vesicle Transport in Non-neuronal Cells	25
		2.3.2 General Features of Axonal Transport of Molecules and Organelles	27
		2.3.2.1 Passage Through the Cell Body	28
		2.3.2.2 Deposition of Rapidly Transported Material within the Axon	31
		2.3.2.3 Reversal of Rapid Axonal Transport	34

3 Method and Materials 38

3.1 Protein Turnaround Study 38

3.1.1 Multiple Proportional Counter (MPC) Technique 38

3.1.2 Bathing Solution 42

3.1.3 Nerve Preparation and Pulse Creation Procedure 42

3.1.4 Lesion Time 49

3.1.5 Data Collection and Analysis 49

3.2 Organelle Turnaround Study 55

3.2.1 Video-enhanced Contrast, Differential Interference Contrast (DIC) Microscopy 55

3.2.2 Bathing Solution 59

3.2.3 Nerve Preparation and Axonal Lesion 60

3.2.4 Image Detection and Recording with Video-enhanced DIC Microscopy 62

3.2.5 Data Collection and Analysis 65

4 Results 66

4.1 Protein Transport 66

4.1.1 Protein Transport in NR Solution 66

4.1.1.1 General Observations 66

4.1.1.2 Transport Rates and Related Parameters 67

4.1.1.3 Turnaround and Retrograde Transport 69

4.1.1.4 Turnaround Time 71

4.1.2 Protein Transport in KG Solution 74

4.2 Transport Reversal of Organelles at a Lesion 75

4.2.1 Organelle Transport in the Vicinity of a Lesion in KG Solution 75

4.2.1.1 General Observations 75

4.2.1.2 Transport Rates 77

4.2.1.3 Reversal of Organelle Transport 77

4.2.1.4 Reversal Dynamics and Quantity 85

4.2.2 Organelle Transport in the Vicinity of a Lesion in NR Solution 88

4.2.2.1 General Observations 88

4.2.2.2 Reversal Dynamics 91

5 Discussion 93

5.1 Protein Reversal Dynamics Proximal to a Lesion 93

5.1.1 Protein Requires > 1.5 h to Turnaround at a Lesion 93

5.1.2 Reversal of Protein is Reduced in Nerves Bathed in KG Solution Compared to that in NR Solution 99

5.2 Organelle Reversal Dynamics Proximal to a Lesion 101

5.2.1 Organelles Require < 10 min to Reverse Transport Direction 101

5.3 Comparison of Transport Kinematics and Reversal Dynamics between Protein and Organelles 104

5.3.1 Association of Protein Translocation with Organelle Transport 104

5.3.2 Dissociation of Protein and Organelle Reversal 107

5.3.2.1 Protein Turnaround is Delayed Compared to Organelle Reversal 108

5.3.2.2 Different Reversal Characteristics between Proteins and Organelles 109

5.4 Relationship of Rapidly Transported Organelles and Newly Synthesized Proteins 110

5.5 Conclusion 116

Reference 118

LIST OF TABLES

Table		Page
1	Composition of Transported Materials	13
2	Morphological Types of Transported Organelles	20
3	Mean ± SEM of Protein Transport Parameters for Nerves Bathed in NR Solution	68
4	Coefficients of Correlation between 10 Transport Parameters and the Lesion Time (t) for Nerves Bathed in NR solution	70
5	Mean ± SEM of the Protein Turnaround Time (Ta)	73
6	Comparison of Protein Transport Parameters between Nerves Bathed in NR and KG Solution	76
7	Mean ± SEM of Organelle Transport Rates	78
8	Mean ± SEM of Organelle Flux in the Vicinities of the Double Lesions	84
9	Transport Rates (Mean ± SD) of Protein and Organelles in the Sciatic Nerve of *Xenopus laevis*	106

LIST OF FIGURES

Figure			Page
1	Exploded View of the Multiple Proportional Counter		39
2	Schematic Representation of the Pulse Creation Procedure		44
3	Lesion Creation Time under MPC Monitoring		47
4	Counts versus Time Plots		51
5	Time versus Position Plot		54
6	Schematic Representation of the Arrangement of the Major Optical Components in the DIC Microscope		57
7	Procedure of Single Axon Preparation for the DIC Microscopy		61
8	Video-enhanced, Differential Interference Contrast Micrographs of a Living Axon from the Sciatic nerve of *Xenopus laevis*		63
9	Turnaround Time (Ta) versus Lesion Time (t)		72
10	(a)	Schematic Representation of the Double Lesion on a Single Axon	81
	(b)	The Results of Organelle Flux in the Vicinities of the Lesions	82
11	Organelle Flux versus Lesion Time Plot of Five Axons from One Nerve Bathed in KG Solution		86
12	Retrograde Organelle Flux versus Anterograde Flux for Axons Bathed in KG Solution		87
13	Correlation of the Distance of Axon Degeneration from the Lesion to the Square Root of Time after Lesioning		90
14	Retrograde Organelle Flux versus Anterograde Flux for Axons Bathed in NR Solution		92
15	Difference of the Protein Turnaround Time (T) Derived at the Actual Turnaround Site from that (Ta) Estimated at the Distal Ligature		95
16	Protein Turnaround Time (Ta) versus Square Root of Lesion Time		97

ABBREVIATIONS

AChE	Acetylcholinesterase.
AF	Fast portion of the anterograde pulse of the radiolabeled proteins.
AS	Slow portion of the anterograde pulse of radiolabeled proteins.
AMP-PNP	5'-adenylylimidodiphosphate.
A-R reversal	Anterograde to retrograde reversal.
ATP	Adenosine triphosphate.
b	A constant ratio (in $mm/h^{1/2}$) of the distance that degenerative change extended from a lesion to the square root of time after lesioning.
C	Image contrast.
C_v	Video-enhanced image contrast.
ChAT	Choline acetyltransferase.
d	The distance (in mm) degenerative change extended from an axonal lesion after lesioning.
DβH	Dopamine-β-hydroxylase.
DIC	Differential interference contrast.
DRG	Dorsal root ganglion.
Δ	Phase difference between two wavefronts.
Δ_b	Bias retardation.
Δ_o	Phase difference introduced by the object under examination.
EGTA	Ethyleneglycol-bis(β-aminoethyl ether)-N,N,N',N'-tetraacetic acid.
EM	Electron microscopy.
ER	Endoplasmic reticulum.
F_1-ATP_{ase}	A mitochondria membrane enzyme.

GA	Golgi apparatus.
HEPES	N-2-hydroxyethyl piperazine-N'-2-ethanesulfonic acid.
HRP	Horseradish peroxidase.
I	The intensity of a light wave.
I_b	The object light intensity.
I_o	The background light intensity.
I_{max}	The maximum light intensity transmitted by the microscopic system.
I_v	Electronic reduction of the background light intensity.
KG	Potassium glutamate solution.
MPC	Multiple proportional counter.
NE	Norepinephrine.
NGF	Nerve growth factor.
NR	Normal frog Ringer solution.
RER	Rough endoplasmic reticulum.
RF	Fast portion of the retrograde pulse of radiolabeled proteins.
SP	Substance P.
t	Time (in h) after lesioning.
T	True protein turnaround time (in h) estimated at the actual turnaround site.
Ta	Protein turnaround time (in h) estimated at the distal ligature.
TH	Tyrosine hydroxylase.

1. INTRODUCTION

The fundamental task of the neuron is to receive, conduct and transmit signals. To perform this function, neurons in general are extremely elongated. Their processes, axons and dendrites, can extend over distances thousands of times that of the cell body and have a cytoplasmic volume thousands of times that of a non-neuronal cell. At the same time, neurons are extremely regionally differentiated. The diversity of function is maintained by regional differences in structural organization and in macromolecular composition. Electron microscopy reveals that the cell body of a typical neuron contains vast numbers of ribosomes. But although dendrites often contain some ribosomes, there are no ribosomes in the axon; therefore, the axon is essentially lacking in capacity to synthesize proteins. Essentially all proteins required to maintain the function and structure of an axon and its terminal are synthesized in the cell body and delivered to their destinations by the process of axonal transport.

Axonal transport can be classified into two broad categories according to the rate of transport: slow and fast. The slow component transports at rates of less than 5 mm/day and the fast at rates approximately one hundred times that of the slow. This thesis will investigate only fast axonal transport.

A wide variety of materials such as proteins, lipids, neurotransmitters, transport motor proteins, and various enzymes are moved by the fast transport system. Electron microscopic autoradiography shows corresponding accumulation between membranous organelles and labeled proteins at an axonal lesion. The movement of optically detectable organelles within axons can be observed directly. It is generally believed that the movement of membranous organelles is mediated through some microtubule-dependent mechanism. Proteins

and other molecules carried by rapid axonal transport are thought to be associated with these organelles as cargo. Upon arriving at its destination, transported material is transferred from the transport system to specific stationary structures. But, at the molecular level, little is known about the form of the attachment or relationship of the cargo proteins or other molecules to their carrier organelles, or whether the association is preserved for the lifetime of the organelle once it is established at the initial phase, or whether the relationship is loose and rebuildable in transit within the axon.

Based on similarities between neurons and other secretory cells in terms of the secretory process, an analogy referred to as the secretory model of the protein/organelle relationship has been drawn (Hammerschlag 1983/1984) between the two types of cells. It was postulated that axonally transported proteins are prepackaged in the region of the Golgi apparatus in the cell body and transported through the axon bound to membranous organelles. The proteins are either confined inside the lumen of the organelles or associated with the membrane as membranous proteins. Upon reaching their destinations, either the organelles *in toto* or budded-off vesicles from the organelles fuse with stationary membrane. The membranous proteins retain their association with the membrane, while the lumen-soluble proteins or proteins noncovalently associated with the lipid bilayer are released upon reaching their final destinations (e.g., during secretion). Thus, proteins and organelles become associated units at the initial phase of axonal transport and maintain this relationship throughout the lifetime of the membranous organelles in the cell.

However, neurons exhibit some unique features in terms of their transport system involving the relationship between transported materials and carrier organelles. For instance, at the neuronal cell body, inhibition of protein synthesis and protein trafficking through the Golgi apparatus prevents export of newly

synthesized proteins and phospholipids, but not optically detectable organelles (Smith et al., 1991; Snyder and Smith, 1990). Then again, within the axon, deposition of rapidly transported proteins is not accompanied by the loss of organelles from the transport system or the decrease in size of these organelles (Snyder et al., 1990). Moreover, at an axonal lesion, protease inhibitor prevents the turnaround of anterogradely transported proteins, but not the reversal of organelles (Smith and Snyder, 1991). Thus, it was suggested that a dynamic protein/organelle relationship may exist, that is, cargo protein molecules may off-load from and up-load to carrier organelles at different points within the neuron.

It is well documented that both anterogradely rapidly transported proteins (Abe et al., 1974; Bisby and Bulger, 1977; Bray et al., 1971; Snyder, 1986a, 1989) and optically detectable organelles (Smith, 1987, 1988) are capable of reversing their transport to the retrograde direction upon encountering a neuronal lesion. However, only recently have efforts been made to understand what mechanism(s) governs the transport reversal of molecules and organelles and to reveal the relationship between the transported proteins and organelles as they undergo transport reversal. The primary purpose of this thesis is to attempt to obtain a better understanding of this relationship by investigating transport reversal of both newly synthesized, rapidly transported proteins and optically detectable organelles at a neuronal lesion under similar conditions.

Sahenk and Lasek (1988) reported that protease inhibitors, leupeptin and E-64, prevent the anterograde-to-retrograde (A-R) reversal of proteins. Electron microscopy results showed that this was accompanied by an accumulation at the axon tip of organelles that morphologically resemble anterograde organelles and a reduction of organelles similar to retrograde organelles. The authors proposed that a morphological change of anterograde organelles may be a necessary step in

A-R transport reversal and that proteolysis may be a critical mechanism to such a conversion. Inhibition of such a mechanism may result in the failure of A-R reversal of organelles and thus in the prevention of turnaround of the proteins which reside on them. This is consistent with Hammerschlag's hypothesis of a tightly bound relationship between protein molecules and carrier organelles.

But, similar studies by Smith and Snyder (1991) drew a different conclusion. Their studies showed that while leupeptin prevents A-R reversal of labeled proteins, it does not prevent reversal of optically detectable organelles at an axonal lesion. It seems that the condition necessary for organelles to reverse transport direction is not sufficient for proteins to do so. It was suggested by the authors that proteins are first off-loaded from incoming anterograde organelles at the site of the lesion and, to return, some proteolytic process is necessary for proteins to up-load to outgoing retrograde organelles which will carry them away from the lesion site. If proteins accumulated at the lesion site are not carried away by their original carrier organelles, proteins and organelles may differ in their time required to undergo reversal. This hypothesis seems to be supported by reports that organelles are able to reverse their transport direction at a lesion within 10 minutes (Smith, 1987, 1988); but, instead of minutes, proteins require hours to reverse their transport direction (Bisby and Bulger, 1977; Sahenk and Mendell, 1980; Snyder, 1986a, 1989). However, comparable data of reversal dynamics of organelles and proteins in the same nerve of the same species under similar conditions is not available. So it is not clear whether protein molecules and organelles normally reverse as a tightly bound unit and proteolysis inhibition causes the dissociation of protein molecules from the carrier organelles and the subsequent prevention of their return, or whether transfer of protein molecules from one organelle to another is a normal step of the reversal process and proteolysis inhibition prevents the reassociation. This work is intended to

investigate the question of whether protein and organelles undergo A-R transport reversal at a neuronal lesion as a tightly bound unit.

If the relationship between protein and membranous organelles is established at an initial phase for the lifetime of the membranous organelles or the proteins, sorting of newly synthesized, transportable proteins may be expected to be made at the organelle level, that is, an organelle will carry only one kind of protein to the same destination. Therefore, the A-R reversal of organelles at a neuronal lesion can be expected to be accompanied by a correspondent reversal of cargo protein molecules. However, if a more dynamic relationship exists, that is, it is loose and rebuildable within the axon, then sorting may be expected at a lower level in a different dimension. In other words, an organelle may carry different proteins to different destinations. Thus, transfer of proteins between anterograde organelles and those undergoing transport reversal at an axonal lesion is possible. As a result, the reversed organelles may off-load their original cargo proteins and return without proteins or with fewer proteins, or they may carry proteins up-loaded at the lesion site which are not those they originally carried to the lesion site. In either case, a difference in reversal dynamics and reversal amounts between carrier organelles and cargo proteins might be expected. If this is the case, multiple pathways for material distribution through different pools by means of fast axonal transport is possible. Thus, the relationship between axonally transported proteins and the carrier membranous organelles is of interest not only because of the importance of the proteins and membrane components in axonal and synaptic functions, but because it may represent the molecular mechanisms involving guidance and delivery. It is also of related interest because it may represent a modification of vesicle transport processes used to convey proteins over less dramatic distances in other cell types.

To test this, parallel studies under similar conditions were designed to investigate *in vitro* the transport reversal of both proteins and organelles in the same nerve from the same species: the sciatic nerve from *Xenopus laevis*. The studies were conducted with two different bathing media: (1) normal frog Ringer (NR) solution, whose composition is compatible with extra-axonal fluid, it allowing the nerve or axon to be situated in a condition that resembles the actual physiological condition; (2) potassium glutamate (KG) solution, which is compatible with intra-axonal function, it allowing the axon to maintain homeostasis and organelle transport up to an axonal lesion. Thus, it is possible to observe organelle transport at a location very close to the lesion.

Protein transport and transport reversal was studied using a position-sensitive detector of ionizing radiation, the multiple proportional counter (MPC). By placing a living nerve with a pulse of radiolabeled protein in opposition to the MPC, it is possible to continuously monitor the axonal transport of the pulse along the nerve for an extended period of time. Organelle transport reversal was studied using video-enhanced contrast, differential interference contrast (DIC) microscopy. The video DIC microscopy is a method capable of detecting particles of various sizes, including those as small as 30-200 nm, and their movement in living axons. Transport rates in both directions, reversal dynamics, and the reversal ratios of both proteins and organelles were estimated.

The aim of this study was to attempt to compare (1) the kinematics of protein and organelle transport as they undergo translocation, (2) transport reversal dynamics and the reversal ratio of proteins and organelles at a neuronal lesion, and (3) the reaction of protein and organelle reversal to the two different bathing media, to reveal whether there is correspondence between proteins and organelles in translocation within the axon and transport reversal at a neuronal lesion. By these means it is possible to conclude whether axonally transported

organelles and proteins undergo transport reversal at a neuronal lesion as an inseparable unit, or whether transfer of proteins from their original carrier organelle to other organelles undergoing transport reversal can occur. It was hoped that the results would provide an indication of the protein/organelle relationship at a neuronal lesion. The existing relationship may have interesting implications for the cellular mechanisms of transport reversal. In addition, the findings may be significant in that they may bring light to the relationship between proteins and organelles at other sites within the neuron.

2. BACKGROUND INFORMATION RELATED TO THE PROBLEM

In this chapter axonal transport related to this work is reviewed. Particular emphasis is placed on the association of rapidly transported protein and other molecules to optically detectable membranous organelles. Since neurons may be considered as secretory cells, and analogies of intracellular trafficking of proteins as well as the form of the protein/organelle relationship can be drawn from well-studied non-neuronal secretory cells, relevant information of intracellular pathways of protein transport in non-neuronal cells is also reviewed. Finally, some features of axonally transported molecules and membranous organelles at different sites within the neuron are described. Similarities and differences between neuronal and non-neuronal cells in terms of the delivery of material are identified. Special attention is focused on the relationship between the transported proteins and other molecules and carrier organelles that may be revealed in these features.

2.1 Historical Development of Axonal Transport

Vast amounts of information on axonal transport have been accumulated; a full scale review is beyond the scope of this thesis. In this section relevant information on axonal transport of both molecules and membranous organelles related to the problem is reviewed. General information on the subject of axonal transport that is not covered in this thesis is available in formal reviews (Grafstein and Forman, 1980; Ochs, 1982; Schwartz, 1979; Snyder and Smith, 1984; Vallee and Bloom, 1991) and reported international conferences on this subject (Smith and Bisby, 1987; Weiss, 1982).

2.1.1 Axonal Transport of Molecules

2.1.1.1 Two Components, Fast and Slow, of Axonal Transport

As early as the middle of last century Waller's work (1852) on degenerative reactions after injury in peripheral nerve showed that the maintenance of the integrity of the axon is critically dependent on its continuity with the cell body. It was suggested that the nerve cell body acts as a nutritive center for the axon and that material is transported from the cell body along the axon and dendrites to the nerve terminals. Later, in 1905, Scott observed similarities between neurons and other secretory cells in their subcellular organization of dense-staining Nissle substance and numerous distinct granules. He then proposed that neurons can be viewed as secretory cells that synthesize their secretions in the cell body and transport them as particles to the nerve terminal for release. Forty years later, in the middle 1940s, Weiss and Hiscoe (1948) laid the experimental foundation for the hypothetical process of axonal transport. They observed swelling of regenerating nerve fibres proximal to a constriction. The swelling was suggested to represent accumulation of axoplasm that normally advanced as a coherent column in an undisturbed nerve fibre. When the nerve constriction was subsequently released, the accumulated axoplasm moved at a rate of 1-2 mm/day. They postulated from these experiments that there is a constant slow axoplasmic flow along the axon that proceeds at a normal average rate of 1 mm/day.

In the following decades a variety of experimental findings supported Weiss' postulate. With the ligature-accumulation technique combined with enzyme assay methods, acetylcholinesterase (AChE), choline acetyltransferase (ChAT), and certain oxidative enzymes were found to accumulate at the cut end of a nerve or at the point of a ligature (Friede, 1959; Hebb and Waites., 1956;

Lubinska et al., 1964). The accumulations were explained by Weiss's axoplasmic flow hypothesis as due to the disruption of transport in the axon. Droz and Leblend (1962, 1963), using ^{3}H-labeled amino acids injected systemically, showed the movement of a wave of radiolabeled protein along the nerve at a rate of 1 mm/day corresponding to that reported by Weiss and Hiscoe.

However, Miani's studies (1960, 1962) of protein and phospholipid transport, labeled with ^{14}C-amino acids and $^{32}PO_4$, respectively, showed a transport rate faster than 1 mm/day. More convincing evidence of a component with a faster transport rate was reported by Lubinska et al. (1964). They studied the accumulation of acetylcholinesterase activity at a neuronal lesion. From their quantitative studies on accumulation rate, they noted a rate of transport of several hundred mm/day, considerably faster than the 1-2 mm/day "slow" rate reported by Weiss and Hiscoe. By the late 1960s the technique of using radioactive tracers to label transportable materials of neurons had been improved to become a powerful tool in the study of axonal transport. Segment analysis is one of the methods that employs radiolabeling to generate more accurate estimates of the transport rates of labeled material (Ochs, 1972). In this method, transport material is locally radiolabeled at the cell bodies of appropriate nerve. The nerve is thereafter cut off into segments at various intervals which are assayed for radiolabel to determine the profile of radioactivity along the nerve. Transport velocities of various components are determined from the rates of displacement of various peaks in the radioactivity profile. For example, the rate of displacement of the front activity along the nerve gives the transport velocity of the most rapidly moving material. Radioactive amino acids have been applied exogenously to the cell bodies of neurons in certain pathways of the peripheral and central nervous systems to label transportable proteins for segment analysis (Goldberg and Kotani, 1967; Grafstein, 1967; Gross, 1973; Gross and Beidler, 1973, 1975; Lasek,

1968a&b; Ochs, 1972; Ochs et al., 1967). This method provides a measure of the entire spectrum of proteins moving down the axons. It was then clearly demonstrated that a second transport component exists, fast axonal transport having a range of velocities of 100-500 mm/day, approximately one hundred times that of the slow movement of 1-2 mm/day originally established by Weiss and Hiscoe.

Individual compositions in the transported material have been identified by labeling the transported materials using different precursor labels and by means of biochemical separation techniques. A wide variety of materials are transported to the axon and the nerve terminal via fast or slow axonal transport. Many different proteins are included. Gel electrophoresis has made it possible to separate a large number of transported proteins, some of which have been identified. In addition to proteins, lipids, neurotransmitters and some small molecules are also transported.

Detailed studies into the form and biochemical composition of the transported materials of the two transport processes (slow and fast) revealed other differential characteristics besides that of transport velocity that distinguishes fast from slow axonal transport. The fast and slow components differ in quantity, composition and subcellular localization of materials transported (for a review see Grafstein and Forman, 1980). It was found that about 80% of the transported radiolabeled protein is carried by slow axonal transport, the remaining 20% by fast axonal transport (McEwen and Grafstein, 1968). The subcellular distribution of the transported materials within the neuron was determined mainly by means of subcellular fractionation (Cancalon, 1979; Carton and Appel, 1973; Lorenz and Willard, 1978; Sabri and Ochs, 1973) and electron microscopic autoradiography (Droz et al., 1973; Hendrickson, 1972; Lentz, 1972; Schonbach et al., 1971; 1973). Of the fast-transported materials most

are membrane-associated and located in a particulate fraction, including a large variety of membranous cellular structures; only a small proportion is soluble (Cancalon and Beidler, 1975; Lorenz and Willard, 1978; McEwen and Grafstein, 1968; Sabri and Ochs, 1973). The biochemical composition of fast-transported material is predominantly membrane constituents (proteins, glycoproteins, phospholipids) and materials that would be associated with membranous organelles or vesicles, including neurotransmitters and transmitter-associated enzymes as well as myosin-like proteins which promote the movement of vesicles and organelles. Slow transport consists mainly of cytoplasmic material that is not associated with the plasma membrane or vesicular fraction (Black and Lasek, 1979, 1980; Hoffman and Lasek, 1975; Schonbach et al., 1973; Willard et al., 1974), including cytoskeletal proteins that make up neurofilaments, microtubules and microfilaments, and numerous cytosolic enzymes that catalyze intermediate metabolism (Lorenz and Willard, 1978; McEwen and Grafstein, 1968; Sabri and Ochs, 1972). However, some particulate material is also slowly transported (McEwen and Grafstein, 1968), and fast axonal transport also carries some cytosolic proteins (Brimijoin and Wiermaa, 1977a; McEwen and Grafstein, 1968).

As a result of detailed analysis of the composition of transported materials and their transport rates, more elaborate components of axonal transport have been revealed. Three subgroups of fast anterograde axonal transport and two of slow axonal transport have been categorized by Lorenz and Willard (1978) according to the composition and transport rate of the transported materials. Table 1 lists the rate components of some of the transported materials.

Table 1. Composition of Transported Materials

Transport group	Velocity (mm/day)	Biochemical composition	Subcellular organelles or structures
FA* I	100 – 500	Proteins (e.g., ion pumps, glucose transporter) Glycoproteins Phospholipids Classic transmitters (e.g., NE, ACh, serotonin) Neuropeptide transmitters (e.g., SP) Transmitter related enzymes (e.g., DβH, AChE)	Plasma membrane 50-150 nm tubulovesicular structures Dense cored vesicles
II	20 – 70	F_1 ATP_{ase}	Mitochondria
III	3 – 20	Myosin-like protein	Contractile elements
SA* IV	2 – 4	Actin Clathrin Calmodulin Soluble enzymes (e.g., ChAT, catechol o-methytransferase)	Microfilaments Clathrin complexes
V	< 2	Tubulin Neurofilament protein triplet	Microtubules Neurofilaments
FR* VI	> 100	Endogenous material Proteins Glycoproteins Phospholipids Lysosomal hydroxylase Presynaptic receptors Exogenous material NGF HRP Tetanus toxin Viruses	Large multivesicular bodies Other prelysosomal structures

* FA, SA and FR stand for fast anterograde, slow anterograde and fast retrograde, respectively.

2.1.1.2 Fast Retrograde Axonal Transport

Lubinska et al. (1964) first used the "isolated segment" technique, in which a nerve was ligated at two sites to create an isolated segment of nerve separated from both the cell body and the nerve terminal, to study axonal transport. It was found that AChE activity accumulated on the distal side as well as on the proximal side of the ligatures placed on canine sciatic nerve. Quantitative studies on accumulation rate revealed movement of this material in both directions to be at the fast rate. This experiment revealed that there is both fast anterograde and fast retrograde axonal transport, and that both proceed independent of continuity with the neuronal cell body. Dahlström (1965) arrived at the same conclusion from studies of the accumulation of catecholamines in ligated rat peripheral adrenergic nerves (Dahlström and Häggendal, 1966, 1967).

The presence of retrograde transport became more evident from work using labeled proteins. Many of the constituents (proteins, glycoproteins, phospholipids) carried by fast anterograde transport also appeared in retrograde transport (see Table 1). It has been shown that a fraction of radioactively labeled, anterogradely transported material is returned by retrograde transport from normal nerve terminals and from neuronal lesions (Abe et al., 1974; Armstrong et al., 1985; Bisby, 1985, 1987; Bisby and Bulger, 1977; Bray et al., 1971; Edström and Hanson, 1973; Snyder, 1986a). Some of the enzymes carried by fast anterograde transport such as AChE and dopamine-β-hydroxylase (DβH) have also been identified in retrograde transport (Brimijoin and Wiermaa, 1977b; Brimijoin and Wiermaa, 1978).

However, the composition of the anterograde and retrograde constituents, although similar, is not identical. As an example, norepinephrine (NE) and DβH were shown to have a common organelle localization (Hörtnagl et al., 1969; Lagercrantz, 1976) and identical anterograde transport rate (Brimijoin and

Wiermaa, 1977b), suggesting that they might be carried by the same organelles down axons. But, NE was found absent from retrograde DβH-containing vesicles (Brimijoin and Wiermaa, 1977b). This might reflect empty DβH-containing organelles or fragments of them returning to the cell body. In addition, analysis of vesicle proteins by polyacrylamide gel electrophoresis shows some differences in labeled proteins between anterograde and retrograde vesicles (Abe et al., 1974; Martz et al., 1989). Some of the anterogradely transported proteins are also present in the retrograde vesicles, some are absent from the retrograde vesicles, and the retrograde vesicles contain some new protein bands that are not present in the anterograde vesicles. Furthermore, some enzymes (e.g., DβH) moving toward the neuronal cell body are inactive (Nagatsu et al., 1976) and receptor affinity is altered (Zarbin et al., 1983). They are presumably destined for degradation or recycling.

In addition to the endogenous material derived from reversal of the anterograde component, retrograde transport also carries exogenous materials such as horseradish peroxidase (HRP) (Broawell and Brightman, 1979; Kristensson, 1970; Kristensson, 1977; Kristensson and Olsson, 1971a&b) and nerve growth factor (NGF) (Johnson et al., 1978; Stockel et al., 1975; Stockel et al., 1976) that are taken up from the extracellular space by the terminal. In addition, detailed studies of the retrograde transport of NGF showed considerable specificity. The uptake of NGF is mediated by specific membrane receptors only on adrenergic and sensory neurons (Hendry et al., 1974; Stoeckel et al., 1975) and transported back to the cell body with a rate comparable to that of fast axonal transport. Based on these findings and the evidence already discussed, it was considered that rapidly transported materials may be contained within membrane-bounded compartments. This notion fits with earlier evidence from AChE and norepinephrine (NE) accumulation (Dahlström, 1965; Lubinska et al., 1964) that

neurosecretory material is transported in the form of membrane-bounded vesicles (Bargmann, 1966).

The purpose of retrograde transport is presumed to be the return of materials to the neuronal cell body for recycling or degradation (Bisby, 1987; Holtzman, 1976; Nagatsu et al., 1976). Impairment of retrograde transport is associated with abnormal functioning of the axon as in the case of acrylamide intoxication (Chretien et al., 1981; Sahenk and Mendell, 1981). The arrival at the cell body of retrogradely transported material from the distal axon may also serve as a signal to inform the cell body of the status of the axon or as a tropic signal (Bisby, 1987). For example, axonal injury was found to cause structural and biochemical changes in the neuronal cell body. The onset of this reaction of the cell body depends on the distance from the site of injury (Watson, 1968), and blockade of retrograde transport to the cell body can delay the onset of such change (Singer et al., 1982). This implies a signal role of retrograde transport to the cell body. In addition, retrogradely transported NGF can induce an increase in cell body tyrosine hydroxylase (TH) and hence the increase of neurotransmitter (Hendry, 1977; Paravicini et al., 1975). In dorsal root ganglion (DRG) neurons containing substance P (SP), reduction in retrograde transport of NGF was been shown to lead to reduction in SP content in DRG (Johnson et al., 1986).

2.1.1.3 Summary

It has been widely recognized that instead of one constant slow movement of axoplasm, two transport processes distinct from each other in rate exist: the fast transport of 100-500 mm/day and the slow of 1-2 mm/day. Fast transport carries mostly membrane-associated material and slow mostly cytoskeleton and soluble proteins. In addition, fast axonal transport is bidirectional, including anterograde transport from the cell body to the nerve terminal and retrograde transport from

the terminal to the cell body. On the basis of the differences in biochemical composition, intracellular localization of the transported material, and transport velocity, it is well accepted that different mechanisms are involved in fast and slow axonal transport. Moreover, material moving at the fast rate may be transported in the form of membrane-bounded organelles or vesicles.

2.1.2 Axonal Transport of Membranous Organelles

The first notion of axonal transport of organelles was a prevision by Scott in 1905. Based on his observation of the similarities between neurons and other secretory cells in their subcellular organization of Nissl substance and distinct granules, Scott proposed that neurons are secretory cells which transport their secretory products to the nerve terminal in the form of prepackaged organelles. Observation of the movements of such organelles in neurites in tissue culture with light microscopy has been reported decades ago (Matsumoto, 1920). However, it is only relatively recently that organelle movements in living axons have been clearly observed and quantitative studies applied due to the development of microscopic techniques that permit the visualization of organelles in living cells. To observe the movement of organelles in living axons requires a microscopic method capable of visualizing organelles and subcellular structures inside living cells in an optically suitable preparation. With such advanced light microscopy as dark field (Cooper and Smith, 1974; Forman et al., 1977; Smith, 1972), phase contrast (Forman, 1982), and differential interference contrast (DIC) (Allen et al., 1969; Kirkpatrick et al., 1972), the fast movement of intra-axonal organelles or vesicles in both the anterograde and the retrograde direction has been clearly demonstrated. Movement velocities have been measured with the aid of combined techniques such as cinemicrographic and computer analysis (Breuer et al., 1975; Forman et al., 1977), photokymography (Berlinrood et al., 1972) and

automated cross-correlation analysis (Smith and Koles, 1976). The velocities of movement of organelles were found to be 1-2 μm/s, generally similar to the fast rates of transport obtained from radiolabeling studies (Burdwood, 1965; Cooper and Smith, 1974; Forman et al., 1977; Smith, 1971,1972).

Quantitative analysis of moving particles by light microscopy showed directional asymmetry: over 90% of the microscopically detectable particles moved in the retrograde direction (Cooper and Smith, 1974; Forman et al., 1977). This observation seemed to contradict biochemical evidence that no less material is transported in the anterograde than in the retrograde direction (Abe et al., 1974; Bisby, 1976; Bray et al., 1971; Edström and Hanson, 1973; Lubinska and Niemierko, 1971). This discrepancy was explained due to the limitation in resolution power of light microscopy (Forman et al., 1977). It was explained as that the majority of particles moving in the anterograde direction are too small to be detected using the light microscope, whereas most of the particles moving in the retrograde direction are large enough to be within the resolution (0.2 μm) of the light microscope. This explanation was supported by the observation of light scattering proximal to an axonal lesion, which increased with time after a lesion was applied, that might be caused by an accumulation of small particles which could not be detected individually (Smith, 1980). In addition, EM examination showed coincident asymmetric accumulation of organelles at an axonal lesion (Smith, 1980; Tsukita and Ishikawa, 1980). Large organelles of diameter 200-500 nm predominated on the distal side of an axonal lesion, and small vesiculotubular membranous structures of diameter 50-150 nm that could not be individually detected by light microscopy accumulated proximal to the lesion. The time course of the accumulation and effect of mitotic inhibitors on accumulation indicated that the accumulated particles arrived by fast axonal transport.

The morphological character of rapidly transported organelles in axons has been studied with EM in mammalian peripheral nerve (Tsukita and Ishikawa, 1980), in amphibian sciatic nerve (Smith, 1980), and in squid giant axons (Fahim et al., 1985). Various types of ultrastructurally different organelles are similar in different animal species. However, directional differentiation was observed. Table 2 summarizes the different morphological types of organelles transported in the two directions. The anterogradely moving organelles consist predominantly of small vesicles and tubulovesicular organelles of diameter 50-150 nm (average 80 nm). Some large dense cored vesicles that resemble secretory granules and a small proportion of mitochondria and organelles that resemble prelysosomes are also present in the anterograde component. Transport of some of the organelle marker proteins (e.g., DβH for neurotransmitter storage granules, mitochondria proteins and lysosome enzymes) matches the transport of these organelles (Partlow et al., 1972; Schmidt et al., 1980; Wooten, 1973). In contrast, retrogradely moving organelles are composed mostly of large organelles of diameter 200-500 nm, including dense cored vesicles, dense lamellar bodies and large multivesicular bodies that resemble lysosomes and prelysosomes. A small proportion of mitochondria, small vesicles and organelles indistinguishable from anterograde organelles and vesicles are also presented in the retrograde group.

Only recently, in the 1980s, has direct observation of the movement of subresolution vesicles become possible with improved DIC light microscopy combined with video enhancement of the image (Allen et al., 1981a&b; Inoué, 1981, 1986). This technique became a powerful optical tool for detecting intracellular organelles and their movements. It allows vesicles or organelles of varying size, including those with diameters as small as 30 nm, in the cytoplasm of a living axon to be viewed in real time and in their native state (Allen et al., 1982; Brady et al., 1982; Fahim et al., 1985; Smith, 1989). The velocity of the organelle

Table 2. Morphological Types of Transported Organelles

Morphological type	Dimension[1]	Accumulation at a lesion[1,2]		Composition[3]	
	(nm)	Prox side	Dist side	Prox side	Dist side
TVO	50-180	dominant	some	>90%	60%
DCV	70-90	some	some	≤10%	≤10%
MITO	280-780	some	some		
DLB	190-480	------	dominant	1%	30%
MVB	160-640	------	dominant		

Abbreviations: Prox, proximal; Dist, distal; TVO, tubular vesicular organelles; DCV, dense cored vesicles; MITO, mitochondria; DLB, dense lamellar bodies; MVB, multivesicular bodies.

References: 1, Smith, 1980; 2, Tsukita and Ishikawa, 1980; 3, Smith and Snyder, 1991.

movement can be measured directly from video images as organelles change position over the course of minutes. Their rate of movement is 0.5-5 μm/s or 45-450 mm/day (average 1-2 μm/sec) (Allen et al, 1982; Forman, 1987; Smith, 1988), similar to the fast rates previously obtained with conventional light microscopy (Cooper and Smith, 1974; Forman et al., 1977). Beyond this, extensive work in this line has resulted in a better understanding of the mechanism of fast axonal transport. In the following section, the present model of the transport mechanism is presented.

2.2 Transport Mechanisms

2.2.1 Mechanisms of Organelle Movement

Recently, great attention has focused on exploring the cellular and molecular mechanism of axonal transport. Extensive studies of axonal transport of organelles using video-enhanced microscopy brought new insights into the mechanism of fast axonal transport. It is generally accepted that membranous organelles and vesicles are the basic units of fast axonal transport.

Optical studies show that the movements of the membranous organelles and vesicles are too sustained and directional to be confused with the continual small Brownian movements caused by random thermal motions (Allen et al., 1985; Allen, 1987; Kendal et al., 1983). These organelles and vesicles move in close association with the microtubules which were subsequently identified by immunocytochemical staining, suggesting that microtubules may play an important role in such movements (Allen et al., 1985; Brady et al., 1985; Vale et al., 1985). A finding from this line of work is from studies on extruded squid axoplasm. When extruded squid axoplasm was placed onto a coverglass, it was found that single cytoplasmic filaments that dissociated from the bulk axoplasm

and bound to the surface of the coverglass supported the movement of vesicles in both directions when ATP was present (Allen et al., 1985; Vale et al., 1985a). When the same filaments were examined in the electron microscope, each of the filaments was identified as a single microtubule (Schnapp et al., 1985). Evidence that microtubules are essential components for organelle transport and that single microtubules can support bidirectional movement of organelles was also revealed in protozoa (Koonce and Schliwa, 1985) and in fibroblasts in culture (Hayden and Allen, 1984). Hence, the conclusion was drawn from these results that organelle movement is generated by a direct interaction between organelles and microtubules.

It has been demonstrated that organelles isolated from axoplasm (Gilbert and Sloboda, 1984) and purified synaptic vesicles (Schroer et al., 1985) show ATP-dependent movement when injected into squid giant axon. Studies of organelle transport in a reconstituted system consisting of microtubules from squid optic lobes (free of any associated proteins), organelle-enriched fraction and soluble supernatant fraction from squid axoplasm showed that the presence of the supernatant enhanced the movement of organelles along the microtubules and stimulated the movement of the microtubules along the coverglass (Vale, et al., 1985b). A similar movement of microtubules on a glass coverslip was also observed with native microtubules in dissociated axoplasm (Allen et al., 1985). The results indicated that a soluble motor molecule may be involved in generating a microtubule-based movement. Later, the use of a nonhydrolyzable ATP analog, 5'-adenylylimidodiphosphate (AMP-PNP), which induces stable binding between organelles and microtubules in isolated axoplasm (Brady, 1985; Lasek and Brady, 1985; Scholey et al., 1985), led to the identification and purification of the soluble motor molecules that generate microtubule-based movement (Vale et al., 1985c). One of these proteins, kinesin, a 380-kD polypeptide with an ATP-sensitive

microtubule-binding site and membrane-bounded organelle-binding site, has microtubule-stimulated ATPase activity and generates unidirectional movement of organelles and glass beads along microtubules towards the plus end of the microtubule (i.e., anterograde *in vivo*) in reconstituted *in vitro* systems and generates movement of microtubules on glass slides (Hirokawa et al., 1989; Hollenbeck, 1988, 1989; Schliwa, 1989; Schroer et al., 1988; Vale et al., 1985a, c, d & e). Cytoplasmic dynein, a multi-subunit protein with dynein-like characteristics such as binding to microtubules and high ATPase activity, produces movement in the opposite direction as kinesin, i.e., towards the minus end of microtubules or retrograde *in vivo* (Gilbert and Sloboda, 1989; Schnapp and Reese, 1989; Schroer et al., 1989; Vale, 1987). These studies indicate that there are two different motors responsible for bidirectional fast axonal transport working through some microtubule-dependent mechanism with kinesin the anterograde motor and dynein the retrograde motor.

2.2.2 Rapidly Transported Materials are Carried by Membranous Organelles

There is no evidence of a separate mechanism for rapid transport of proteins and other molecules. They are therefore thought to be transported as cargo in association with membranous organelles and vesicles. Considerable evidence supports this model. Evidence from biochemical analysis shows that rapidly transported molecules are predominantly membrane associated and located in the particulate fractions (Lorenz and Willard, 1978; McEwen and Grafstein, 1968). Double-labeled proteins and membrane phospholipids show similarities in transport rates, temperature dependence, transport inhibition by mitotic inhibitors, and subcellular fraction distribution (Abe et al., 1973). In addition, light microscopy and EM autoradiography show associated transport and

accumulation of rapidly transported proteins and membranous organelles and vesicles (Tsukita and Ishikawa, 1980). Also, retrograde transport of tracer molecules such as HRP and NGF show membranous compartment involvement and can be cytochemically demonstrated in membranous organelles (Hendry et al., 1974; Kristensson and Olsson, 1971; LaVail and LaVail, 1974, 1975). Moreover, optically detectable organelles and vesicles move at velocities of 0.5-5 μm/s (or 40-450 mm/day), generally coincident with the transport rates of proteins and other molecules. Meanwhile, particle movement along the microtubules requires ATP (Brady et al., 1982) and can be interrupted by low temperatures and by mitotic inhibitors (Hammond and Smith, 1977; Kendal et al., 1983), similar to protein transport that is ATP-dependent (Ochs, 1974) and interrupted by mitotic inhibitors (Abe et al., 1973; Edström and Mattsson, 1972; Hanson and Edström, 1977) and low temperature (Brimijoin et al., 1979; Edström and Hanson, 1973; Gross, 1973; Ochs and Smith, 1975). This suggests that the transport of optically detectable membranous organelles and radioactive labels are different aspects of the same process. Thus, it is generally accepted that membrane-bounded organelles mediate fast axonal transport through some microtubule-dependent mechanism, and that the transported molecule is associated with the membrane of the organelle or contained within the membrane compartment.

2.3 Relationship of Rapidly Transported Molecules to Membranous Organelles and Vesicles

Vesicle transport as a system for distribution of membrane, proteins, lipids, and other molecules between different compartments inside the cell is a very common phenomenon in most eukaryotic cells (Farquhar, 1985; Kelly, 1985; Rothman, 1985; Schliwa, 1984). Fast axonal transport in neurons is thought to be

a mere extension of such an intracellular traffic system over a dramatic distance. It would be of value to review the intracellular traffic of proteins and their relationship with carrier membranous organelles in well-studied non-neuronal cells before focusing on that in neurons.

2.3.1 Protein Traffic via Vesicle Transport in Non-neuronal Cells

Almost all proteins in eukaryotic cells are synthesized on a single class of ribosomes in the cytosol of the cell body. They are categorized into two major groups (for review of the protein transport pathway see Burgess and Kelly, 1987; Kelly, 1985; Palade, 1975; Pfeffer and Rothman, 1987). One group of proteins is released into the cytosol after its synthesis has been completed. Most of these proteins remain in the cytosol as permanent residents. Those with sorting signals are subsequently transported across respective membranes into mitochondria, nuclei and peroxisomes through an energy-dependent mechanism. The journey from their synthesis to these organelles is by diffusion. The other group of proteins, destined for secretion, as well as those destined for the endoplasmic reticulum (ER) and the Golgi apparatus (GA), the lysosomes, and the plasma membrane, are cotranslationally imported into the ER from the cytosol through some energy-dependent translocation mechanism because of a signal that is generally located at their amino terminus (for review of protein translocation across membrane see Blobel, 1982; Verner and Schatz, 1988; Walter and Lingappa, 1986; Wickner and Lodish, 1985). Some of these proteins will pass completely into the ER lumen when their synthesis is completed, while others will remain anchored in the ER membrane as membrane proteins.

Membrane proteins are attached to the lipid bilayer of a membrane in two major forms. (1) Some are attached to the membrane by a covalent linkage to the lipid molecules via an oligosaccharide or fatty acid chain as integral membrane

protein. Some of these integral membrane proteins (transmembrane protein) extend across the lipid bilayer of the membrane with their hydrophobic regions through the membrane where they interact with the hydrophobic tails of the lipid molecules, their hydrophilic regions exposed to water on both sides of the membrane. Others may be anchored to the membrane solely by a covalently attached lipid. (2) Others are associated with membrane indirectly by noncovalent interactions with integral membrane proteins as peripheral membrane proteins. Thus, a relationship between newly synthesized proteins and the ER membrane is built up either during or immediately following protein synthesis. These proteins thus become membrane associated, either confined inside the lumen of the membrane compartment or associated with the membrane in the forms of integral membrane protein or peripheral membrane protein. Many of the peripheral membrane proteins can be released from the membrane by relatively gentle extraction procedures, such as exposure to solutions of very high or low ionic strength or extreme pH, which interfere with protein-protein interactions but leave the lipid bilayer intact (Helenius and Simons, 1975; Montal, 1986). In contrast, the tightly bound integral membrane proteins can be released only by disrupting the bilayer with detergents or organic solvents.

All proteins except permanent residents of the ER are then exported to the GA by means of shuttle vesicles. Oligosaccharide chains are added to almost all of the protein molecules destined for the GA while they are still in the ER. The GA includes three biochemically specialized compartments (cis, medial, trans) (Rothman, 1985), each containing a unique set of enzymes. As the various newly synthesized glycoproteins pass through the GA, each one is post-translationally modified according to its final destination by a series of glycosylation, sulfation or acylation reactions. In the trans-compartment of the GA, the proteins are sorted and packaged for delivery according to their final destinations. All of the

proteins that pass through the GA, except those that are retained there as permanent residents, are distributed through either signal-dependent, receptor mediated, selective pathways or signal-independent, non-selective, default pathways into a particular type of membranous vesicle which transports them to their ultimate destinations (e.g., plasma membrane, constitutive secretion, regulated secretion, lysosome). The transport of membrane and membrane-associated proteins or other molecules across each membrane compartment is mediated by the budding and fusion of transport vesicles during which the relationship between membrane and membrane-associated molecules and thus their topological orientation is preserved, except when the lumen-soluble proteins or proteins noncovalently associated with the lipid bilayer are released upon reaching their final destinations (e.g., during secretion). Thus, the relationship between the membrane and the membrane-associated proteins is maintained throughout their lifetime in the cell.

In this model of protein transport, membrane-associated proteins such as endocytotic proteins or other molecules would be transported back to lysosomes or the GA utilizing a similar but reversed pathway (Fishman and Fine, 1987; Snider and Roggers, 1986; Stoorvogel et al., 1988; for review see Steinman et al., 1983; Thilo, 1985).

2.3.2 General Features of Axonal Transport of Molecules and Organelles

Some evidence implies that a similar relationship exists between rapidly transported protein and organelles in neurons. This was first suggested by Scott in 1905 based on his observation of the similarity between the subcellular organization of the Nissl substance and numerous distinct granules in neurons and non-neuronal secretory cells. Over decades, this postulate was further elaborated. As discussed earlier, considerable evidence supports the idea that

proteins and other molecules are rapidly transported in association with membranous organelles in neurons. Based on this and other evidence (discussed below), Hammerschlag (1983/84) proposed a model in which the relationship of proteins to their carrier membranous organelles is analogous to that of proteins destined for secretion and the plasma membrane in the well-studied non-neuronal secretory cell model. In brief, this model states that once packaged in the GA into different organelles with specific destinations, proteins remain associated with membranous organelles throughout the lifetime of the organelles in the cell. In this model we may expect parallel transport kinematics between proteins and organelles.

However, this model can not explain findings that a difference in transport kinematics exists between axonally transported organelles and protein at different points within the axon (Smith et al., 1991; Smith and Snyder, 1991; Snyder et al., 1990). Thus, a more dynamic model of the relationship between the carrier organelles and cargo proteins was suggested by those authors. It was suggested in this model that protein molecules may off-load from and up-load to carrier organelles at some points within the axon.

The following sections describe some observed features of axonal transport of protein molecules and membranous organelles at different sites within the axon that provide some evidence for the two described models of the relationship between transported protein and organelles.

2.3.2.1 Passage Through the Cell Body

Some evidence suggests that, in neurons, newly synthesized, rapidly transported proteins go through a pathway in a membrane-associated form similar to that of proteins destined for secretion in non-neuronal cells. Labeled, newly synthesized proteins appear to pass sequentially from the rough ER (RER), to the

GA, to the axon (Droz and Koening, 1970) followed by fast axonal transport (Grafstein and Forman, 1980). The rapid axonal transport of newly synthesized proteins or lipids is interdependent on the synthesis of both proteins (Grafstein et al., 1975; Schwartz, 1979) and phospholipids or cholesterol (Longo and Hammerschlag, 1980; Sherbany et al., 1979). Interference with the synthesis of either reduces the amount of fast-transported material into the axon. Thus, the interrelationship between newly synthesized proteins and membrane-component lipids built at the initial phase seems necessary for fast axonal transport. This is consistent with the scheme that fast axonal transport distributes macromolecules through membrane-bounded organelles and vesicles. This routing of rapidly transported proteins from the RER, through the GA complex, to the axon in a membrane-associated form has been confirmed by the affects of agents that disturb intracellular trafficking of newly synthesized proteins without affecting their synthesis. The Ca^{2+} requirement in protein intracellular trafficking seems a common feature in non-neuronal cells that probably triggers the fusion of vesicles with membrane (Tartakoff and Vassalli, 1978). The Ca^{2+} antagonist, Co^{2+}, when added to the bathing medium of the neuronal cell body, was found to reduce the amount of exported leucine-labeled, newly synthesized proteins to the axon, while the level of protein synthesis was unaffected (Lindsey et al., 1981; Hammerschlag, 1980). Meanwhile, ultrastructural evidence has shown that the reduction in export of protein to the axon was accompanied by a proportional increase in smooth-membrane vesicles and a decrease in the amount of recognizable GA. The results were interpreted by the authors as due to an accumulation of transition vesicles because of their reduced fusion with Golgi membrane and subsequent reduced addition of new Golgi membrane which caused reduced transport from the RER to the GA (Hammerschlag and Stone, 1982). Moreover, in the presence of Co^{2+}, the amount of transport of galactose (a

sugar known to be added to glycoprotein in the GA) labeled glycoprotein was reduced to a greater extent, indicating a similar affect of Co^{2+} on another step of transport from the GA to the axon. Results of similar studies showed that monensin, a sodium ionophore (Hammerschlag, 1982), and brefeldin A (Smith et al., 1991), an agent that causes disassembly of the cis- and medial-compartments of the GA, prevent proteins destined for fast axonal transport from leaving the GA without affecting protein synthesis.

On the other hand, Hammerschlag and Stone (1987) have reported that Co^{2+} and monensin inhibit export of radiolabeled protein to the axon, but they have little or no effect on the export of the fast transported enzymes AChE and adenylate cyclase. It was suggested by the authors that a large storage pool of fast-transported proteins might exist distal to the GA where Co^{2+} and monensin act. Evidence of such a pool has been reported for fast transported proteins (Berry, 1980; Goodrum and Morrell, 1982, Morin et al., 1991). It was suggested by Morin et al. (1991) that a possible advantage of such a pool might be to maintain a sufficient supply of neuropeptides during prolonged periods of high activity, which, unlike classical transmitters, can not be synthesized at the nerve terminal to meet the increased demand. Under such conditions, if export from such a storage pool were coupled to a neuron's electrical activity, then the increased demand for peptide transmitter could be met rapidly without requiring new protein synthesis. However, it is not known if the proteins are stored in packaged organelles.

Similar findings have been reported by Smith et al. (1991) in which cycloheximide, puromycin, and brefeldin A have been shown to inhibit profoundly the export of labeled protein to the axon, but not that of optically detectable organelles. The independence of organelle transport and the synthesis of proteins could be explained by the storage pool of fast-transported material.

However, another possibility suggested by the authors is also appealing, that is, that anterogradely transported organelles are formed by recycled membrane that arrives in the cell body via retrograde transport. In this case, organelle transport may be independent of protein synthesis and newly synthesized proteins may be up-loaded to pre-existing membranous organelles. This explanation is consistent with the evidence of recycling of synaptical vesicles in the cell body, presumably through the GA (Laduron, 1984; Levy et al., 1990).

2.3.2.2 Deposition of Rapidly Transported Material within the Axon

Axonal transport serves to maintain the structure and function of an axon and terminal by delivering needed macromolecules synthesized in the neuronal cell body. Rapidly transported proteins (Gross and Beidler, 1975; Muñoz-Martmez et al., 1981; Ochs, 1975; Snyder, 1989), glycoproteins (Armstrong et al., 1987; Forman et al., 1972; Goodrum and Morell, 1982), lipids (Bisby, 1985; Haley and Ledeen, 1979; Toews et al., 1987) and other molecules such as NE (Brimijoin and Wiermaa, 1977b) and SP (Brimijoin et al., 1980) have been shown to be deposited to stationary structures within the axon following the passage of a wave of rapidly transported material, with only a proportion of the rapidly transported material reaching the nerve endings. A similar deposition of retrogradely transported proteins that originate from reversed anterogradely transported proteins at a neuronal lesion has also been reported (Snyder, 1989).

The distribution of transported material between the axon and the nerve terminals varies according to the length of the axon. The total amount of material deposited within the axon is found to be proportional to the length of the nerve. In short axons such as the goldfish optic system, only approximately 30% of the radiolabeled protein remains in the axon (Forman et al., 1972). On the contrary, in the 30 cm long garfish olfactory nerve, as much as 80% of the radioactivity is

deposited within the axon (Cancalon and Beidler, 1975, 1977; Gross and Beidler, 1975). The amount of transported proteins that are deposited at each nerve segment was found to be a constant proportion of the transported protein in the moving phase, and the profile of material retained along the nerve follows an exponential function (Gross and Beidler, 1975; Muñoz-Martmez et al., 1981; Snyder, 1989). Thus, besides sending molecules to the synapses, fast axonal transport provides the axon with materials in quantities proportional to the amount of nerve which has to be sustained. Based on the knowledge of exponential deposition of transported material, it was suggested that the deposition of rapidly transported material from the moving phase to a relatively stationary structures may be a passive process.

Local conditions of the axon may actively modulate the deposition of transported materials. Increased deposition of proteins in regenerating nerve has been reported by a number of authors (Bisby, 1978; Chan et al., 1989; Griffin et al., 1976, 1981; Harry et al., 1989; Tessler et al., 1980). It reflects a response of the neuron to the increased demand for axonally delivered macromolecules as the regenerating axon grows. Alteration of deposition of rapidly transported materials was seen in neuropathic conditions of axon as well. For instance, in acrylamide-induced neuropathy, deposition of rapidly transported glycoproteins within the axon is selectively increased (Bradley and Willard, 1973; Chretien et al., 1981; Harry et al., 1989). The enhanced deposition of glycoproteins was explained as a response of the neuron to repair damaged axolemma due to a possible preferential damage of glycoproteins by acrylamide.

Another phenomenon that suggests an active deposition process is that different molecules are deposited preferentially at different sites. Most of the fucose-labeled glycoproteins are rapidly transported to and accumulated in nerve terminals, while a few are more evenly distributed along the axon and nerve

terminal (Bennet, 1973; Forman et al, 1972; Goodrum and Morell, 1982; Karlsson and Sjöstrand, 1971; Toews et al., 1982). This is different from the case with rapidly transported proteins in general. Many of the aminoacid-labeled, rapidly transported proteins are deposited in the axon and nerve terminal, but a few distinct polypeptides are preferentially transported to nerve terminals (Cancalon and Beidler, 1977; Weiss et al., 1978). Selective delivery of sulfoproteins to the nerve terminal was reported by Stone et al. (1984a&b, 1987). Regional differential deposition of different lipid molecules has also been reported (Toews et al., 1987).

Little is known about the mechanisms by which rapidly transported macromolecules are deposited, or the relationship between transported molecules and carrier organelles or vesicles during the deposition process. According to the secretory model, upon reaching their destination, either the individual organelles *in toto* or budded-off vesicles from these organelles fuse with stationary membrane as a result of recognition of a cytoplasmic marker on the organelle or budded-off vesicle by a receptor on the stationary structure or through a cytoplasmic docking receptor (Hammerschlag, 1983/1984; Hammerschlag and Stone, 1987; Stone and Hammerschlag, 1987). Thus, the transported molecules are deposited as part of the membranous organelle and the molecule/organelle relationship is preserved during the deposition process.

However, very little information regarding the involvement of organelles in deposition of transported molecules is available. A comparative study of protein and organelle transport showed that the deposition of rapidly transported, newly synthesized proteins is not accompanied by the loss of rapidly transported anterograde organelles from the transport system or the decrease in size of these organelles (Snyder et al., 1990). The authors suggested the possibility that the deposited labeled proteins may be released from intact transported vesicles. Thus,

deposition of macromolecules at a stationary structure may be a result of their dissociation from transported carrier organelles. Toews et al. (1987), based on their finding of differential deposition of individual lipid molecules, proposed a mechanism of single lipid molecules unloading to stationary structures as a result of dissociation of lipid molecules from membranous transported organelles, either by actual contact of the membranous transport organelles with stationary membranes in the axons or through specific lipid transfer proteins.

2.3.2.3 Reversal of Rapid Axonal Transport

Rapid transported molecules and optically detectable organelles are known to be capable of reversing their transport direction in the axon under certain conditions. Reversal of anterogradely transported proteins is known to take place (1) at normal nerve terminals (Abe et al., 1974; Bisby, 1987; Bisby and Bulger, 1977; Bray et al., 1971; Edström and Hanson, 1973), (2) at a neuronal lesion (Bisby and Bulger, 1977; Bray et al., 1971; Frizell and Sjöstrand, 1974; Schmidt et al., 1980; Snyder, 1989), (3) at the junction between the parent and the daughter axons of regenerating nerve (Chan et al., 1989), and (4) at the tip of regenerating axons (Bulger and Bisby, 1978). At an axonal lesion, turnaround of anterogradely transported proteins seems a regular feature. It has been demonstrated in frogs (Abe et al., 1974; Edström et al., 1987; Partlow et al., 1972; Snyder, 1986, 1989), in chicken (Bray et al., 1971; Hässig et al., 1991), and in rats (Bisby and Bulger, 1977; Schmidt et al., 1980). But, turnaround of retrogradely transported proteins could not be demonstrated (Hässig et al., 1991; Schmidt at al., 1980). In contrast, optically detectable organelles have been shown to undergo both A-R and R-A reversal at an axonal lesion (Smith, 1988). In addition, retrogradely transported organelles may also undergo transport reversal in the neuron cell body (Smith et al., 1991). This is a conjecture based on the finding

that inhibition of protein synthesis and protein trafficking through the Golgi apparatus prevents export of newly synthesized proteins and phospholipids from the cell body, but not the export of anterograde organelles (Snyder and Smith, 1991), implying that these organelles may be derived from arriving retrogradely transported organelles that undergo transport reversal at the cell body.

Transport reversal is controlled by the local conditions of the axon or nerve terminal. Studies of transport of radiolabeled protein in intact nerves show that a small fraction of labeled protein originally transported to the terminal undergoes transport reversal to participate in retrograde transport (Abe et al., 1974; Bisby and Bulger, 1977). At an artificial ending caused by an axonal lesion, axonal injury causes an increase in the quantity of returned, newly synthesized protein (Bisby and Bulger, 1977). The reversal returns to a normal value when regeneration at the injured site proceeded (Bulger and Bisby, 1978). But, it remained elevated when regeneration was prevented. Some pharmaceutical and axonopathic conditions affect transport reversal at a nerve terminal or axonal lesion as well. Sahenk and Mendell (1980) reported a delay in the time of onset and a reduction in the amount of retrograde transport of metabolically labeled protein due to a failure in the turnaround process in the distal axon caused by zinc pyridinethione toxicity. Local application of protease inhibitors, leupeptin and E-64, resulted in a similar effect of prevention of protein reversal at a neuronal lesion (Sahenk and Lasek, 1988).

However, it is not understood what mechanism governs the transport reversal of material or the relationship between the cargo proteins and other molecules and the carrier organelles as they undergo transport reversal. Sahenk and Lasek (1988) found from their studies on the effect of leupeptin on protein transport reversal that the prevention of protein reversal by the protease inhibitor was accompanied by an accumulation at the severed axon tip of membranous

organelles that morphologically resemble anterograde organelles and a reduction of organelles morphologically similar to retrograde organelles. They concluded from their results that the morphological conversion of transported organelles is necessary for the A-R reversal process. Proteolysis is probably a critical step in such a process. Inhibition of protein reversal is a consequence of failure in such a mechanism. This explanation is in agreement with the tightly bound secretory model of the protein/organelle relationship.

However, although morphological differences between anterograde organelles and retrograde organelles originating from the nerve terminal have been observed by a number of authors (Fahim et al., 1985; Smith, 1980; Tsukita and Ishikawa, 1980), there is no known biochemical criterion for distinguishing anterograde organelles from retrograde organelles. Almost all morphological types of retrograde organelles are also found in the anterograde organelle population, only the percentage of each kind differs between the two groups of organelles. Smith and Snyder (1991) reported that there is a relatively large percentage (63%) of small, retrogradely transported organelles in normal axons that are morphologically indistinguishable from those dominant in the anterograde group. Moreover, organelles that reverse their transport direction to retrograde at a lesion are predominantly (> 80%) small vesicles indistinguishable from anterograde organelles. Thus, it is argued that a morphological change is not a prerequisite condition for A-R transport reversal, at least at an axonal lesion. This was supported by the observation that during transport reversal, organelles move back and forth with a large amplitude indicating a fully reversible switch-like process (Smith, 1987, 1988). In addition, similar studies on the effect of leupeptin on transport reversal by Smith and Snyder (1991) showed that while leupeptin prevents the A-R reversal of newly synthesized proteins, it does not prevent reversal of organelles at an axonal lesion. It was therefore suggested

(Smith and Snyder, 1991) that transport reversal of organelles is not operated by an irreversible mechanism such as proteolysis, but that reversal of proteins is. This adds supportive evidence for a dynamic protein/organelle relationship.

If proteins and organelles reverse transport direction at a lesion under different mechanisms, they must be separated during such process. Consequently, they may display different reversal dynamics. The primary goal of this thesis is to examine the reversal dynamics of both proteins and organelles in the same nerve from the same animal under similar experimental conditions to see whether there is correspondence between proteins and organelles during transport reversal. Such information may reveal some aspects of the protein/organelle relationship in neurons.

3. METHODS AND MATERIALS

In this chapter techniques and experimental procedures used in this study are described. Two sets of experiments with specific techniques were performed to study transport reversal of proteins and of organelles respectively.

The first section of this chapter describes the protein turnaround study. The multiple proportional counter (MPC), the nerve preparation, the radiolabeled pulse creation procedure, the experimental bathing solutions, and the procedure for making a nerve lesion are detailed. Following this, the method of quantitative data analysis of turnaround time is discussed.

The second section of this chapter deals with the organelle turnaround study. The video-enhanced contrast, differential interference contrast (DIC) light microscopy technique used for observing organelle movement, the nerve preparation for DIC microscopy, the axonal lesion, and the experimental bathing solutions are described. Then, the quantitative data analysis is discussed.

3.1 Protein Turnaround Study

3.1.1 Multiple Proportional Counter (MPC) Technique

The methods of studying transport kinematics and reversal dynamics using the MPC have been described in published works (Snyder, 1982, 1984, 1986a&b; Snyder and Smith, 1984). Following is a summary of the MPC technique.

The multiple proportional counter (Snyder, 1982, 1984; Snyder and Smith, 1984) is a position-sensitive detector of ionizing radiation (Figure 1). It is composed of a series of single rectangular proportional radiation counters arranged side by side in a linear array and which share a common gas flow

Figure 1. Exploded View of the Multiple Proportional Counter (MPC)
A sample of ionizing radiation is placed on the entrance window of the counter. Beta particles escaping from the sample will penetrate, if of sufficient energy, the window and enter the counter. They will be confined to one specific proportional counter by the collimators. The anode wires operate at a positive potential (V_A) with respect to the grounded outer walls. The current signal caused by the radiation at the anode wires is amplified, passed through a lower-level discriminator to a binary converter, and stored in a memory unit. (Modified from Snyder, R.E. and Smith, R.S., in "Axoplasmic Transport", Weiss, D.G., Ed., Basel, Springer-Verlag, 1982, p442. With permission.)

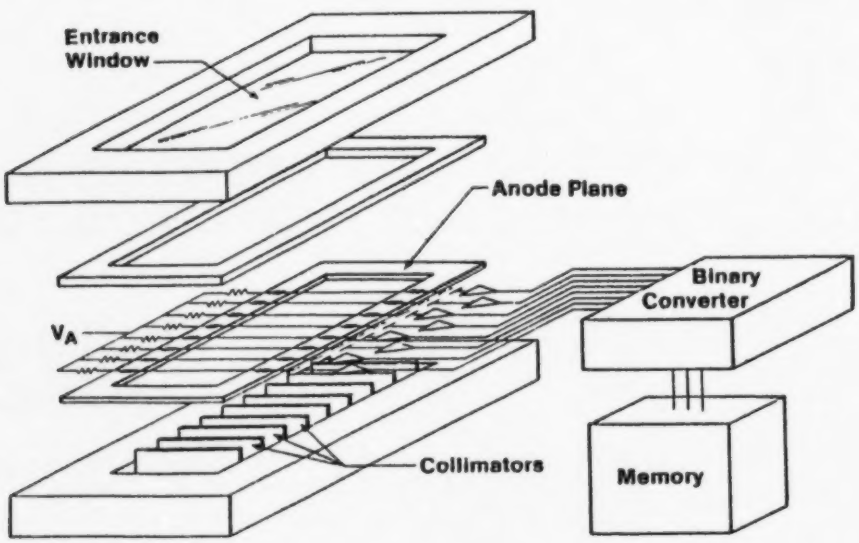

system. Each of the counters acts independently and is capable of detecting β-particles emitted from radionuclides such as ^{14}C, ^{32}P, ^{45}Ca and, in this work, ^{35}S. Each counter is a rectangular chamber with one side an entrance window consisting of 10-μm aluminized mylar for the passage of ionizing radiation. Each counter has an internal width of 2.68 mm and is separated from its adjacent counters by 0.50-mm-thick brass septa which serve as collimators to limit the trajectory of the β-particles in the direction parallel to the axis of the array of counters. Thus, the MPC offers a spatial resolution of 3.18 mm. Each counter contains an anode wire made of 20-μm-diameter gold-plated tungsten wire placed at width median of the chamber 3.18 mm below the entrance window of the detector. One end of each anode wire is connected through a 10-MΩ resistor which serves to decouple the anode signals from one another, to a common positive potential of 1100 to 1200 V with respect to the grounded outer walls, and the other end, the output, via a decoupling capacitor to a preamplifier. The multiple counter has an outer aluminum structure which provides a gas-tight compartment and, in addition, electrostatic shielding. The counter operates in the proportional region of the gas-amplification curve.

The initial process in the proportional counter is the formation of ion pairs in the gas volume by the ionizing radiation that enters the detector through the entrance window. Subsequently, the positive ions and electrons move towards the oppositely charged electrodes. Under the influence of the electric field, the free electrons produced by the ionizing radiation accumulate rapidly at the positive electrode where they result in secondary ionization. In the so-called proportional-counter region, the initial ionization produced by each particle is amplified linearly by secondary ionization. This process repeats itself until an avalanche of electrons reaches the positive electrode, causing a current signal to flow in the external circuit through the power supply. All of the primary

electrons will produce an avalanche, giving a pulse at the anode which is proportional to the size of the avalanche. The signals from the preamplifiers are conducted to amplifiers followed by lower-level discriminators that remove electronic noise pulses. The amplifier/discriminator unit converts the analog signals above a minimum level to logic signals. The signals from the discriminators enter a binary encoding system and are then stored in a memory unit.

By placing a living nerve with a moving pulse of radiolabeled proteins in opposition to the MPC, it is possible to continuously monitor the axonal transport of the pulse along the nerve for an extended period of time via the β-particles that escape the nerve and enter the detector. The collimators confine the ionizing particles originating from the nerve to well defined regions in space. The MPC yields a distance-time relationship of radioactivity change along a nerve from a single preparation. Therefore, the MPC is able to detect the movement of the pulse of radiolabel in the anterograde direction and the accumulation of the radioactivity at a distal ligature following its arrival. Upon encountering such a lesion, a proportion of the anterogradely transported protein reverses its direction to retrograde transport. The MPC is capable of detecting the movement in the retrograde direction of a smaller pulse which consists of a fraction of the anterogradely transported protein that turned around at the distal ligature (Snyder, 1986a&b). Parameters of not only the anterograde transport of the labeled protein but also the turnaround and the retrograde transport of the protein as dissociated processes are obtained from single preparations as described below. This allows us to explore the dynamics of protein turnaround and retrograde axonal transport of protein.

3.1.2 Bathing Solution

One of the following two solutions was used as the bathing medium for the nerve preparations during these experiments. Solution 1, normal Ringer (NR) solution, a physiological saline which is compatible with the extra-axonal fluid had the following composition (mM): NaCl, 112; KCl, 3.0; $MgSO_4$, 1.6; $CaCl_2$, 3.0; Glucose, 5.5; HEPES (N-2-hydroxyethyl piperazine-N'-2-ethanesulfonic acid), 3.0. The solution was adjusted to pH 7.40 ± 0.02 with NaOH and/or HCl and was gassed with oxygen before use. Solution 2, potassium glutamate (KG) solution, which was compatible with intra-axonal function, had the following composition (mM): potassium glutamate, 120; $MgSO_4$, 2.0; $CaCl_2$, 2.0; EGTA (potassium salt), a Ca^{2+} chelator, 4.0; HEPES, 5.0; ATP, 2.0. In some experiments ATP was not added to the bathing solution. The solution was adjusted to pH 7.00 ± 0.02 with KOH and gassed with oxygen. The major difference between the two solutions that is critical, except for the high concentration of sodium and chloride in the NR instead of the high potassium concentration in the KG, was that Ca^{2+} was buffered with EGTA and ATP was added to support the axonal transport mechanism in the KG solution. Ringer solution was used as a basic bathing medium for all of the nerve preparations during dissection. After a lesion had been placed, either the NR or the KG solution was used for each of the two groups of nerve preparations.

3.1.3 Nerve Preparation and Pulse Creation Procedure

Female adult specimens of *Xenopus laevis* (Nasco Scientific, U. S. A.) were anesthetized by submersion in a 2% aqueous solution of urethane (ethyl carbamate, Sigma Chemical Co.) for 20-30 minutes and then sacrificed. A sciatic nerve, usually 60-80 mm in length, in continuity with its ninth dorsal root

ganglion (DRG) was isolated. A thread (6-0) was tied to the distal end of the nerve. During the dissection the preparation was bathed in NR solution.

Figure 2 shows the time course of the pulse creation procedure. Immediately following dissection, the nerve preparation was placed in a two-compartment tray containing NR, with the ganglion and its roots in one compartment (0.025 ml) and the sciatic nerve extended to the second compartment (20 ml) through a passage 3 mm in diameter and 3 mm in length. The passage was then sealed with silicon grease which separated the two compartments without causing any harmful effect to the nerve and its axonal transport. The Ringer solution in the ganglion compartment was removed and replaced with 0.025 ml of NR solution which contained 0.25 mCi of L-^{35}S-methionine at a specific activity of 1000-1400 Ci/M (Amersham or New England Nuclear). Following a 1-h period which allowed the radiolabeled methionine to enter into the cell bodies and become incorporated into newly synthesized proteins, the radioactive solution in the ganglion compartment was removed and the compartment rinsed twice and refilled with nonradiolabel-containing NR solution. After an additional 3.5-h period during which time newly synthesized proteins were exported into the axons, the nerve was severed 4 mm distal to the ganglion to prevent further transport of radiolabel into the axons. Thus, a pulse of radiolabel at the proximal end of the sciatic nerve was created.

The nerve was next rinsed in 1 ml of fresh NR for 5 minutes. The solution used at this time and for subsequent procedures contained in addition 1.0 mM of nonradioactive methionine to reduce the incorporation of contaminant ^{35}S-methionine in non-neuronal cells of the nerve. In a dish containing NR solution, the standard length of the nerve with its perineural sheath still on was measured and recorded using the method of Chan et al. (1980). The nerve trunk

Figure 2. Schematic Representation of the Pulse Creation Procedure

0–1 h

A sciatic nerve (N) 74 mm in length with its ninth dorsal root ganglion (G) in continuity was placed in a two-compartment tray. The passage between the two compartments was sealed with silicone grease. The nerve cell bodies in the G-compartment were bathed in 0.025 ml of NR containing 0.25 mCi of L-^{35}S-methionine and the nerve in the N-compartment in plain NR. A 1-h incubation period was allowed during which radiolabel would enter the cell bodies and become incorporated into newly synthesized protein.

1–4.5 h

Radioactive NR was removed from the G-compartment which was then rinsed and refilled with plain NR. An additional 3.5-h period allowed newly synthesized protein to be exported into the axons.

4.5–6.75 h

Four-millimeter nerve immediately distal to the ganglion was removed to prevent further export of radiolabel into the axons from the cell bodies. Thus, a pulse of radiolabel was generated. The nerve was then rinsed in fresh NR containing 1.0 mM non-radioactive methionine. A standard length of the nerve was then measured. The nerve was next desheathed and rinsed in 200 ml of NR for about 2.25 h while the pulse of radiolabel moved distally.

6.75 h

By this time fast transported radiolabel, at 7.5 mm/h, had moved distally for about 15 mm, and slow transported radiolabel, at 3-4 mm/d, as well as axonally non-transportable radiolabel will not have reached this point. The 10-mm proximal piece of nerve was cut off to reduce the contamination. The nerve of 60 mm in length with a narrow pulse of fast transported radiolabel was then moved to a one-compartment tray for MPC monitoring.

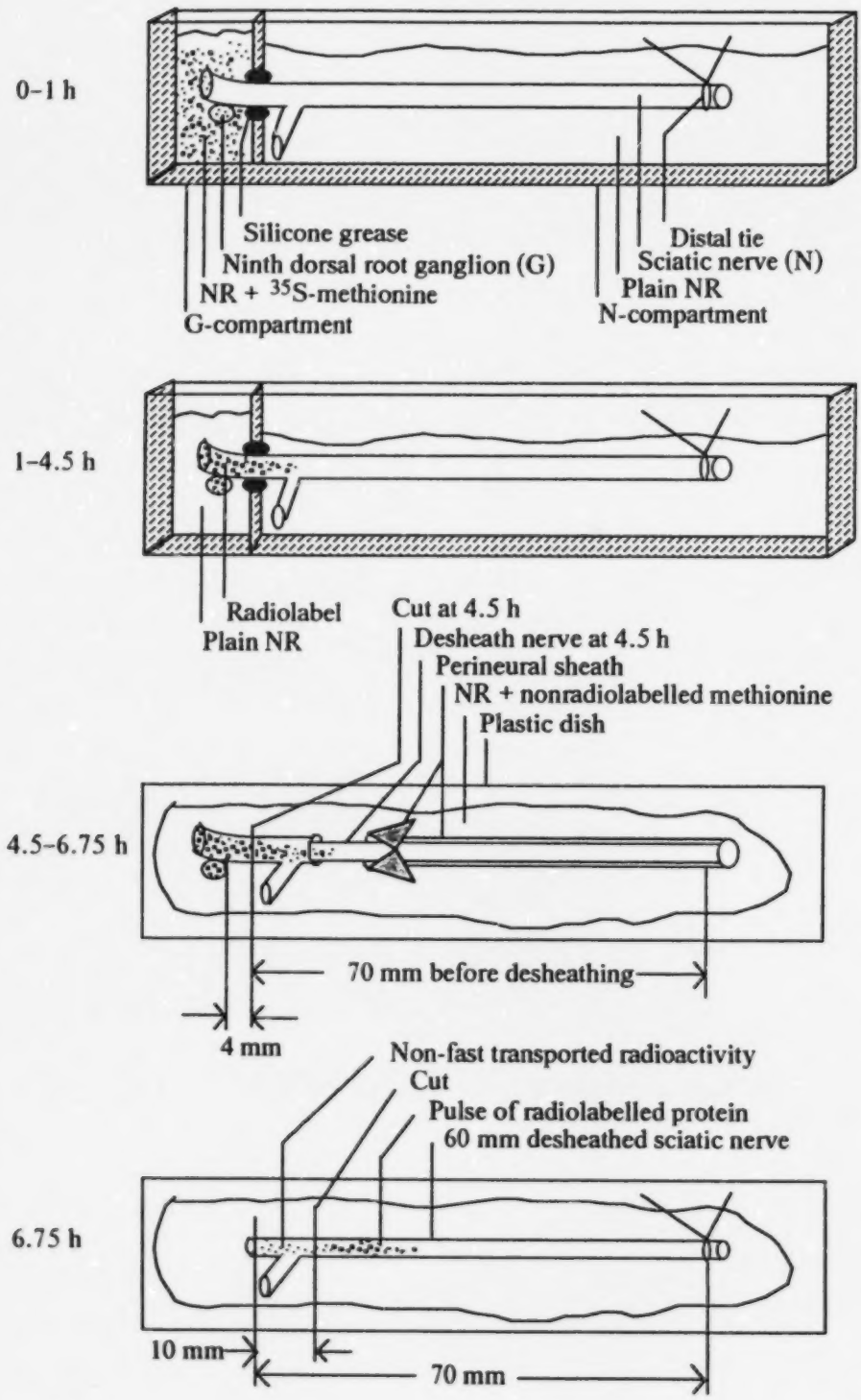
0–1 h
Silicone grease
Ninth dorsal root ganglion (G)
NR + 35S-methionine
G-compartment
Distal tie
Sciatic nerve (N)
Plain NR
N-compartment
1–4.5 h
Radiolabel
Plain NR
Cut at 4.5 h
Desheath nerve at 4.5 h
Perineural sheath
NR + nonradiolabelled methionine
Plastic dish
4.5–6.75 h
70 mm before desheathing
4 mm
Non-fast transported radioactivity
Cut
Pulse of radiolabelled protein
60 mm desheathed sciatic nerve
6.75 h
10 mm
70 mm

with its perineural sheath has a banded appearance due to the wavy disposition of the nerve fibres within the perineural sheath. Under a binocular microscope, the nerve was stretched to a point where the bands just disappeared. The recorded length was used as a reference for later realignment. The ligature at the distal end of the nerve was then removed. The nerve was carefully desheathed on a piece of NR-solution-wetted filter paper and rinsed in 25 ml of NR. The distal ligature was put back at the previous place of the nerve. The nerve was then transferred to 200 ml of NR and gently agitated for 2.25 h while the pulse of radiolabel moved distally, leaving behind contamination caused by diffusion. The proximal 10 mm of the sciatic nerve was next cut off to eliminate or reduce the contamination; therefore, a 45-65 mm long sciatic nerve with a narrow pulse of newly synthesized radiolabeled protein was prepared for monitoring the movement of the labeled proteins along the axons.

Another thread was tied at the proximal end of the nerve. The nerve was placed in a one-compartment tray with a 3.6-μm mylar floor and containing about 170 ml of NR or KG solution, with the threads attached to the ends of the nerve holding it in position and contacting the floor of the tray (see Figure 3a). A second loose tie was placed 10-15 mm proximal to the initial distal ligature with the thread attached to screw devices on the walls of the tray for later constriction of the nerve. A piece of gauze stretched over a plastic frame was used to gently press the nerve against the floor of the tray. A pump device was used to circulate the bathing solution. The one-compartment tray was finally placed on the top of the entrance window of the MPC for continuous monitoring of the movement of the pulse of radiolabeled proteins along the sciatic nerve. The radiation which was emitted from within the nerve and which penetrated the floor of the tray entered the detector through the entrance window and was detected by the MPC. The radioactivity and its position was displayed on an oscilloscope and

Figure 3. Lesion Creation Time under MPC Monitoring

(**a**), A schematic representation of the nerve positioned in a one-compartment tray and its relation to the MPC. A 63 mm nerve (N) is placed in a tray filled with NR, with threads tied at both ends holding it in position and a press (P) gently pressing it against the mylar floor (MF) of the tray. A loose thread is placed proximal to the distal end of the nerve. The ends of the thread are attached to the screw devises (S) on the walls of the tray for later constriction of the nerve. The tray is then placed on the entrance window (EW) of the MPC and bathing solution is circulated.

(**b-d**), Schematic counts-vs-position plots at various times following removal of the nerve from the animal (T) to show the time of lesion creation (t). **b**, The distal tie was placed at the time of removal of the nerve and MPC monitoring started about 6.75 h later. At the beginning of MPC monitoring (T = 6.75 h) the front of the pulse of radiolabel was 17 segments (or 54 mm) proximal to the distal tie. It took about 7.2 h for the pulse to reach the distal tie according to the known transport rate of 7.5 mm/h. In this case the loose tie was not tighten and the lesion time prior to the arrival of the pulse at the distal ligature is t = 6.75 + 7.2 = 14 h. **c**, In this case, the loose tie, which was 14 segments (or about 45 mm) distal to the front of the pulse at the beginning of MPC monitoring (T = 6.75 h), was tied at this time to generate a lesion time of t = 6 h. **d**, In this case, the loose tie was tied when the front of the pulse reached the tie segment (at time T = 12.75 h) and the lesion time is t = 0 h.

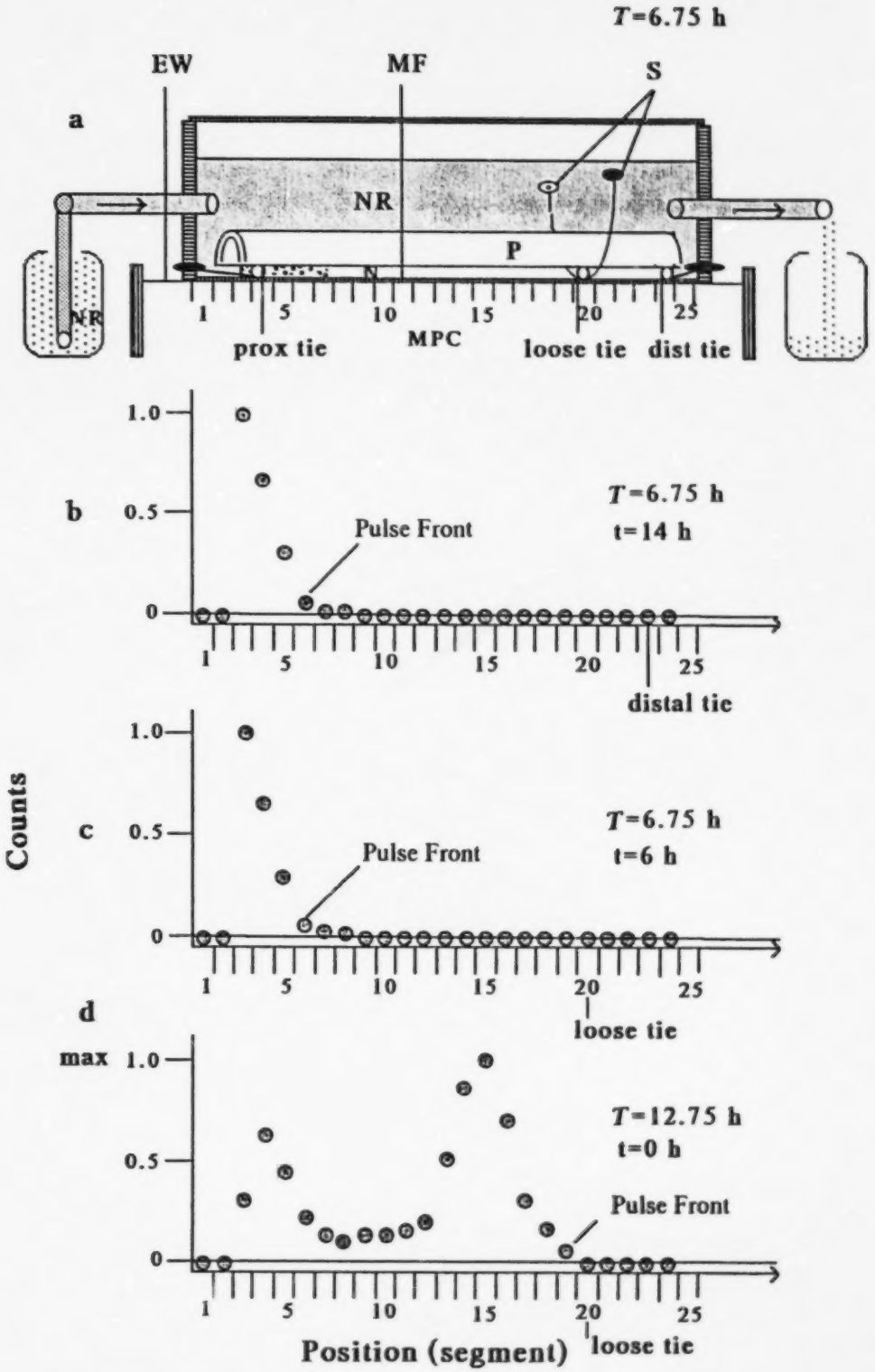
T=6.75 h
EW
MF
S
a
NR
P
N
NR
1
5
10
15
20
25
prox tie
MPC
loose tie
dist tie
1.0
0.5
0
b
T=6.75 h
t=14 h
Pulse Front
distal tie
Counts
c
T=6.75 h
t=6 h
Pulse Front
loose tie
d
max
T=12.75 h
t=0 h
Pulse Front
loose tie
Position (segment)

recorded in the form of counts-vs-position spectra in 1000-s blocks on disk for subsequent quantitative analysis. Experiments were performed at a temperature of 23-23.5^0 C.

3.1.4 Lesion Time

In this work, counts-vs-position spectra were sent to an oscilloscope such that the shape and location of the pulse of radiolabel along the nerve was displayed on the screen. Knowing the location of the front of the pulse along the nerve, and according to a previously reported fastest transport rate of 180 mm/day (7.5 mm/h) (Snyder, 1986), the loose knot placed near the distal end of the nerve was tied at different times in different preparations so that the time period from constricting the loose ligature to that when the front of the pulse of radiolabel arrived at the ligature ranged from 0 to 6-7 hours (defined as the lesion time). Figure 3b-d illustrates 3 situations with lesion times of 0, 6 and > 10 h. In the case of 0 h (Figure 3d), the loose tie was constricted when the front of the pulse just arrived at the segment to be ligated; in the case of 6 h (Figure 3c), the loose tie was tighten when the pulse was about 45 mm proximal to it; in the case of > 10 h (Figure 3b), no second ligature was placed, reversal occurring at the ligature placed at the distal end of the nerve after dissection at the beginning of the experiment.

3.1.5 Data Collection and Analysis

Counts-vs-position spectra were recorded from the pulse radiolabeled nerve for about 20 hours. Two to four background spectra, recorded from the one-compartment tray before placing the nerve in the tray, were averaged to correct all records for room background. The data recorded were rearranged to be plotted as the counting rate (counts/hour) as a function of time for each

3.18-mm segment of nerve (counts-vs-time plot). Figure 4 shows the counts-vs-time plots from some segments of one nerve. The series of counts-vs-time plots from all the segments of the nerve reveals the movement of the pulse of radiolabeled protein along the nerve as a function of time. The early pulse of radiolabel is the anterograde pulse which started at the proximal segment of the nerve and moved anterogradely towards the distal ligature. It reached the distal ligature several hours later resulting in accumulation of radioactivity at the ligature. The later pulse of smaller amplitude is the retrograde pulse which originated at the ligature following arrival of the anterograde pulse and moved retrogradely. A plateau of radioactivity remained behind the anterograde pulse in each segment following passage of the pulse represents deposition of radiolabel from the rapidly moving system to a stationary phase.

Transport rates and turnaround time required for the transport reversal of radiolabeled protein at the lesion were calculated for each preparation using techniques described by Snyder (1986a). Eight times were calculated from selected counts-vs-time plots which are the arrival times of five parts of the anterograde pulse at the specific nerve segment: 0.1AF and 0.25AF, when the anterograde pulse first reached 10% and 25% of its maximum counting rate; AP, when the anterograde pulse reached its maximum counting rate; 0.25AS and 0.1AS, when the anterograde pulse fell to 25% and 10% of its maximum counting rate above the plateau between the anterograde and the retrograde pulse; and the departure times of three parts of the retrograde pulse from the specific nerve segment: 0.1RF and 0.25RF, when the retrograde pulse first reached 10% and 25% of its maximum counting rate above the plateau; and RP, when the retrograde pulse reached its maximum counting rate. Counts-vs-time plots from the nerve segments in which the anterograde and the retrograde pulse were separated by the stationary plateau, a region free of moving activity (e.g.,

Figure 4. Counts versus Time Plots

The plots were recorded from one preparation. Each plot shows the time course of the activity through a 3.18-mm segment of nerve. Nineteen plots were obtained for this specific nerve. Only 8 are shown. The distance of the segment from the proximal end of the nerve is given in each plot. The series of plots shows that an early pulse of radiolabel moved anterogradely and reached the distal ligature (57.15 mm from the proximal end of the preparation) in 6–8 h and resulted in accumulation of radioactivity at the ligature. Later, a smaller pulse (indicated by the arrow) of radiolabel moved retrogradely. The retrograde pulse became indistinguishable from the plateau in the proximal segments about 40 mm proximal to the distal ligature.

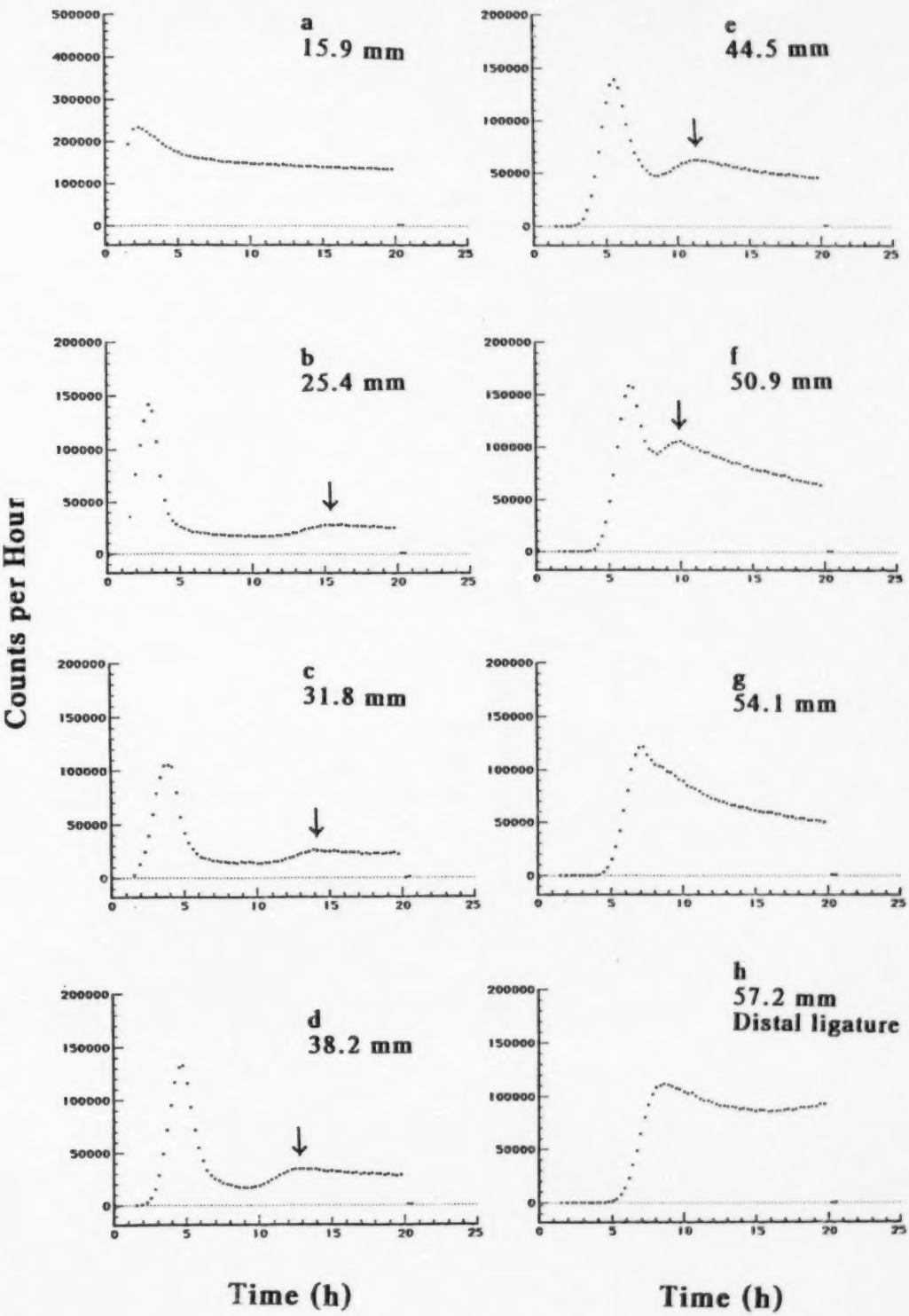
a
15.9 mm
e
44.5 mm
b
25.4 mm
f
50.9 mm
c
31.8 mm
g
54.1 mm
d
38.2 mm
h
57.2 mm
Distal ligature
Counts per Hour
Time (h)
Time (h)

Figure 4c-e), were used to calculate all eight times. The arrival times of the slow portion of the anterograde pulse and the fast portion of the retrograde pulse were not calculated at the segments where the two pulses were not clearly separated (e.g., Figure 4f). Similarly, the arrival times of the fast portion of the anterograde pulse were not able to be calculated from counts-vs-time plots of proximal nerve segments in which the anterograde pulse had partially passed prior to recording (e.g., Figure 4a&b).

The calculated times were then plotted as a function of position of each corresponding segment (time-vs-position plot) (see Figure 5). A straight line was fitted to each of the eight sets of times using a weighted least-squares technique. The reciprocal slopes of the fitted straight lines gave the transport rates of the eight respective parts of the pulses. Extrapolation of the 0.1(0.25)AF and 0.1(0.25)AS lines to the proximal ligature gives the width of the anterograde pulse at the segment. Extrapolation of the lines to the position of the distal ligature yielded the time when the anterograde pulse arrived at this segment, the time when the retrograde pulse departed, and the time interval between the arrival of the anterograde pulse and the departure of the retrograde pulse from the distal ligature which was defined as the turnaround time, the time required for the reversal of transport to occur at the distal ligature. The turnaround time, specified as the time period from first arrival of radiolabel at the ligature to the first departure of radiolabel from the ligature, was calculated for each preparation and used in subsequent analysis.

Figure 5. Time versus Position Plot

Time-vs-position plot for the preparation whose counts-vs-time plots are shown in Figure 4. Data points show the times at which selected portions of the anterograde and retrograde pulses reached each segment of the nerve. The lines are least-squares fits to the data points. The reciprocal slopes of the fitted lines are the transport rates. Extrapolation of the times of 0.1AF and 0.1RF to the position of the distal ligature yielded the turnaround time (Ta) required for protein to reverse transport at the ligature.

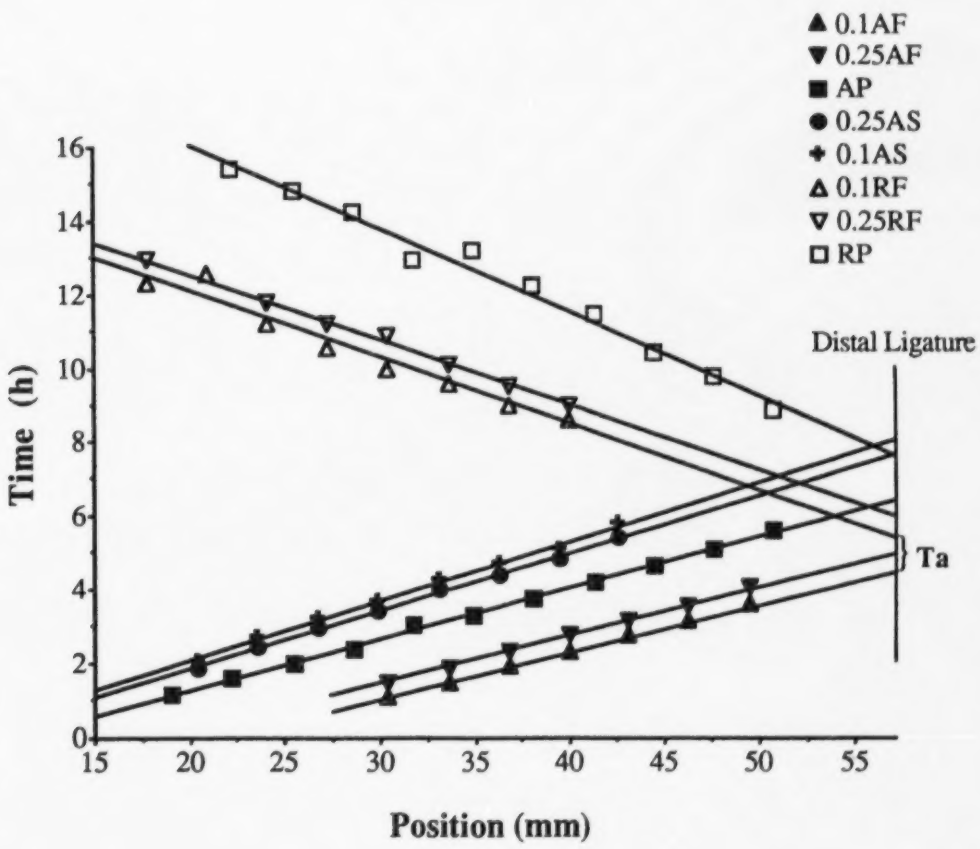

3.2 Organelle Turnaround Study

3.2.1 Video-enhanced Contrast, Differential Interference Contrast (DIC) Microscopy

Detailed information on the video DIC technique and its use in detecting organelle transport in living axons can be found in published works (Allen et al., 1969; Allen et al., 1981a&b; Allen, 1983, 1985; Inoué, 1986; Smith, 1989). Following is a summary of the video DIC technique.

When light passes through an unstained cell, the amplitude of the light waves scarcely changes and the structural details of the cell cannot be seen in the ordinary way even if the image is highly magnified. However, the phase of the light wave is altered by its passage through the cell according to the cell's refractive index which is correlative with the thickness and/or density of different parts of the cell. Light passing through a relatively dense or thick part of the cell, such as the nucleus or an organelle, is retarded and its phase consequently shifted relative to light that passes through a surrounding thinner or less dense region of the cytoplasm. When the two sets of waves are brought to combine, they interfere with each other such that the amplitude of the resultant wave is altered, thus changing the resultant intensity or brightness. The phase change introduced into the object beam by the presence of the specimen is converted into an amplitude difference. Small phase differences thus become visible by exploiting the interference effects. Differential interference contrast (DIC) microscopy is one of the methods which introduces contrast into nonabsorbent objects, the living cell, and makes visible the transparent object by exploiting interference effects produced when recombining the waves.

Since each organelle which travels at the rapid-transport speed may represent a region of refractive index which differs from that of the surrounding

cytoplasm, such organelles may be detectable by DIC microscopy. Figure 6 outlines the arrangement of the major optical components in the microscope. The general working principle of the DIC microscope is, in brief, first to produce plane-polarized light waves which then strike a beam-splitter, a modified Wollaston prism, combined with the condenser. The incident beam is split into two mutually coherent components that are capable of interfering, forming two laterally separated beams of light with a very small lateral displacement or shear. When the beams pass through the object, their phases shift corresponding to the gradient in the optical path difference which is determined by the refractive index and thickness of the object under examination. After passing through the object, the plane wavefronts are deformed. Above the objective a second modified Wollaston prism combined with the analyzer is used as a beam combiner to combine the two beams and meanwhile introduce a constant phase difference (Δ_b), or bias retardation, between them which is instrumentally controllable. The wavefronts interfere with each other. The intensity (I) of the emergent beam is a function of the phase difference (Δ) between the wavefronts which is the sum of the bias retardation and the gradient in phase difference (Δ_o) introduced by the object (Allen et al., 1969; Allen, et al., 1981a):

$$I = I_{max}\mathrm{Sin}^2(\Delta/2) \qquad (3.1)$$

where I_{max} is the maximum intensity transmitted by the system. Since $\Delta_o = 0$ in the background, the background intensity I_b is then given as

$$I_b = I_{max}\mathrm{Sin}^2(\Delta_b/2) \qquad (3.2)$$

Figure 6. Schematic Representation of the Arrangement of the Major Optical Components in the DIC Microscope.

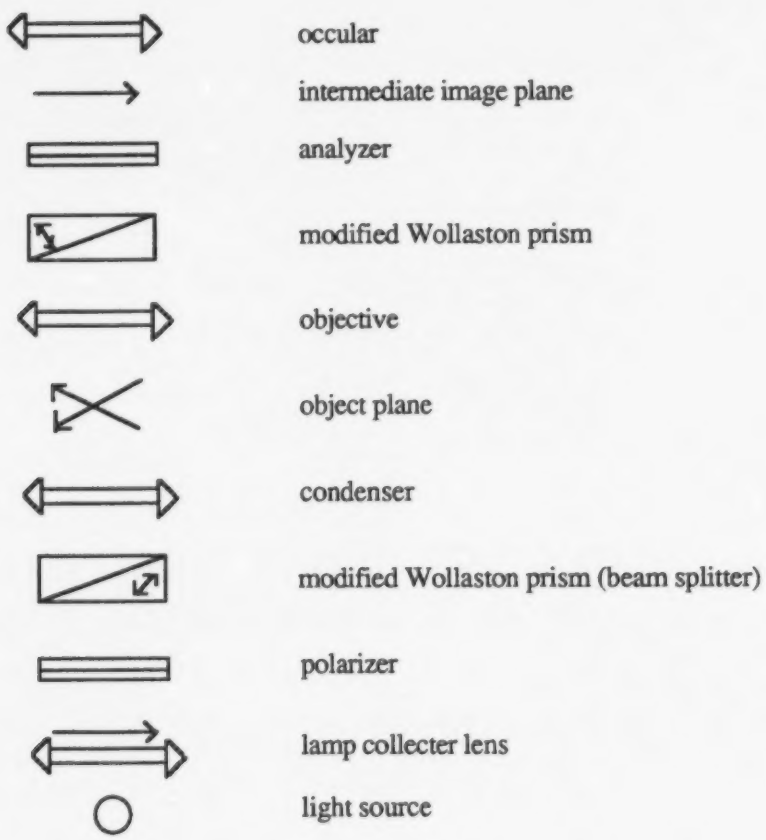

Note: oriented arrows represent the axial location of field planes.

while the object intensity I_o is

$$I_o = I_{max}Sin^2[(\Delta_b + \Delta_o)/2] \qquad (3.3)$$

Therefore, wherever interfaces (at organelles, membranes, fibrils, etc.) introduce gradients of optical path difference, the contrast of the object against background ($I_b - I_0 \neq 0$) is achieved by converting a small phase difference into an intensity difference.

Image contrast (C) is defined as the difference in brightness or intensity between that of the background (I_b) and that of the object (I_o) divided by the background intensity (I_b):

$$C = (I_b - I_o)/I_b \qquad (3.4)$$

Since I_b and I_o are functions of the bias retardation, the contrast of the image of an object against background $I_b - I_o$ varies as a function of the bias retardation (Δ_b). Since organelles moving in the axons are very small, high resolution and high magnification are required in order to see them. Therefore, the specimen under examination is required to be very thin and a high magnification objective lens with a high numerical aperture is usually required for good results. Under ideal optical conditions that produce maximal signal $I_b - I_o$ [when $\Delta_b = \pi/2$, which is out of the operating range in high extinction methods (Allen et al., 1981a; Inoué, 1986)], the background intensity (I_b) is relatively high which causes the object to be nearly invisible (Allen, 1983). In video-enhanced DIC microscopy, the microscopic image is recorded with a video camera. The signal due to background illumination is subtracted electronically without diminishing the difference ($I_b - I_o$) in intensity of the background I_b and the object I_o under study.

The enhanced image contrast C_v may therefore be expressed as (Allen et al., 1981a&b, 1983, 1985)

$$C_v = (I_b - I_o)/(I_b - I_v) \qquad (3.5)$$

where I_v is the electronic reduction in signal level introduced by an offset in the camera applied to darken the background in the video image without affecting the difference in brightness that constitutes the video signal. Thus, the visual contrast of video-DIC image is enhanced by electronically decreasing the denominator of equation (3.4). Organelles as small as 50 nm in diameter and their movement can be detected in extruded squid axoplasm (Allen et al., 1982; Brady and Lasek, 1982). Moreover, since images produced by video cameras are in an electronic form, they can be digitized, sent to a linked computer, and processed in various ways to enhance and extract latent information invisible to the eye. With real-time image processing such as background subtraction and frame averaging, the computer-assisted video-DIC microscope makes it possible to detect small particles with diameters of 50-100 nm and their movement in single myelinated axons (Smith, 1989).

3.2.2 Bathing Solution

Two studies were conducted using different bathing solutions. Ringer solution was used as the basic bathing medium for all of the experiments. After an axonal lesion was made, either NR or KG solution (see section 3.1.2) was used for the nerve preparation of each of the two groups.

3.2.3 Nerve Preparation and Axonal Lesion

Figure 7 illustrates the procedure of nerve preparation for DIC microscopy. A sciatic nerve 50-60 mm in length from the same species as used in the protein transport study was isolated and desheathed using a similar method as that adopted in the protein transport study. During dissection and desheathing, the nerve preparation was bathed in NR solution.

The nerve was then treated for about 10 minutes with a 1% trypsin (Sigma Chemical) in NR solution which allows the axons to be more readily isolated without damage (Smith et al., 1985). The nerve was next rinsed in plain NR and then transferred onto a microscope cover glass which had a thin layer of silicone grease on the edges, with the nerve bathed in sufficient NR or KG solution. The bundle was teased in the center of the middle region of the nerve with fine needles to expose individual axons. A drop of silicone oil (Dow Corning 710) was applied to the center of the teased area of the nerve (which gently pressed the isolated axons against the cover glass). A 10-25 μm wide lesion was made on isolated axons by crushing them against the underneath cover glass with a fine wire 25 μm in diameter. A microscope slide was then placed over the preparation. The silicone oil supported the isolated axons against the surface of the top cover glass and mechanically stabilized the preparation so that optimum optical conditions were achieved. Either NR or KG solution was perfused into the latent chamber between the top cover glass and the microscope slide so that the nerve preparation was bathed in the appropriate medium.

In other preparations, double lesions with a separation of 300-500 μm were made on individual axons and the preparations bathed in KG solution.

Figure 7. Procedure of Single Axon Preparation for DIC Microscopy

1. Dissect a sciatic nerve 50-60 mm long.
2. Desheath the nerve.
3. 1% trypsin treatment.
4. Rinsing.
5. Isolating single axons and making axonal lesion (see text for details).

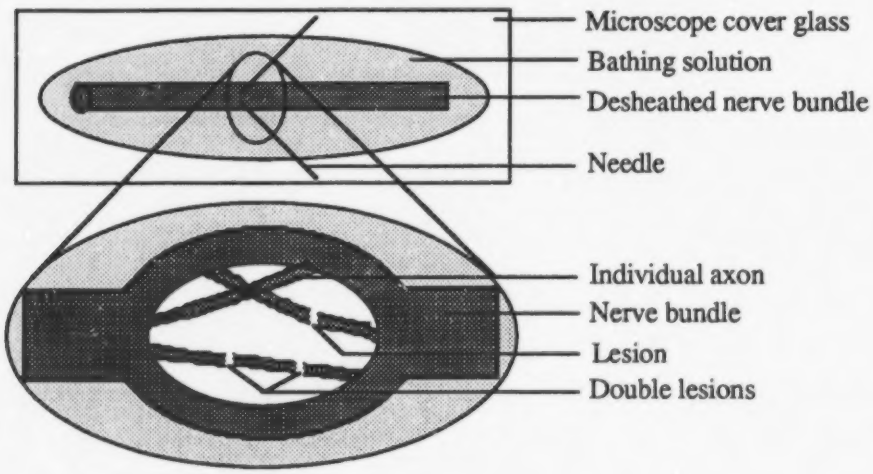

6. Mounting preparation on microscope slide.

3.2.4 Image Detection and Recording with Video-enhanced DIC Microscopy

Individual myelinated axons were viewed with differential interference contrast (DIC) microscopy (Zeiss photomicroscope; objective X63, NA 1.4). A 100-W quartz-halogen lamp with a band-pass green filter (peak transmission at 550 nm, bandpass 60 nm) was used to provide Köhler illumination. The specimen was viewed with an oil-immersion lens. The image was detected with a television camera (DAGE MTI) with a chalnicon tube that resulted in a differential interference contrast (DIC) image of the living axon with much detail obscured by low spatial frequency structures and with only very few moving organelles.

Further image enhancement was achieved by real-time digital processing of the television signal, the DIC image, using Quantex Corporation computing equipment (DF-80 spatial filter and DS-50 processor). A detailed description of the method has been given by Smith (1989). The DIC image was high-pass filtered to remove low-spatial-frequency deep shadows and highlights originating in the myelin, followed by noise reduction by frame averaging and contrast enhancement so that the detailed image of fine axonal structure was improved. At this stage, most of the rapidly transported organelles still could not be detected since they were particulates not larger than 50 nm in diameter. The image of the stationary cellular structure had to be removed to manifest the moving elements. A moving exponential time average of the high-pass image was taken as a background image representing stationary structure, and this averaged image was subtracted from the unaveraged current high-pass image which contained both moving elements and stationary components, thus resulting in detection of the moving elements. Electronic noise in the resultant image was reduced also by the exponential averaging process. The final output was the image of the living axon at a magnification of 12000X which revealed most clearly and mainly the moving elements which were the rapidly transported organelles (Figure 8).

Figure 8. Video-enhanced, Differential Interference Contrast Micrographs of a Living Myelinated Axon from the Sciatic Nerve of *Xenopus laevis*

The video micrographs were taken at a time interval of 1 second. The time sequence is shown at the upper-left corner of each micrograph. The longitudinal axis of the axon cylinder runs from bottom to top of each micrograph. Many moving organelles are revealed. Examples of the anterogradely moving organelles are indicated by the single-lined arrows and of the retrogradely moving organelles by the double-lined arrows. Movement of the organelles can be seen by comparison of their positions in the sequential micrographs. M represents myelin. Scale bar = 5 μm.

2
M
1
M
4
M
3
M

3.2.5 Data Collection and Analysis

Axons from individual preparations were viewed as soon as possible after the axonal lesion was created, and the images of axon segments of interest, 200-1000 μm proximal to the lesion, were video-taped intermittently for about 2 hours for subsequent analysis. All experimental procedures were performed at a room temperature of 23-24^0 C.

Subsequently, parameters of organelle transport such as velocity and traffic density were measured for each individual axon. Organelle transport velocity was estimated by measuring the time required for individual organelles to move across a unit length (5 μm) of axon segment. Organelle traffic was measured as the number of organelles in the microscope focal plane (approximately 0.5 μm in depth) that crossed a unit diameter (1 μm) of axon segment in a unit time period (1 min). Inference of organelle reversal dynamics was then drawn from the parameters of anterograde and retrograde transport of organelles in the vicinity of the lesion.

4. RESULTS

In this chapter the results of transport reversal of protein and of organelles are presented in two sections. In each section, the transport kinematics and related parameters are estimated first, then, reversal dynamics are assessed from the parameters of anterograde and retrograde transport in the vicinity of a neuronal lesion.

4.1 Protein Transport

4.1.1 Protein Transport in NR solution

Twenty-one nerves were studied using NR solution as the bathing medium during all of the experimental stages. All nerves were treated similarly with the exception of a different lesion time prior to the first arrival of the anterogradely transported pulse of radiolabeled protein at the lesion site. Special attention was placed on the lesion creation time with the intention to create comparable experimental conditions to those of organelle transport because this time is uncontrollable in the organelle experiment.

4.1.1.1 General Observations

All nerves examined displayed qualitatively similar counts-vs-time plots (see Figure 4) except for the presence of a retrograde pulse in some nerves. All of the preparations showed an anterograde pulse of radiolabeled protein. Eighteen of the 21 nerves showed a retrograde pulse.

The plots recorded from the central segments of a nerve showed a typical pattern of radioactivity change with time. The more distal of these segments

showed an absence of radioactivity before the radiolabeled protein had reached the segment. Then, a pulse of radiolabel reached, peaked, and passed through the segment representing the passage of the anterograde wave of radiolabel. Following passage of the anterograde pulse was a plateau which represented radiolabeled protein deposited to a stationary phase from the rapidly moving system. Later in time, a second pulse of smaller amplitude arrived which resulted from the passage of a wave of retrogradely transported labeled protein that had originated at the distal ligature. After reaching a maximal value the counting rate decreased slowly, leaving a broadened pulse tail when the retrograde pulse passed through the segment. Moving proximally, the retrograde pulse broadened and finally became indistinguishable from the plateau in the more proximal segments 30-40 mm proximal to the distal ligature. The counts-vs-time plot from the distal ligature segment showed initially no radiolabel, followed in time by a rapid increase to a maximum counting rate that corresponded to the arrival and accumulation of the anterograde pulse.

4.1.1.2 Transport Rates and Related Parameters

Anterograde transport rates were estimated for all the preparations. Retrograde transport rates were estimated for the 18 (out of 21) nerves which showed a retrograde pulse. The mean rates and other transport parameters are presented in Table 3. Two-tailed Student's t-tests showed no statistically significant difference in anterograde transport rates between preparations with and without a retrograde pulse. The combined mean anterograde transport rates of both groups and the mean rates of retrograde transport of the 18 nerves were within the range of presumed normal values presented in a previous report (Snyder, 1986a).

Table 3. Mean ± SEM of Protein Transport Parameters for Nerves Bathed in NR Solution (Temperature = 23°C)

Parameter[a]	Group 1[b] (n = 18)	Group 2[c] (n = 3)	P[d]	Combined (n = 21)	Previous Report[1] (n = 10)	P[e]
Transport Rates (mm/day)						
0.1AF	182.9 ± 3.2	177.1 ± 4.3	n.s.[f]	182.4 ± 2.8	180.8 ± 2.2	n.s.
0.25AF	178.9 ± 3.3	174.7 ± 1.7	n.s.	178.4 ± 2.9	179.6 ± 1.7	n.s.
AP	174.5 ± 3.4	171.7 ± 10.1	n.s.	174.1 ± 3.0	171.6 ± 2.3	n.s.
0.25AS	161.9 ± 2.6	159.7 ± 8.0	n.s.	161.5 ± 2.3	158.5 ± 2.9	n.s.
0.1AS	159.1 ± 3.4	155.7 ± 7.7	n.s.	158.6 ± 3.0	153.7 ± 3.0	n.s.
0.1RF	158.5 ± 9.1				158.5 ± 7.3	n.s.
0.25RF	145.5 ± 6.7				145.6 ± 4.7	n.s.
RP	109.0 ± 3.9				110.3 ± 3.5	n.s.
r/a	0.097 ± 0.011[g] 0.093 ± 0.008[h]				0.108 ± 0.010	n.s.

Reference: 1, Snyder, 1986a.

[a] See text for the definitions for the parameters.

[b] Preparations in group 1 showed a retrograde pulse of radiolabel.

[c] Preparations in group 2 did not show a retrograde pulse of radiolabel.

[d] Probability of significance test of the means between group 1 and group 2 based on two-tailed Student's t-test.

[e] Probability of significance test of the means between combined data (of group 1 and group 2) and previously reported data based on two-tailed Student's t-test.

[f] n.s., not significant at $\alpha = 0.05$ level of significance.

[g] The values were obtained from the sixth segment proximal to the distal ligature.

[h] The values were the average over the fifth to seventh segments proximal to the distal ligature.

The absence of a retrograde pulse in three nerves might have resulted from the failure of a protein turnaround process at the local lesion, from a reduction in the amount of turnaround of radiolabel to a level insufficient to be detected, or from a failure in the retrograde transport system. Considerable evidence suggests that anterograde and retrograde transport share the same basic transport elements, only with different molecular transport motors, so the turnaround process probably involves a switch between motors. The unaffected anterograde transport in the three nerves which failed to show a retrograde pulse compared to that in nerves which showed a retrograde pulse suggests that these three nerves had a functioning transport system. Thus, the absence of a detectable retrograde pulse of radiolabel is more likely due to a failure or considerable decrease in transport reversal of radiolabeled protein rather than dysfunction of the subsequent retrograde transport.

Since the lesion existence time prior to the first arrival of the anterograde pulse of radiolabeled protein at the ligature (named as lesion time, t) is the only factor that differed among all the preparations, a correlation analysis was carried out. No correlation was found between anterograde and retrograde transport rates and the time period (t) that a lesion existed before radiolabel reached the lesion. The coefficients of correlation (r) for all eight rates are below 0.20 ($n = 21$ for anterograde transport rates, $n = 18$ for retrograde transport rates); (refer to Table 4). Therefore, it is concluded that the time period that a nerve lesion existed had no effect on transport rates.

4.1.1.3 Turnaround and Retrograde Transport

Due to counting statistics and small fluctuations with time in the counting rate of the anterograde deposition following the passage of the anterograde pulse through a segment of nerve, a counting rate associated with the retrograde pulse

Table 4. Coefficients of Correlation Between 10 Transport Parameters and the Lesion Time (t) for Nerves Bathed in NR Solution

Parameter	r	P	n
0.1AF	0.006	0.977	21
0.25AF	0.113	0.632	21
AP	0.144	0.539	21
0.25AS	-0.043	0.848	21
0.1AS	-0.086	0.711	21
0.1RF	0.136	0.595	18
0.25RF	0.206	0.584	18
RP	0.004	0.984	18
Ta	-0.620	0.006	18
r/a	0.100	0.694	18

Lesion Time (t): time period (in h) between creation of the lesion and the arrival of radiolabeled protein.

0.1AF, 0.25AF, AP, 0.25AS, 0.1AS, 0.1RF, 0.25RF and RP: the transport rates (in mm/day) of five parts of the anterograde pulse of radiolabel and three parts of the retrograde pulse of radiolabel (see text for the definitions).

Ta: turnaround time (in h) required for protein to reverse transport at the distal ligature obtained as the time interval between the arrival of the fastest portion of the anterograde pulse and departure of the fastest portion of the retrograde pulse of radiolabel (defined in Figure 5).

r/a: protein reversal ratio obtained as the ratio of peak amplitude of the retrograde pulse above anterograde deposition plateau to peak amplitude of the anterograde pulse of radiolabel.

r: coefficient of correlation between the listed parameters and the lesion creation time (t) prior to the arrival of radiolabel at the distal ligature.

P: probability of significance test of the coefficient of correlation.

(superimposed on the anterograde deposition plateau) of less than 1-2% of the maximum counting rate of the anterograde pulse cannot generally be detected. In the present experiments, 18 out of 21 nerves showed a detectable retrograde pulse. This result is close to the previous reported data from similar experiments in which about 20% of the nerves bathed in Ringer solution failed to show a detectable retrograde pulse (Smith & Snyder, 1991; Snyder, 1986a).

In an attempt to measure the size of the retrograde pulse, the ratio of the maximum counting rate of the retrograde pulse above the plateau to that of the anterograde pulse (r/a) was measured from those distal segments which showed a clear plateau between the two pulses (see Figure 4c&d). As an example, the mean (± SD) ratio for the sixth segment proximal to the distal ligature from the 18 preparations was 0.097 ± 0.047 (range: 0.047-0.239), which is similar to a previously reported value of 0.108 ± 0.036, range: 0.036-0.172 (Snyder, 1986a). The averaged (± SD) ratio from the fifth to the seventh segments proximal to the distal ligature was found to be 0.093 ± 0.035 (range: 0.045-0.176). The value varied considerably between preparations, being below detection limits for the three nerves that did not show a retrograde pulse. But the difference in the r/a ratios was not found to correlate with the lesion time which ranged from 0 h to about 13 h (r = 0.10, n = 18, refer to Table 4). Thus, it is suggested that the amount of protein turned around at the lesion does not change during the first 10 hours after the lesion is created.

4.1.1.4 Turnaround Time

The time required for protein to turn around at the lesion, defined as the turnaround time (Ta), was determined for the nerves that showed a detectable retrograde pulse. Table 4 shows that the turnaround time (Ta) is correlated with the lesion time (t) (r = 0.62). Figure 9 gives a plot between Ta and t for the

Figure 9. Turnaround Time (Ta) versus Lesion Time (t)

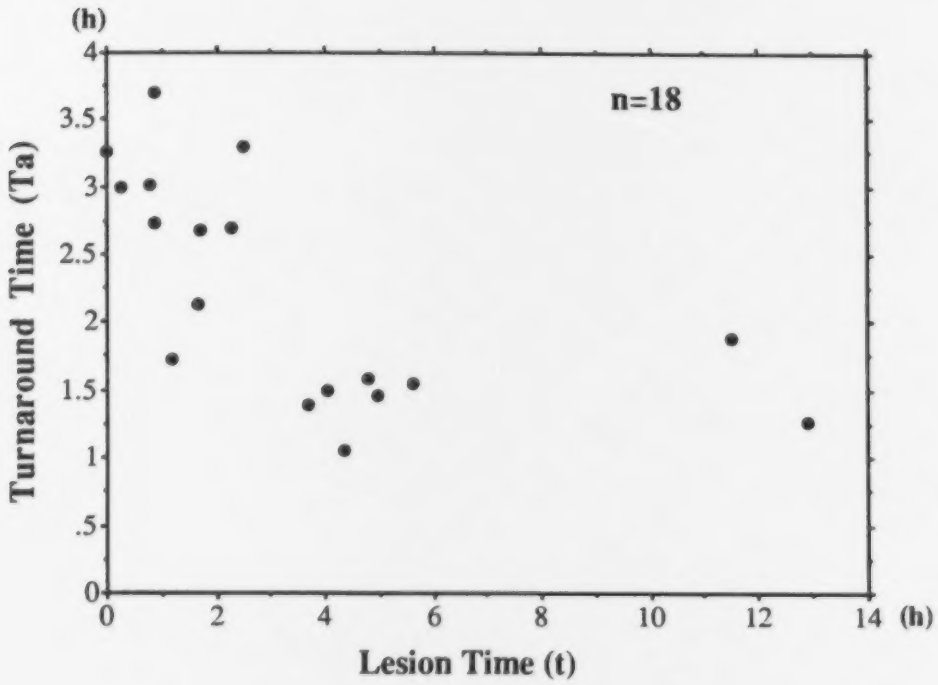

Table 5. Mean ± SEM of the Turnaround Time (Ta)

Lesion Time t (h)	Ta (h)	n	P	Combined Value
$t \leq 1$	3.14 ± 0.16	5		
$1 < t \leq 2$	2.18 ± 0.28	3		
$2 < t \leq 3$	2.39 ± 0.12	2		
$3 < t \leq 6$	1.43 ± 0.08	6	} n.s.*	1.46 ± 0.08
$t \geq 6$	1.58 ± 0.31	2		

* n.s., not significant based on two-tailed Student's t-test at $\alpha = 0.05$ level of significance.

corresponding nerve preparation. Turnaround times varied among preparations from 1 h to 3 h. Turnaround time had the maximum value of about 3 h when $t < 1$ h (refer to Table 5), which is to be compared with that of organelle turnaround (see below). When t was longer, Ta decreased correspondingly and reached an equilibrium value of 1.46 ± 0.08 h (mean ± SEM) when $t > 3$ h, which is similar to that (1.49 ± 0.15 h) of previous studies under similar experimental conditions (Snyder, 1986a).

The difference in turnaround time among preparations with different lesion times might be explained as that the local condition for turnaround requires a certain period of time to develop after the lesion was placed. Another explanation for the difference in turnaround time is that the turnaround site progressed proximally from the lesion site with time due to degenerative changes along the axon and to the diffusion of extracellular molecules. Therefore, in the case of a longer lesion time, the turnaround site would be correspondingly more proximal from the ligature. Thus, the actual turnaround time at this more proximal turnaround site would be greater than the turnaround time calculated at the ligature, the additional time period equal to that required for the radiolabel to travel the distance from the more proximal actual turnaround site to the distal ligature and back to the turnaround site (this point will be expanded upon in Chapter 5).

4.1.2 Protein Transport in KG Solution

Six nerves were studied using the same method but with KG solution instead of NR solution as the bathing medium after the distal lesion was created. Counts-vs-time plots from nerve preparations bathed in KG solution showed qualitatively similar anterograde transport of the pulse of radiolabeled protein and subsequent accumulation of the radioactivity at the distal ligature. Comparison

of the transport rates of the anterograde pulse to the results from preparations using NR solution as the bathing medium revealed no significant differences (Table 6).

However, only three out of the six nerves with KG solution as the bathing medium exhibited a detectable retrograde pulse. Moreover, of the three nerves bathed in KG solution which exhibited a recognizable retrograde pulse of radiolabel, the amplitude of the retrograde pulse was very small. The average r/a ratio from the fifth to seventh segments proximal to the ligature was found to be 0.030 ± 0.006 ($\pm$ SEM) which is below the minimum value of the range of r/a ratio for nerves bathed in NR solution ($P < 0.01$, Table 6). It is thus concluded that the protein turnaround at a lesion in nerves bathed in KG solution was significantly reduced compared to that in nerves bathed in NR solution. Retrograde transport rates and the turnaround time were estimated for only one of the nerves bathed in KG solution due to the limited amplitude of the retrograde pulse. The retrograde transport rates were within the range of respective parameters for nerves bathed in NR; the turnaround time was 1.74 h (lesion time = 4.42 h).

4.2. Transport Reversal of Organelles at a Lesion

4.2.1 Organelle Transport in the Vicinity of a Lesion in KG Solution

4.2.1.1 General Observations

Thirty-seven axons were examined from 11 preparations using KG solution as the bathing medium after a lesion was made. Axons were able to be viewed with video microscopy as soon as 10 minutes after an axonal lesion was produced. The axonal lesion was recognized as a region 25-50 μm in width that

Table 6. Comparison of Protein Transport Parameters between Nerves Bathed in NR or KG solution

Parameter[a]	KG group[b] (n = 6)	NR group[c] (n = 21)	P
Transport Rates (mm/d)			
0.1AF	176.1 ± 9.0	182.4 ± 2.8	n.s.[d]
0.25AF	170.6 ± 8.0	178.4 ± 2.9	n.s.
AP	172.4 ± 3.6	174.1 ± 3.0	n.s.
0.25AS	159.2 ± 5.0	161.5 ± 2.3	n.s.
0.1AS	150.7 ± 7.0	158.6 ± 3.0	n.s.
r/a	0.030 ± 0.006[e]	0.093 ± 0.008[f]	0.008
range (min–max)	0.020 – 0.039	0.045 – 0.176	

[a] See text for the definitions for the parameters.

[b] KG group: nerves bathed in potassium glutamate solution.

[c] NR group: nerves bathed in normal Ringer solution. Values (except r/a ratio) are the average of both groups which showed and did not show retrograde pulse.

[d] n.s., not significant based on two-tailed Student's t-test at $\alpha = 0.05$ level of significance.

[e] n = 3

[f] n = 18

was structurally discontinuous; the axon contained liquefied axoplasm and intracellular debris. No organelles were observed moving across this area. Sometimes, the two ends of the axon were apparently separated. Next to the edge of the damaged area the axon was crowded with accumulated organelles for up to 50 μm, accumulation increasing with time. In the vicinity of the lesion, as close as 50 μm adjacent to the edge of the lesion, the axon showed structural continuity. Active bidirectional organelle transport continued up to the end of the intact axis cylinder close to the lesion area.

4.2.1.2 Transport Rates

The transport velocity of organelles was measured from the images of preparations in which no close axonal lesion was made. Organelles were divided into two groups according to their apparent diameter: > 0.2 μm or ≤ 0.2 μm. The results are presented in Table 7. It is noticeable that the transport rates of organelles of the same size moving in both directions are similar. The difference in velocity is related to the size of the organelles, not to their transport direction. Large organelles have a velocity of about 1.5 μm/s, approximately 70% of that (2 μm/s) of the small sized organelles. These rates are similar to protein transport rates.

4.2.1.3 Reversal of Organelle Transport

Since the axonal lesion had cut off the flow of transported organelles through the lesion area, the majority of the normally retrogradely moving organelles originating distal to the lesion would have vacated the region 200 μm proximal to the lesion within 5 minutes after the lesion was made according to the known organelle transport rates (refer to Table 7). [The minimum transport rate of the small retrograde organelles is $>$ 250 μm/5 min. Since the mean ($\pm$ SD)

Table 7. Mean ± SEM of Organelle Transport Rates (Temperature = 23-24°C)

	Transport Rates (μm/s)		
Organelle Size	Anterograde	Retrograde	P
Small (≅ 0.2 μm)	2.11 ± 0.08 (n = 89) (or 182 mm/day) (range 0.57–4.11)	2.13 ± 0.14 (n = 50) (or 184 mm/day) (range 0.87–6.25)	n.s.*
Large (≥ 0.2 μm)	1.50 ± 0.15 (n = 27) (or 130 mm/day) (range 0.49–3.45)	1.42 ± 0.07 (n = 111) (or 123 mm/day) (range 0.19–4.05)	n.s.
P	< 0.002	< 0.001	

* n.s., not significant based on two-tailed Student's t-test at $\alpha = 0.05$ level of significance.

retrograde transport rate of the large organelles is 1.42 ± 0.75 μm/s, which is slower than that of the small organelles, 84% of the large organelles had a transport velocity of ≥ 200 μm/5 min (mean - 1 SD). In addition, the large organelles consisted of < 50% of the retrograde organelle population (Smith and Snyder, 1991). Therefore, more than 90% of the retrograde organelles would have departed from the region 200 μm proximal to a lesion within 5 min.] Even the slowest moving organelles (0.19 μm/s, the slowest value of retrograde transport rates, see Table 7) originating distal to the lesion would have vacated this area in less than 20 minutes. But, when the axons were observed about 200 μm proximal to the lesion 7-30 min after the lesion was created, retrogradely moving organelles were observed. Thus, the organelles observed moving away from the lesion were thought to have originated from the lesion area, either from the anterogradely moving organelles that turned around upon encountering the lesion or from newly recruited organelles at the lesion. This result is consistent with that reported by Viancour (1990) from studies on organelle flux in distal segments of severed crayfish giant axons, in which the author reported a slower than expected decrease in organelle flux after transection. Similarly, the delayed decline of organelle flux was explained by the author as possibly a result of transport reversal of organelles and/or recruitment of new organelles to the transport system.

Evidence that supports the turnaround of organelles is that occasionally organelles were viewed directly under the microscope to change transport direction in the vicinity of the lesion. This is consistent with a previous report by Smith (1988) in which the author traced the movement of organelles and observed organelles change direction of movement in the vicinity of an axonal lesion. Furthermore, the reversal hypothesis is supported by the notion that retrogradely moving organelles originating from the lesion area are similar in size

to anterograde organelles, while the retrogradely moving organelles from normal nerve terminals are composed of a larger percentage of large organelles (Smith, 1987, 1988; Smith and Snyder, 1991). If the retrogradely moving organelles are reversed anterograde organelles, then the retrograde organelle flux will depend on the arrival of anterograde organelles at the site of the lesion. On the other hand, if the retrogradely moving organelles are newly recruited organelles, then the retrograde organelle flux may be independent of the supply of anterograde organelles but dependent on the injury itself since the formation of new organelles by an endocytotic process at the injured nerve ending or from damaged intracellular structures at the lesion area is probably triggered by the injury.

To test the two possibilities, a second lesion was applied 300-500 μm proximal to the first on three individual axons to deprive the first lesion of a continuous supply of anterogradely moving organelles. Figure 10a illustrates the two lesions which create two longer (about 25 mm) segments and a shorter (300-500 μm) center segment in an individual axon. According to the known organelle transport rates (refer to Table 7), more than 90% of the organelles normally moving in the axon would be cleared from the central segment 10-15 min after lesioning, while in the two longer segments organelles would continue to flow towards the lesions for about 4 hours based on an average organelle transport rate of 6.4 mm/h.

Under the microscope the damage or alteration of the axon due to the lesions was seen to be confined to a very small area close to the lesions. Normal intracellular structures and moving organelles were viewed up to 25-50 μm of a lesion. In the middle of the isolated segment of axon between the two lesions, intracellular structure was normal. Organelle traffic in both directions was measured over a period of about 1.5 hour at locations of about 200 μm proximal

Figure 10.

a. Schematic Representation of the Double Lesions on a Single Axon

In the shorter central axonal segment the two lesions will deprive each other of incoming organelles within 10-15 min post-lesioning. In the longer proximal and distal segments organelle supply towards the lesions will not be exhausted for a relatively long time (about 4 h based on the combined mean organelle transport rate of 6.4 mm/h). Organelle flux in both directions was measured at locations P, C and D during a period of about 1.5 h post lesioning.

b. The Results of Organelle Flux in the Three Locations Plotted Against Lesion Time (t)

Figure 10a

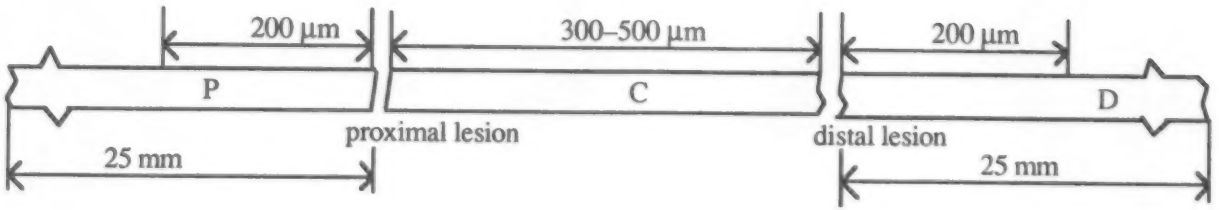

Figure 10b.

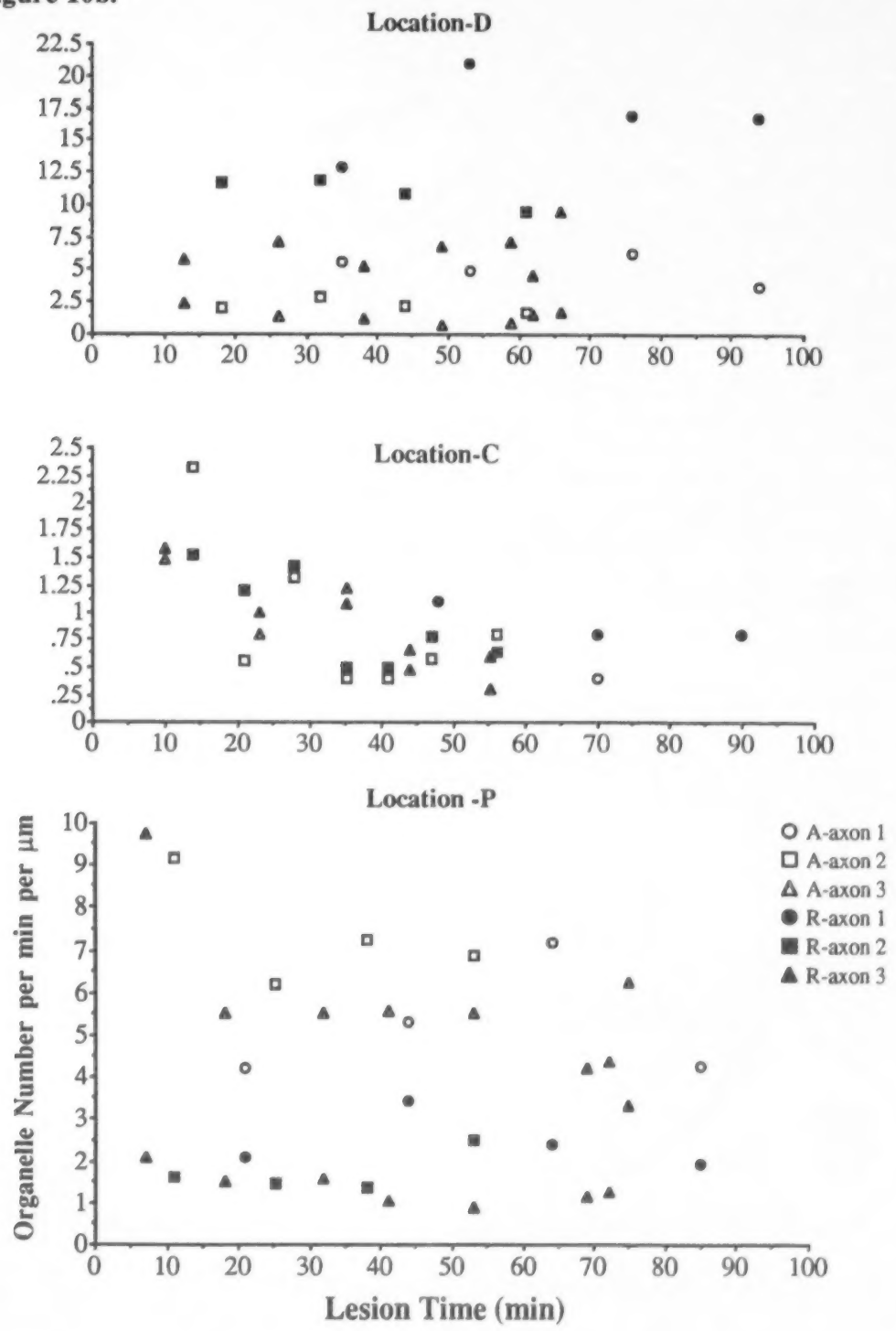
Location-D
Location-C
Location -P
Organelle Number per min per µm
Lesion Time (min)
A-axon 1
A-axon 2
A-axon 3
R-axon 1
R-axon 2
R-axon 3

to the proximal lesion (location P), at the center of the segment between the two lesions (location C), and 200 μm distal to the distal lesion (location D). Figure 10b plots the organelle flux at the three locations from the three axons against the lesion time. Results from the three axons studied showed similar patterns of organelle behavior. In the region between the two lesions (location C) organelle traffic in both directions was decreased dramatically 10 min after lesioning compared to traffic at the other two locations. Organelle flux continued to decline with time to a relatively stable level 40 min after lesioning, with an average (± SEM) anterograde organelle flux of 0.63 ± 0.09 per min per μm and retrograde organelle flux of 0.71 ± 0.07 per min per μm (Table 8). The lowered organelle flux continued even 90 minutes after lesioning, suggesting that this relatively short segment of axon was alive and reserved the capacity to sustain transport. On the other hand, organelle fluxes at the other two locations which were not deprived of organelles moving towards the lesions were relatively constant throughout the 1.5 h experimental time. Therefore, average organelle fluxes in the longer segments were calculated from all the data points obtained during the 1.5 h post-lesioning. One-tailed Student's t-test shows that the average traffic densities of organelles moving in both directions in the central segment 40 min post-lesion were reduced to 20-40% of the mean organelle flux in the respective directions away from the lesion in the proximal segment (location P) and the distal segment (location D) (Table 8). This result proved that a significant number of organelles did not move across the lesion area. The decrease in organelles moving in the central segment is likely due to the shortage of supply of organelles caused by the second lesion and not to the loss of transport ability. The result was explained as that the proximal lesion prevented the delivery of anterograde organelles to the distal lesion which resulted in a dramatic decrease in transport reversal and subsequent decrease in organelle

Table 8. Mean ± SEM of Organelle Flux in the Vicinities of the Double Lesions*

	Organelle Number per min per μm				
Transport Direction	Location-P	$P_{P\text{-}C}$**	Location-C	$P_{C\text{-}D}$**	Location-D
Anterograde (A)	6.08 ± 0.41	< 0.0001	0.63 ± 0.09	< 0.0025	2.59 ± 0.45
Retrograde (R)	1.85 ± 0.19	< 0.0002	0.71 ± 0.07	< 0.0001	10.47 ± 1.24
n	16		8		15

* Data was obtained from three axons shown in Figure 10b. Value is the average of all data points at location P and D, and data points 40 minutes after lesioning at location C.

** Probability of unpaired, one-tailed Student's t-test of organelle fluxes between locations P and C ($P_{P\text{-}C}$), and between locations C and D ($P_{C\text{-}D}$) shown in Figure 10.

traffic moving away from the distal lesion. The dependence of organelles moving away from a lesion on the arrival of organelles moving towards the lesion supports the concept of organelle reversal.

4.2.1.4 Reversal Dynamics and Quantity

The reversal of anterograde organelles proximal to the lesion was evaluated as the ratio of the organelle traffic moving away from the lesion to that moving towards it. Anterograde traffic and retrograde (reversed anterograde) traffic were obtained from the same axonal segment at a location about 200 μm proximal to the lesion from 37 axons from 11 nerves bathed in KG solution. Data from each axon was collected as soon as possible, 10-30 minutes after the lesion was produced, and continued for up to 2 hours. Figure 11 is the plot of organelle flux against lesion time of 5 axons from one nerve preparation and shows the pattern of organelle transport within that period of time. Ten to thirty minutes after the lesion, active bidirectional transport was viewed. Organelle flux moving away from the lesion reached a near equilibrium level 10 minutes after the lesion. No significant correlation was found between the organelle flux and the time within the first 2 h after the lesion was created. Therefore, the reversal ratio was calculated from all the data points obtained during the 2 hours.

Figure 12 plots the retrograde organelle flux (R_{KG}) against the anterograde flux (A_{KG}). It shows that the retrograde flux is correlated with the anterograde organelle flux. A least-squares fit yielded a straight line $R_{KG} = 0.56 + 0.25A_{KG}$ ($n = 78$, $r = 0.66$, $P < 0.001$). The result suggests that retrograde organelle flux is dependent upon the arrival of anterograde organelles at the lesion, possibly because the transport reversal of organelles moving towards the lesion is the major source of organelles moving away from the lesion. The intercept of the fitted line represents the portion of organelle flux moving away from the lesion

Figure 11. Organelle flux versus Lesion Time Plot of Five Axons from One Nerve Bathed in KG Solution.

Each point represents the number of organelles per min per μm of axon segment at various times after the axonal lesion was created. A represents organelle flux in the anterograde direction and R the retrograde direction. No significant correlation was found between the organelle fluxes and the time post-lesioning.

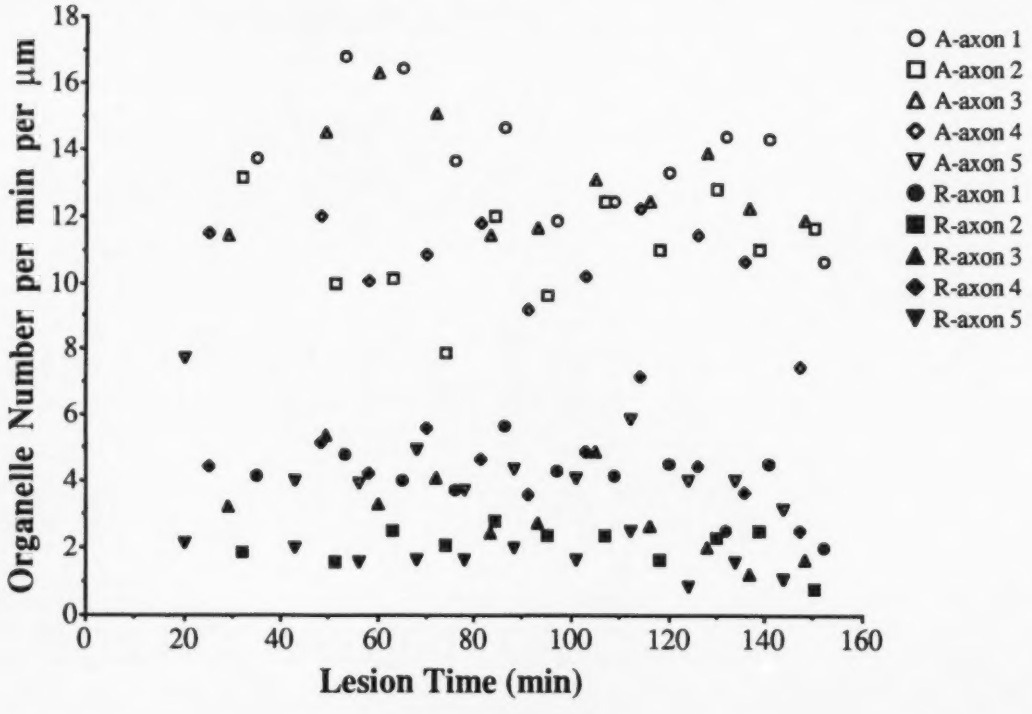

Figure 12. Retrograde Organelle Flux versus Anterograde Organelle Flux for Axons Bathed in KG Solution

The data were obtained at locations about 200 μm from a lesion in 37 axons from 11 nerves bathed in KG solution. Where R_{KG} represents the retrograde organelle flux and A_{KG} the anterograde organelle flux. A least-squares fit yielded the straight line $R_{KG} = 0.56 + 0.25A_{KG}$ (the standard deviation of the intercept is ±0.31 per min per μm and ±0.03 of the slope, n = 78).

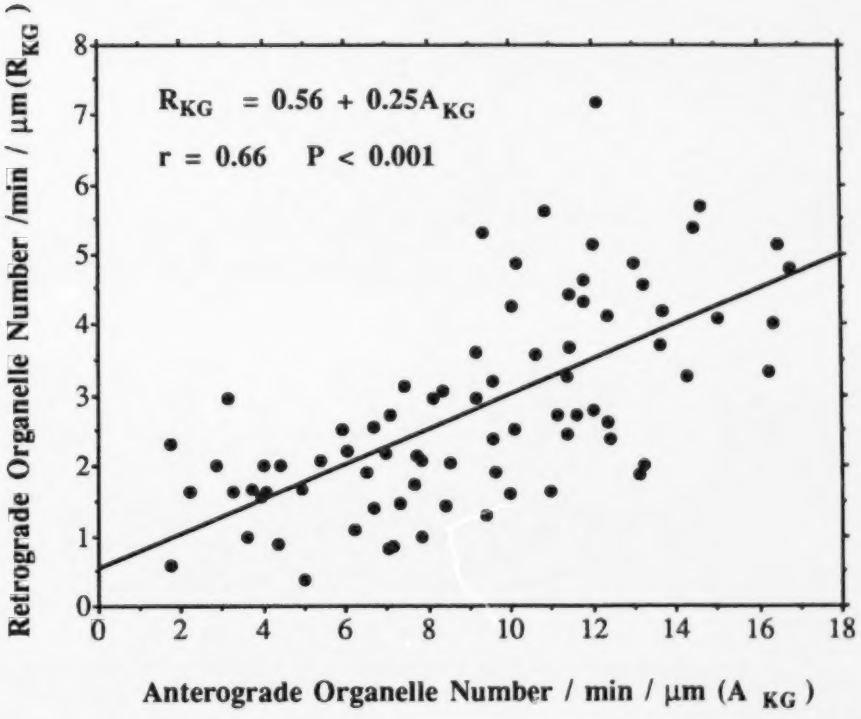

that is independent of the organelles moving towards the lesion. Recruitment of new organelles at the lesion area was considered as a possible source of this portion of retrograde organelles. This result is consistent with that of the double lesion experiment. A two-tailed Student's t-test showed that the retrograde organelle flux (0.56 ± 0.31 per min per μm [± SD]) at the intercept of the fitted line is not different from the value of organelle flux (mean ± SEM, 0.71 ± 0.07 per min per μm) obtained in the central segment of double lesioned axons ($P > 0.05$). It was therefore concluded that about 25% of the anterogradely transported organelles were able to reverse their transport direction in the vicinity of a lesion within < 10 minutes upon encountering the lesion. Recruitment of new organelles into the transport system might account for a small percentage of the organelle population moving away from the lesion.

4.2.2 Organelle Transport in the Vicinity of a Lesion in NR Solution

4.2.2.1 General Observations

Twenty-seven axons were examined from 11 nerves with NR solution as the bathing medium after lesioning. Like axons bathed in KG solution, the axonal myelin and axis cylinder were incomplete and discontinuous in the lesion area, usually over a length of 25-50 μm. Next to the lesion the axon underwent degenerative changes. The axon contained liquefied axoplasm and discontinuous fragments of intra-axonal structure. No moving organelles were observed in this region. The degenerative changes gradually became less severe further away from the lesion up to a region where the axon showed almost normal intra-axonal structure and organelles moving in both directions began to appear. The distance from the lesion to this region extended up to 1000 μm in some axons 30 minutes after the lesion was created and continued to progress

away from the lesion with time. The organelles moving away from the lesion were thought to be organelles whose transport direction had reversed, as discussed in organelle reversal in axons bathed in KG solution. If this were true, the reversal site must have progressed from the lesion to the edge of the degeneration region since beyond this region no moving organelles were observed.

The degenerative changes were possibly due to the membrane barrier being destroyed: ions whose intracellular and extracellular concentrations were normally regulated to produce a concentration gradient across the membrane could now diffuse down the concentration gradient, and might trigger functional and structural changes in an axon. If this is the case, the distance (d) that an ion could reach through diffusion from the edge of the lesion and cause subsequent degenerating change and dysfunction of organelle transport within the axon would follow the well known relationship (Carslaw, 1959; Crank, 1957; Smith, 1988):

$$d/t^{1/2} = b \qquad (4.1)$$

where t is the time after the lesion is created and b is a constant. The distance (d) from the lesion to the edge of degeneration was measured under the microscope at various times t (ranging 0.5-1.5 h) from the same axon. Figure 13 is the $d/t^{1/2}$ plot for two axons. The mean coefficient b estimated accordingly was 0.80 ± 0.43 mm/h$^{1/2}$ ($\pm$ SEM) (n = 7). Thus, in axons bathed in NR solution, the transport reversal site progressed away from a lesion 600 ± 300 µm in 30 min, and 800 ± 400 µm in 1 h after the lesion was created.

Figure 13. Correlation of Distance of Axon Degeneration from the Lesion to the Square Root of Time after Lesioning

Results from two axons to show the progress of degenerative change from an axonal lesion. Each data point represents the distance (d) from the edge of the lesion to the edge of the degenerative region plotted against the square root of the lesion time (t). The distance at lesion time zero was taken as zero.

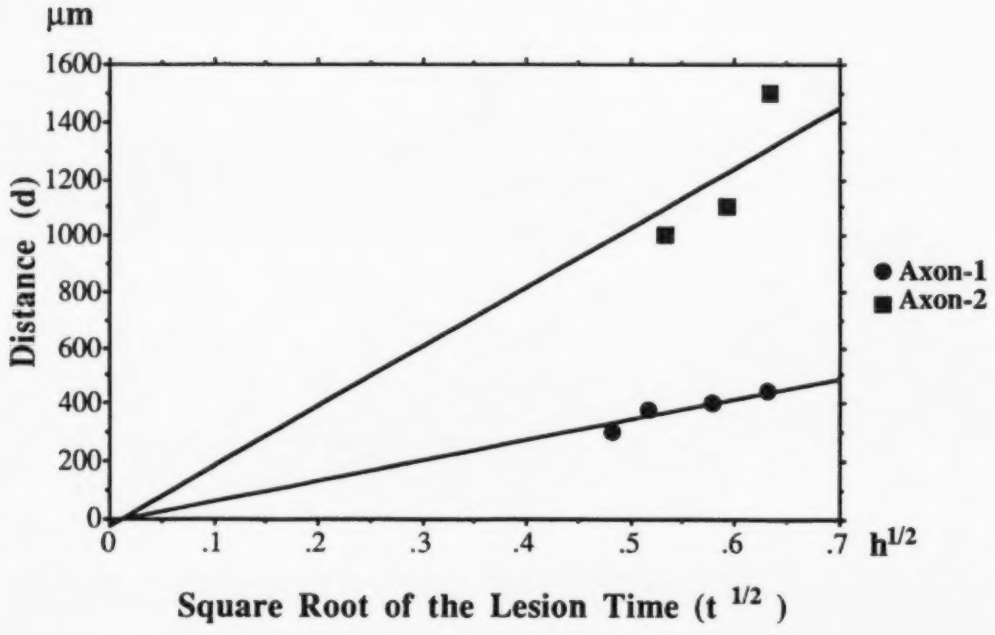

4.2.2.2 Reversal Dynamics

Due to the progressive degenerative change, organelle flux could not be measured at the same location for the same period of time as for axons bathed in KG solution. Data on organelle traffic were collected at locations where the degenerative change was less severe and the axon showed moving organelles within a period of 15-120 min after the axonal lesion was created. Figure 14 plots the retrograde organelle flux (R_{NR}) against the anterograde organelle flux (A_{NR}) obtained from 27 axons in 11 nerves bathed in NR solution. It shows that the retrograde organelle flux is correlated with that of the anterograde flux, similar to the result obtained from axons bathed in KG solution. A least-squares fit yielded a straight line: $R_{NR} = 0.86 + 0.24A_{NR}$ ($n = 49$, $r = 0.63$, $P < 0.001$). A comparison of the fitted linear regression model with that yielded from data obtained from axons bathed in KG solution shows the two models are statistically coincident, i.e., with parallel slopes ($P > 0.5$) and equal intercepts ($P > 0.2$). The combined slope is calculated as 0.25 and the intercept as 0.68/min/μm. Therefore, a similar conclusion was drawn on the same basis as that from the KG experiment. In summary, it was concluded that about 25% of anterogradely transported organelles in axons bathed in either KG or NR solution were able to reverse their transport direction in the vicinity of a lesion in less than 10-15 minutes. A small number of new organelles 0.68/min/μm might be recruited into the transport system at the lesion site during a short period (about 2 h) after lesioning.

Figure 14. Retrograde organelle flux versus anterograde organelle flux for Axons Bathed in NR Solution

The data were obtained from 27 axons of 11 nerves bathed in NR solution. R_{NR} represents the retrograde organelle flux and A_{NR} the anterograde organelle flux. A least-squares fit yielded the straight line $R_{NR} = 0.86 + 0.24A_{NR}$ (standard deviation of the intercept is ±0.24 per min per µm and ±0.04 of the slope, n = 49).

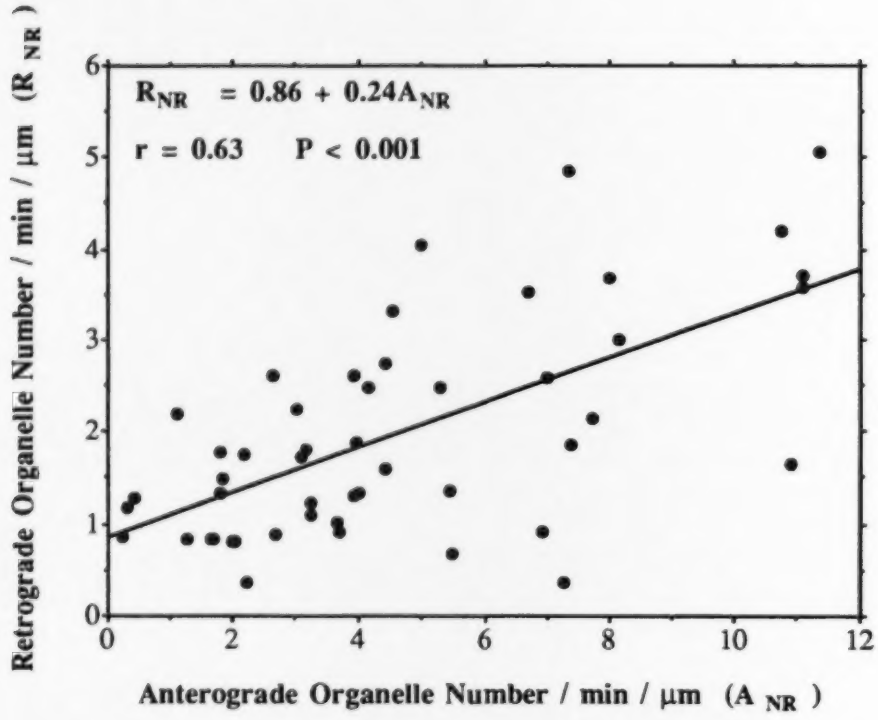

5. DISCUSSION

In this work, studies of the turnaround at a neuronal lesion of both axonally transported organelles and newly synthesized protein were conducted under similar experimental conditions on the same nerve from the same animal species. In this chapter, (1) the reversal dynamics of protein and of organelles are examined separately, (2) a comparison of the reversal dynamics and of the transport kinematics is made between protein and organelles and (3) the possible relationship between protein and organelles implied by their reversal and transport characteristics is discussed.

5.1 Protein Reversal Dynamics Proximal to a Lesion

5.1.1 Protein Requires > 1.5 h to Turn Around at a Lesion

The turnaround time of protein is defined here as the time required for material to reverse its transport direction following arrival at a lesion. It is estimated as the time period between the first arrival and the first departure of material from a lesion. Protein turnaround time was measured from preparations bathed in NR solution. The results show that there is a correlation between the protein turnaround time (Ta) and the time period (t) between the creation of the lesion and the arrival of the radiolabeled protein at the lesion. The Ta reached a maximum value of 3.14 ± 0.08 h (mean ± SEM) when $t < 1$ h, and gradually decreased as t became greater, eventually reaching a minimum equilibrium level of 1.46 ± 0.08 h (mean ± SEM) when $t > 3$ h, the equilibrium level being in agreement with the result from similar experiments ($t \approx 6$ h) reported by Snyder (1986a). One explanation for the difference in protein turnaround time among

the preparations with various t is considered to be that the protein reversal mechanism, which may not be present in intact axons (Schmidt, 1980), developed gradually after the lesion was created. Bisby and Bulger (1977) reported in their study on protein turnaround using rat sciatic nerve that injured axons require 0 ? h to develop the ability to reverse protein axonal transport and that it requires 1.9–2.4 h for protein to turn around.

Another explanation for the decrease in turnaround time with increasing t is that the turnaround site progressed proximally from the edge of the lesion with time after lesioning due to degenerative changes within the axon adjacent to the lesion. Degeneration was observed directly under the microscope in preparations bathed in NR. The distance (d) that the degenerative change extended from the lesion was proportional to the square root of time after lesioning [$d = bt^{1/2}$, $b = 0.80 \pm 0.43$ mm/$h^{1/2}$ (mean ± SEM)]. Thus, the actual turnaround site of organelles progressed proximally at the same rate or greater than the edge of the degenerated region where the axon structure was normal and the capacity for bidirectional transport was preserved. As t increased, the protein turnaround site would be increasingly more proximal to the ligature. Thus, the measured protein turnaround time (Ta) calculated at the distal ligature would be less than the true turnaround time (T) at this more proximal turnaround site (Figure 15) with

$$Ta = T - d(1/0.1AF + 1/0.1RF) \qquad (5.1)$$

where 0.1AF (0.1RF) is the transport rate of the fastest portion of the anterograde (retrograde) pulse, and, as above, d is the distance between the turnaround site at the edge of the degenerating region and the distal ligature which is presumed to follow $d = bt^{1/2}$. Thus, equation (5.1) can be expressed as:

Figure 15. Difference of the Protein Turnaround Time (T) Derived at the Actual Turnaround Site from that (Ta) Estimated at the Distal Ligature
Transport rate plot used to show the turnaround times calculated at the distal ligature (Ta) and at the actual turnaround site (T) presumed to have progressed away from the distal ligature due to degenerative change in nerves bathed in NR solution. The counts-vs-time plots for this particular preparation are shown in Figure 4. Proximal ligature was at 0 mm, distal ligature at 57.2 mm. Lesion time was 12.9 h prior to the first arrival of the anterograde pulse at the distal ligature. d denotes the distance between the edge of the degeneration region and the distal ligature. 0.1AF represents the transport rate of the fastest portion of the anterograde pulse and 0.1RF that of the retrograde pulse.

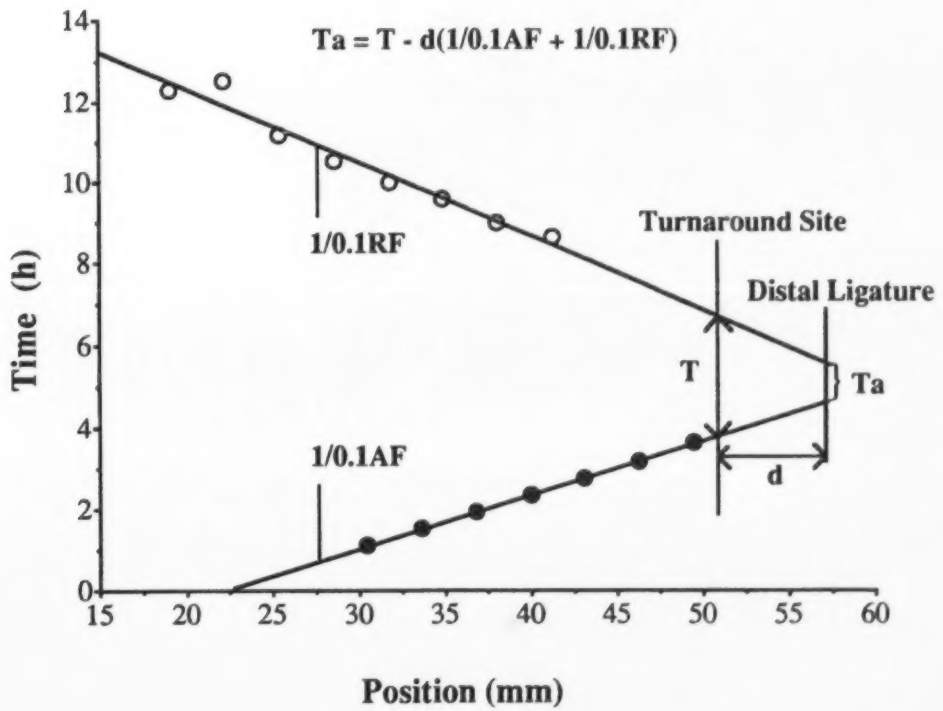

$$Ta = T - b(1/0.1AF + 1/0.1RF)t^{1/2} \quad (5.2)$$

If this is true, then plotting Ta against $t^{1/2}$ will result in a straight line. Figure 16 shows this could be the case. A least-squares fit yielded T = 3.28 ± 0.29 h (± SD) and b(1/0.1AF + 1/0.1RF) = 0.64 ± 0.16 $h^{1/2}$ (± SD). Using measured values of 0.1AF (182 mm/d) and 0.1RF (159 mm/d) resulted in b = 2.3 ± 0.41 mm/$h^{1/2}$ (± SD), somewhat larger than the value of 0.80 ± 0.43 mm/$h^{1/2}$ (± SEM) estimated from optical data. On this basis, the results suggest that it requires at least 1.5 h, probably about 3 hours, for protein to turn around when encountering a neuronal lesion.

However, it could be argued that some proteins that arrive at the lesion area of the nerve can turn around instantly. The 3-h delay of the initiation of retrograde transport of the label could be explained as due to uneven turnaround of different fractions of the proteins. The mean width of the radiolabeled pulse estimated at the proximal ligature was found to be 18.1 mm at 10% of the peak amplitudes. The arrival of the tail (0.1AS) of the pulse at the lesion was estimated to be 3.17 ± 0.11 h (± SEM) (n = 18) later than that of the front (0.1AF). If the turnaround of the first proteins to arrive had been delayed or did not occur at all, and the last proteins to arrive had been first to turn around, it would result in about a 3-h delay of the origin of retrograde transport of the label. In fact, the time interval between the arrival of the slowest portion (0.1AS) of the anterograde pulse and the initiation (0.1RF) of the retrograde pulse at the turnaround site away from the ligature was estimated as to be close to zero [mean ± SD, 0.08 ± 0.42 h]. This concept is appealing since the fastest retrograde transport rate (159 mm/day) of the label that turned around at the lesion is similar to the slowest rate (159 mm/day) of the anterograde transport of the label. But, if

Figure 16. Protein Turnaround Time versus Square Root of Lesion Time
The apparent turnaround time (Ta) was derived from transport rate plots at the distal ligature. A least-squares fit yielded a straight line: $Ta = T - b(1/0.1AF + 1/0.1RF)t^{1/2}$, where $T = 3.28 \pm 0.29$ h (± SD) is an estimate of the true turnaround time and $b(1/0.1AF + 1/0.1RF) = 0.64 \pm 0.16$ $h^{1/2}$ (± SD).

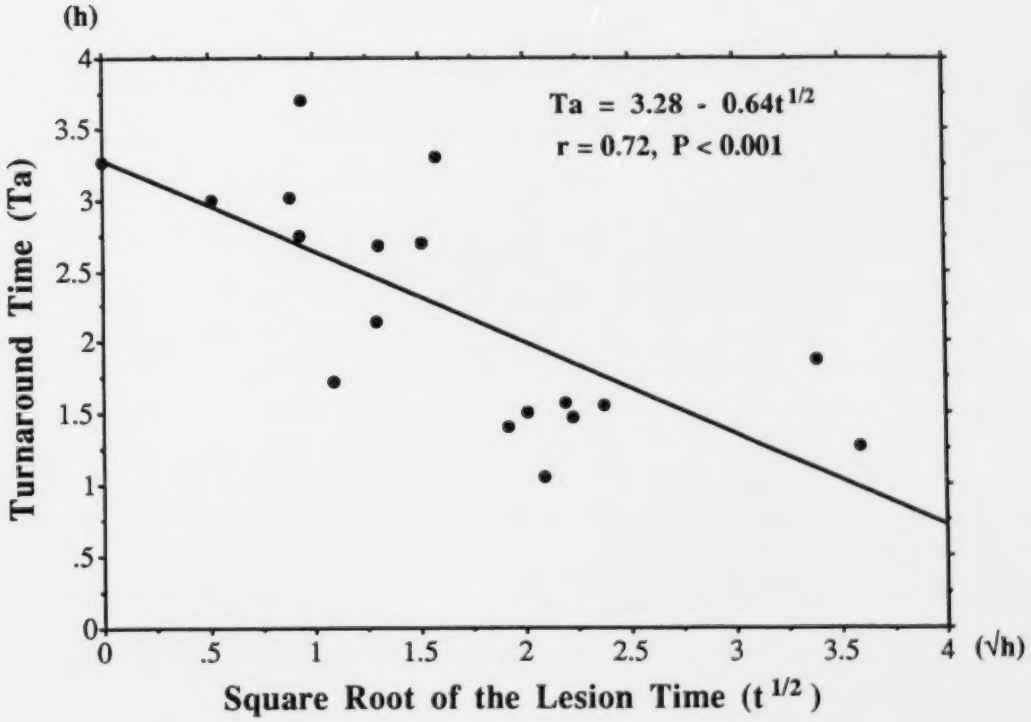

this were the case, the amount of labeled proteins that turned around at the lesion instantly would be < 10% of the amount of the anterograde pulse. Moreover, although the present result shows that proteins that turned around resulted in a retrograde pulse of about 10% of the peak amplitude of the anterograde pulse, the retrograde pulse had a relatively broad tail. The r/a ratio (0.093 ± 0.008), calculated as a reference of transport reversal, underestimates the true relative amount of reversal of the labeled protein since the width of the retrograde pulse was not taken into account. Snyder (1989) reported that about 25% of the anterogradely transported proteins turned around at the lesion within 3 h following arrival of the anterograde pulse at the lesion. Thus, at least 60% of the protein in the retrograde pulse originated from the faster portion of the anterograde pulse which arrived at the turnaround site before the departure of the retrograde pulse. In addition, the estimated departure time of the peak of the retrograde pulse from the turnaround site was 2.84 ± 0.50 h (SD) after the arrival of the slowest portion of the anterograde pulse at the distal ligature, again suggesting that the turnaround of more than 50% of the labeled protein in the retrograde pulse was delayed. Furthermore, this portion of the labeled protein would transport retrogradely with a rate slower than its anterograde transport rate. Thus, it was concluded that proteins, or at least some of them, require a longer time than organelles to reverse transport direction at a neuronal lesion. The retrograde transport of the protein with a slower rate than that of the anterograde transport of the label could then be explained as a change of the transport mechanism (e.g. different vector).

5.1.2 Reversal of Proteins is Reduced in Nerves Bathed in KG Solution Compared to that in NR Solution

The results described here show that with physiological saline (NR) as the bathing medium, a proportion of anterogradely transported radiolabeled protein reversed its transport direction proximal to a neuronal lesion. But, in potassium glutamate (KG) solution, which is compatible with intra-axonal function, the reversal of labeled protein and subsequent retrograde transport of the label completely failed in some cases or was significantly reduced compared to that in NR solution. Anterograde transport rates revealed no difference between preparations bathed in NR or KG solution, suggesting that the transport system was not affected by factors in the bathing medium. The result suggests that it is likely the protein-reversal process rather than the transport phase that is affected by the local environment induced by the neuronal lesion. Injury of the axon itself seems not to be the factor which causes the difference in turnaround of protein at the lesion between the preparations in different bathing media since the lesion was created in the same fashion in all the experimental preparations. The trigger factor thus could have been related to the ion composition of the two bathing solutions.

Turnaround of material at a nerve terminal is a feature of normal axonal transport (Schmidt, 1980). The phenomenon that protein turnaround occurs at both normal nerve terminals and axonal lesion ends bathed in physiological saline but not when bathed in KG solution suggests that protein turnaround at an axonal lesion may share a common mechanism with that at nerve terminals, and the operation of this mechanism may be triggered by a signal from the extra-axonal fluid. Among the extra-axonal ions that are present in NR and absent in KG, Ca^{2+} seems a logical candidate as a trigger. In intact axons, intracellular free Ca^{2+} concentration is regulated at a level of about 10^{-7} M, and its

extracellular concentration is kept relatively high at 1–2 mM. Ion fluxes driven by a single action potential through voltage-gated Ca^{2+} channels can significantly alter the Ca^{2+} concentration transiently in the axoplasm which triggers different cellular processes. However, Na^{+}, K^{+}, and Cl^{-} fluxes through their voltage-gated channels are of no use as a trigger because they are so small in relation to their intra-axonal concentration that they do not significantly alter the ion concentration inside the axon. Changes in intracellular Ca^{2+} levels by artificial injection of Ca^{2+} into the cytoplasm of axon terminals have been shown to trigger exocytosis and subsequent endocytosis, the latter a source of retrograde organelles, at nerve terminals during synaptic transmission (Katz, 1967; Smith and Augustine, 1988). In injured axons bathed in NR solution having a Ca^{2+} concentration of 3 mM, extra-axonal Ca^{2+} could diffuse freely into the axoplasm through the damaged region of axonal membrane. The increase in intra-axonal Ca^{2+} concentration might subsequently trigger the protein-reversal process. However, we can not reject the possible effects of other ions. But, the findings (Sahenk et al., 1988; Smith and Snyder, 1991) that leupeptin, a Ca^{2+}-activated protease inhibitor, prevented reversal of newly synthesized protein proximal to a neuronal lesion supports the possibility of Ca^{2+} involvement. The possibility that protein reversal involves a Ca^{2+}-dependent proteolysis is consistent with the results of Martz et al. (1989) who showed that during anterograde-to-retrograde transport reversal, proteins are reduced in molecular weight by a post-translational mechanism such as proteolysis.

5.2 Organelle Reversal Dynamics Proximal to a Lesion

5.2.1 Organelles Require < 10 min to Reverse Transport Direction at a Lesion.

It is not possible at present to label anterogradely transported organelles to monitor their reversal or other fate when they encounter an axonal lesion. Occasionally, individual organelles were seen to reverse direction, but in general evidence for organelle reversal was drawn from parameters of anterograde and retrograde transport of organelles in the vicinity of the lesion. The results reported here show that active organelle transport in both directions was observed at a location 200 μm proximal to the lesion (in KG solution 7-120 min after lesioning) or at the edge of the degeneration region (400-1100 μm proximal to the lesion in NR solution 15-120 min after lesioning). It is generally presumed that organelles that are present in an axonal segment at the time of lesioning will continue to move towards their respective destinations after lesioning. Therefore, retrograde organelles that originated distal to the lesion, even the slowest ones, are expected to vacate the region between the lesions and observation site 5-20 minutes after lesioning according to the known organelle transport rates. The axon at the lesion was seen to be structurally discontinuous, and no organelles were observed moving across this region. It is thus unlikely that organelles that originated distal to the lesion could move across this damaged area. Therefore, the retrograde organelles moving in the region proximal to the lesion are thought to have originated at the site of the lesion. This presumption is consistent with the observation of persistent organelle transport in isolated segments of crayfish axons (Viancour, 1990). Two possible sources of the retrograde organelles in the present study were considered: (1) transport reversal of anterograde organelles arriving in the proximal vicinity of the lesion and

(2) recruitment of new organelles formed at the site of lesion. The possibility of transport reversal was supported by the fact that organelles were occasionally viewed to change transport direction in the vicinity of the lesion, and by the result that the retrograde organelle flux (R) is correlated with that of anterograde (A), with a R/A ratio of 25%. A second lesion applied 300-500 μm proximal to the first to cut off the anterograde organelle flow towards the first lesion caused a sharp decrease in retrograde organelle traffic from the first lesion. Forty minutes post-lesioning, organelle flux in both directions in the region between the two lesions fell to a level of 20-40 % of the organelle flux on the other sides of the lesions. This result further evidences the dependence of the retrograde organelle flux upon the arriving anterograde organelles at the lesion. On the other hand, in the case of recruitment of new organelles which probably formed from some injury-induced endocytotic process or from damaged intracellular structures at the lesion area, a shortage of anterograde organelles towards the lesion would not be expected to affect the retrograde organelle flux. The sharp decline in organelle flux indicates that recruitment of new organelles, if it did occur, did not constitute a significant proportion of the organelle population moving away from the lesion. In addition, this result eliminated the possibility of organelles moving across the lesion area as a source of the retrograde organelles since the second lesion did not limit the supply of organelles that originated distal to the first lesion. Therefore, the retrogradely moving organelles proximal to the lesion shortly after lesioning, at least the majority of them, are likely to represent reversed anterograde organelles.

It is possible that the sharp decline in organelles moving in both directions in the short axonal segment between the two lesions is due to the loss of transport ability. However, the results show that the axonal segment survived morphologically during the experimental period of about 1.5 h. While the

organelle flux in both directions between the two lesions declined with time, they reached a stable level 40 minutes post-lesioning which, although significantly reduced, remained steady during the rest of the experimental period (about 1 h). This indicates that the short axonal segment between the two lesions sustained the ability to transport. Evidence that organelle transport can persist for reasonably long periods in transected axonal segments has been reported by other researchers (Matsumoto et al., 1981; Viancour, 1990). In the present study, the time dependence of the reduction in organelle flux suggests that the organelle decline could have been related to the gradual depletion of organelle supply. The persistence of organelle flux long after the exhaustion of the supply of organelles that entered the transport system before lesioning is similar to that of the proportion of retrograde organelle flux that is independent of the anterograde organelle flux obtained from the single lesion experiments. If no new organelles were recruited into the transport system, then the persistent organelle flux which is independent of the supply of the organelles from the transport system could mean that a small percentage of organelles can switch transport direction more than once upon encountering a lesion and continuously shuttle back and forth. On the other hand, it is possible that some newly formed organelles by some injury-induced mechanisms could continuously enter into the transport system. This is very likely because it probably serves a role in distribution of materials obtained from the local environment which is necessary for the long-term survival of the transected axonal segment. The results reported are in general consistent with studies on the long-term survival of distal segments (2-3 mm long) of severed giant axons of the crayfish in which persistent organelle flux remained for weeks (Viancour, 1990). Newly recruited vesicles were concluded to be a possible source of the organelles observed in the surviving axonal segments. Injury-induced endocytosis of tracer proteins placed extracellularly to severed

giant axons of crayfish could represent a mechanism for recruitment of material that forms transported vesicles (Meyer and Bittner, 1978; Viancour et al., 1988). Moreover, transected unmyelinated axons of frog optic nerve were reported to have survived and continued to take up exogenous tracer protein and transport it for two months postaxotomy (Matsumoto et al., 1981), suggesting the existence of some injury-induced endocytotic mechanisms. However, if new recruitment is a source of retrograde organelle flux observed proximal to the lesion in the present study, such a source would account for only a small percentage (< 20-40%) of the retrograde organelle population during the first two hours post-lesioning. Transport turnaround of organelles moving towards the lesions would be the major source of the organelles moving away from the lesions.

It was therefore concluded that about 25% of the anterogradely moving organelles were able to reverse their transport direction in less than 10-15 min upon encountering an axonal lesion. Newly recruited organelles at the site of the lesion may account for a small percentage of retrograde organelles proximal to the lesion.

5.3 Comparison of Transport Kinematics and Reversal Dynamics between Protein and Organelles

5.3.1 Association of Protein Translocation with Organelle Transport

Transport rates for different components of fast axonal transport such as proteins and membrane phospholipids have been intensively investigated (for a review see Grafstein and Forman, 1980). The finding that labeled phospholipids and rapidly transported proteins exhibit similarities in transport rates (Abe et al., 1973; Grafstein et al., 1975; Longo and Hammerschlag, 1980) has given rise to the proposal that rapidly transported proteins may be associated with membrane

components, possibly in the form of transport vesicles or organelles. The movement of particles inside living axons has been observed directly and the transport rate of organelles has been measured in various preparations (Allen et al., 1982; Cooper and Smith, 1974; Forman et al., 1977; Koles et al., 1982). However, a direct comparison of the transport rates of protein and organelles is difficult due to differences in animal species, type of nerve and experimental conditions in the various studies.

In this study, transport rates of rapidly transported, newly synthesized proteins and optically detectable organelles were estimated from the sciatic nerve of *Xenopus laevis* under similar experimental conditions. The rates are summarized in Table 9. The results show that coefficients of variation of organelle transport rates (35-50% for anterograde and retrograde) are larger than those of protein rates (< 10% for anterograde transport, 10-20% for retrograde transport). The difference in measurement scales for protein and organelle transport might account for the difference in the variation of transport rates. The variation of organelle transport rates measured on a micro-scale of μm/s represents an instantaneous value. Since the movement of an organelle is not uniform (Kendal et al., 1983), variation in transport rates measured on a large scale such as for protein might be averaged to a lower level. Other than this, the estimated values show that the maximum anterograde rates of protein and organelles are very close. But, the ranges of transport rates of organelles are wider than those of proteins. This might be explained as due to organelle transport rates being measured from all transported organelles, but that protein rates might represent only a fraction of the fastest transported, newly synthesized proteins measured from a relatively narrow pulse of metabolically radiolabeled proteins. In the present experimental protocol a narrow pulse of radiolabel was created by cutting off the cell body shortly after the label was exported into the axon. Thus, the

Table 9. Transport Rates (Mean ± SD) of Protein and Organelles in the Sciatic Nerve of Xenopus laevis

	Protein		Organelles	
Transport Rates	mm/d*	(μm/s)	(mm/d)	μm/s*
Anterograde Fast	182 ± 11.9	(2.11)	(180)	2.11 ± 0.76
Range		(1.83 – 2.37)		0.57 – 4.11
Anterograde Slow	159 ± 12.1	(1.84)	(129)	1.50 ± 0.76
Range		(1.59 – 2.38)		0.49 – 3.45
Retrograde Fast	159 ± 27.8	(1.84)	(184)	2.13 ± 0.98
Range		(0.97 – 2.66)		0.87 – 6.25
Retrograde Slow	<109 ± 11.5	(1.26)	(123)	1.42 ± 0.75
Range		(1.44 – 3.4)		0.19 – 4.05
Temperature	23°C		23–24°C	

Note:

* Unit is the measuring scale.

Source: refer to Table 3 and Table 7.

pulse contained only faster released label. Although there is no evidence that the slower released material is transported at rates different from those of the faster released material, this procedure does narrow the observation range of the label. The transport velocity of organelles measured on a micro-scale may not represent the translocation of organelles on a larger scale as that for protein because the movement of organelles may not be uniform. But, the results do indicate that protein-transport rates are within the capacity of organelle transport. This result adds a supportive line of evidence to the notion that translocation of proteins within the axons may be associated with organelle transport. This is supported by considerable evidence that both protein transport (Abe et al., 1973; Hanson and Edström, 1977) and organelle transport (Brady et al., 1982; Kendal et al., 1983; Hammond and Smith, 1977) are ATP-dependent and can be similarly inhibited by mitotic inhibitors, such as colchicine.

The maximum retrograde transport rate of protein was found to be slower than that of the anterograde rate of protein transport and slower than that of the retrograde rates of organelle transport. This could mean either that only the protein that was carried by slower organelles could reverse transport direction or that protein which turned around was transferred to slower organelles during transport reversal.

5.3.2 Dissociation of Protein and Organelle Reversal

Reversal of protein (Abe et al., 1974; Bisby and Bulger, 1977; Bray et al., 1971; Schmidt et al., 1980; Snyder, 1989) and organelles (Smith, 1987, 1988) at an axonal lesion have been reported earlier. The new contribution of this work is the finding that the reversal of protein and organelles display different characteristics. Rapidly transported, newly synthesized proteins and organelles

differ in reversal dynamics and react differently to the local environment to which they are exposed.

5.3.2.1 Protein Turnaround is Delayed Compared to Organelle Reversal

The retrograde transport of organelles (Cooper and Smith, 1974; Smith, 1980; Tsukita and Ishikawa, 1980) and labeled material (Armstrong et al., 1985; Bisby, 1987; Bisby and Bulger, 1977; Brimijoin and Helland, 1976) originally synthesized in the cell body and anterogradely transported to the nerve terminal, and presumably turned around at the nerve terminal, has been demonstrated by a numbers of researchers. Although the exact site of reversal of transport in intact axons is not clear, injured axons have been shown to develop an ability to reverse axonal transport at a local lesion (Abe et al., 1974; Bisby and Bulger, 1977; Bray et al., 1971; Partlow et al., 1972; Schmidt et al., 1980). Bisby and Bulger (1977) reported a time period of 0.8 h for an injured axon to develop the ability to reverse axonal transport, and a turnaround time for labeled proteins accumulated at a crush of 1.9–2.4 h. Other authors suggest a longer turnaround time of 30 hours or more for protein at a neuronal lesion (Schmidt et al., 1980). Armstrong et al. (1985) suggest a turnaround time at a nerve terminal for phospholipids ranging from 12 h to 2 weeks. But, results from Smith's studies (1987, 1988) show that organelles are able to reverse transport direction at a lesion within 10 minutes. These results display a large difference in reversal dynamics between transported molecules and organelles. But, it is not clear if the difference indicates a different course of reversal since comparative data of the reversal dynamics of proteins and organelles is not available. In this study, an attempt has been made to design comparable experimental conditions for estimating reversal kinematics of proteins and organelles from the same nerve of the same animal species.

The results reported here show that retrograde organelle flux proximal to a lesion resumes within less than 10 min after being stopped by lesioning, and is presumed to result from the reversal of arriving anterograde organelles at the lesion. But, the initiation of the retrograde transport of radiolabeled proteins requires at least 1.5 h, more likely about 3 h after the first arrival of the label at a neuronal lesion. This is concluded to mean that turnaround of proteins, at least more than 50% of them, is delayed by hours compared to that of organelles.

5.3.2.2 Different Reversal Characteristics between Proteins and Organelles

The results reported here show that the amount of protein turnaround in the vicinity of a lesion was reduced in nerves bathed in KG solution compared to that in NR solution. It was explained as a result of low Ca^{2+} concentration in the axoplasm which depressed the protein-reversal process. In contrast, the present results show that organelle reversal was not affected by the same factor(s) in the local environment that affected protein reversal. The results show that both solutions support bidirectional organelle transport, and there is no significant difference in the reversal ratio obtained from axons bathed in KG or in NR solution. The different behavior between protein and organelle reversal is interpreted to mean that the reversal of protein and organelles might be under different mechanisms. It may be that the turnaround of protein proximal to a neuronal lesion is a Ca^{2+}-dependent process, while that of organelles is not. This explanation is supported by the findings of Smith and Snyder (1991) that leupeptin prevents reversal of newly synthesized protein proximal to a neuronal lesion, but not the reversal of organelles.

5.4 Relationship of Rapidly Transported Organelles and Newly Synthesized Proteins

The results reported here suggest a dissociation of proteins and organelles when they reverse their transport direction upon encountering a neuronal lesion. Protein turnaround is delayed by hours compared to minutes for organelles. One possible explanation for the dissociation of proteins and organelles during transport reversal is that they are transported by separate mechanisms, whereas the correlation observed between them during axonal translocation might be pure coincidence. However, there is no evidence that separate mechanisms are responsible for rapid protein transport and organelle transport. On the contrary, considerable evidence discussed above indicates that newly synthesized proteins are transported in association with membranous organelles or vesicles. Together with other evidence, axonally transported proteins are thought to be prepackaged into organelles with different destinations in the Golgi apparatus and remain tightly bound to organelles throughout the life of the organelles (the so-called secretory model), as are those in non-neuronal secretory cells (Hammerschlag, 1983). In this model the transport and reversal dynamics of proteins would be coincident with those of organelles. If this is the case, the difference in turnaround time between proteins and organelles can be understood only if the presumptions are justifiable that labeled proteins are associated with only a subgroup of the organelles and that the reversal of this specific group of organelles is delayed from that of the other organelles which turn around immediately at the lesion. This seems possible because the results show that only 25% of the anterograde organelles arriving at the lesion area reverse their transport direction without delay. The presence of a heterogeneous population of transport organelles which deliver newly synthesized proteins to the axonal and terminal targets has been documented by Morin and co-workers (1991). In

their work, subcellular fractionation of rabbit optic nerve resolved two populations of rapidly transported membranous organelles. Both carried integral synaptic vesicle membrane protein and other proteins. Both were immunoreactive to the transport motor protein kinesin, indicating they are transported by the same mechanism. One population was found to be rapidly exported to the axon from the cell body and bound for the axolemma and nerve terminal. It was suggested by the authors that this group of organelles is coincident with the category of "constitutive" secretory vesicles using Kelly's (1985) terminology. The other population was slowly released to the axon and bound exclusively for the nerve terminal, and a candidate for the "regulated" secretory vesicles. In summary, the two populations of organelles differ from each other in the distribution of proteins, the kinetics of release from the cell body and probably the kinetics of secretion at the nerve terminal. They may differ in reversal dynamics as well. In our experiment a narrow pulse of label was created by removing the cell body shortly after radiolabel was exported into the axon. Thus, the majority of the labeled protein in the pulse may be associated with the fast-released subgroup of organelles. If the two subgroups of organelles are indeed characterized by different reversal dynamics, we may expect the fast-released population to have a longer turnaround time since the turnaround of more than 50% of the label in the retrograde pulse is likely delayed. Recent findings by Hässig et al. (1991) suggest that the molecular forms of AChE intended for functional nerve endings undergo a greater degree of transport reversal at a neuronal lesion than those destined for the axolemma. This was suggested to be the result of packaging in different organelles which may have different capacities to reverse transport direction. This argument implies a non-random process of organelle transport reversal.

The results of the protein-transport studies show that the retrograde transport rates of the labeled protein that turned around from the anterograde pulse are slower and have a greater dispersion than the anterograde rates. On the other hand, the transport rate of organelles is independent of the direction of transport but is inversely related to organelle size. The slower retrograde rate of protein transport compared to that of anterograde transport suggests that the population of organelles that carried the retrogradely moving pulse of radiolabel have a greater proportion of large organelles. If protein remains associated with organelles during transport reversal, then the altered protein transport rate after turning around in the vicinity of a lesion could be either a result of selective reversal of large organelles, or a result of a morphological change of smaller organelles into larger ones without dissociation of the protein that resides on them during transport (Sahenk and Lasek, 1988).

However, if protein molecules remain associated with their organelles during transport reversal, factors that alter protein reversal would similarly affect organelle reversal. But, the results of the leupeptin study by Smith and Snyder (1991) and the present KG study show that conditions that reduce or prevent protein reversal do not affect organelle reversal. These results suggest that rapidly transported proteins are separated from organelles during transport reversal. If this is the case, to undergo transport reversal off-loaded protein must up-load to other organelles that are themselves undergoing transport reversal. The delay of protein turnaround compared to that of organelles can then be explained as a result of dissociation of protein from arriving organelles and reassociation with other organelles at a later time in the vicinity of a lesion. The supposition of protein transfer between vectors during reversal provides a possible explanation for the result that the retrograde transport rate of proteins that turned around proximal to a neuronal lesion is slower and more dispersed

than that of anterograde transport. If this assumption is correct, the result that in KG solution with a relatively low Ca^{2+} concentration only protein but not organelle reversal was depressed suggests that the reassociation of proteins to organelles necessary for protein to return may be a Ca^{2+}-dependent process, probably protease involved (Smith and Snyder, 1991). This explanation supports a dynamic model of protein/organelle relationship (Smith et al., 1991; Snyder et al., 1990; Smith and Snyder, 1991) which suggests that protein molecules may off-load from and up-load to carrier organelles at some points within the axon.

The dissociation of proteins from carrier organelles was found to occur in processes other than transport reversal. Earlier work in this laboratory has shown that in sensory sciatic nerves of *Xenopus*, a fraction of newly synthesized, rapidly transported proteins is deposited to a stationary phase without a parallel loss of vesicles from the transport system or a reduction in size of the transport vesicles (Snyder et al., 1990). The result was interpreted to mean that proteins were released from their carrier vesicles. An independent study by Armstrong et al. (1987) has shown that glycoproteins are accumulated at the nodes of Ranvier and redistributed to the internodal region within a period of 7 days. The redistribution could be explained as a result of selective deposition of some of the transported labeled molecules released from transport organelles and their subsequent redistribution through some mechanisms slower than organelle transport, such as diffusion. A study on the axonal transport of proteins and organelles at the junction between parent axons and their growing daughter sprouts has shown that a large portion of rapidly transported proteins is deposited to a stationary phase in the daughter axons (Chan et al., 1989), while some organelles that failed to traverse the junctional region reversed their direction of transport. Therefore, the unloading of proteins from anterogradely moving membranous organelles was suggested by the authors.

On the other hand, there is evidence that protein may be loaded onto pre-existing membranous organelles. It has been shown that brefeldin A, an agent that disassembles Golgi apparatus, inhibits the export of labeled protein into the axon, but not that of optically detectable organelles (Smith et al., 1991). One possibility suggested by the authors is that the anterogradely transported organelles are formed from recycled retrograde organelles that are loaded with protein from a storage pool in the cell body.

If the argument of protein reassociation is tenable, there must be a post-translational mechanism, other than that used in the secretory model, responsible for attaching protein to and releasing protein from the membranous organelles. Experimental evidence suggests that a storage pool of rapidly transported protein exists in the neuronal cell body. However, it is not clear whether or not the proteins in the storage pool exist in association with transport organelles. Kinesin, a direct marker of rapid transport, was shown to be associated with rapidly transported membrane (Morin et al., 1991; Pfister et al., 1989); it is also distributed in a soluble pool in fibroblasts (Neighbors et al., 1988). In addition, routine isolation of kinesin from soluble brain extracts suggests a large soluble pool in the axon. Based on these observations, it was suggested (Morin et al., 1991) that there may be a post-translational mechanism for converting soluble kinesin to a membrane-associated form. There might also be a mechanism responsible for the release of kinesin from the transport organelle during transport reversal, allowing the organelle to bind cytoplasmic dynein, (which is believed to be responsible for the retrograde transport of organelles). About 15-25% of the fast axonally transported protein is soluble (McEwen and Grafstein, 1968; Sabri and Ochs, 1972). For example, tyrosine hydroxylase (TH), a soluble protein, and DβH, a membrane protein, are also found in both the soluble and the particulate subcellular fractions of rabbit sciatic nerve, and both undergo

rapid axonal transport (Brimijoin and Wiermaa, 1977b). This suggests that both of the enzymes may be transported partly in reversible association with organelles. If such a mechanism does exist, we may expect that proteins whose function is membrane associated may be stored in a soluble form in the cytosol. On the other hand, cargo proteins of axonal organelle transport may not be limited to those whose function requires them to be compartmentalized. Some cytosolic proteins may be transported through fast axonal transport by reversible association with membranous organelles. This offers a strategic advantage for protein transport in neurons to overcome the problem of efficient protein supply over the long distance from the site of protein synthesis to the site of protein use. Although oversupply of cytosolic proteins through slow axonal transport might be a strategy in neurons for sufficient supply of protein over such long distances, it might not meet the demand of the axon and terminal for proteins with short half-lives. Therefore, multiple pathways for material distribution through different pools by means of rapid axonal transport seems a logical solution in neurons. On the contrary, in non-neuronal cells, the short distance between the site of protein synthesis and that of the site of function poses no such demand for organelle transport of cytosolic protein because distribution through diffusion is sufficient.

This postulate is not necessarily contradictory to the secretory model of vesicular protein transport used in non-neuronal cell types because multiple pathways are likely to co-exist, just as constitutive and regulated pathways of exocytosis co-exist in neurons (Burgess and Kelly, 1987). This more dynamic pathway may be a modification of protein transport in adaptation to transport of proteins and other molecules over more extreme distances, and be compatible with its rapid responsive functions.

5.5 Conclusion

The primary aim of this work was to investigate reversal dynamics of rapidly transported organelles and newly synthesized proteins at a neuronal lesion with the intention to reveal some aspects of the protein/organelle relationship. Two methods were employed. Organelle transport was studied in single living axons with video-enhanced, differential interference contrast microscopy. Protein transport was studied using metabolic radiolabeling. Transport of the radiolabel in the nerve was detected using a position sensitive detector of ionizing radiation, the multiple proportional counter. Experimental conditions were approximated. Two bathing media, normal Ringer (NR) and potassium glutamate (KG) solutions, compatible, respectively, with extra-axonal fluid and intra-axonal function were used for both organelle and protein studies. The same nerve from the same species was used for both organelle and protein studies. Dynamic information on transport and transport reversal was obtained for both organelles and protein. A comparison of transport and reversal dynamics between organelles and protein allowed inferences to be drawn regarding their relationship.

This work shows that there is general consistency in transport kinematics between rapidly transported proteins and optically detectable organelles. It supports the hypothesis that proteins are transported in association with organelles. However, under similar conditions the reversal of proteins at a neuronal lesion is not parallel with that of organelles. Transport reversal of proteins, at least for some of them, is delayed by hours compared to that of organelles. In addition, nerves bathed in KG solution show a reduced protein reversal but not a similar reduction of organelle reversal. If rapidly transported proteins and membranous organelles reverse their transport direction at a lesion as an associated unit, then a presumption that there are two or more subclasses of organelles, distinct in reversal mechanism, must be made to explain the observed

reversal difference between proteins and organelles. On the other hand, the difference in transport reversal suggests that a dynamic relationship might exist between rapid axonally transported proteins and organelles. That is, protein may dissociate from carrier organelles and reassociate with membranous organelles during transport reversal. Neither model can explain all aspects of transport reversal and other phases of axonal transport of protein and organelles. Together with other findings, it is proposed that multiple forms of the protein/organelle relationship may co-exist in neurons.

The reversal mechanism of axonal transport remains far from understood. This work was not specifically designed to explore such mechanisms. However, the results do provide some suggestive information on this issue that leads the way for further studies. If a tightly bound relationship between protein and organelles is retained during transport reversal, selective transport reversal of different subclasses of organelles should be expected. If a dynamic relationship does exist, the reversal of organelles and proteins, at least for some of them, must be under different mechanisms. It is likely that some Ca^{2+}-dependent process is involved in protein turnaround, but not in organelle reversal. Local conditions of the axon may also play an important role in transport reversal. Unloading of cargo protein molecules might be a necessary step in organelle transport reversal.

REFERENCES

Abe T., Fink B. R. and Miauddaugh M. 1973. Rapid transport of phosphatidylcholine occurring simultaneously with protein transport in the frog sciatic nerve. *Biochem. J.* 136: 731-740.

Abe T., Haga T. and Kurokawa M. 1974. Retrograde axoplasmic transport: its continuation as anterograde transport. *FEBS Lett.* 47: 272-257.

Allen R. D. 1987. The microtubule as an intracellular engine. *Sci. Am.* 256: 42-49.

Allen R. D. and Allen N. S. 1983. Video-enhanced microscopy with a computer frame memory. *J. Microsc.* 129: 3-17.

Allen. R. D., David G. B. and Normarski G. 1969. The Zeiss-Nomarski differential interference equipment for transmitted light microscopy. *Z. wiss. Mikr. Mikrotech.* 69: 193.

Allen R. D., Allen N. S. and Travis J. L. 1981a. Video-enhanced differential interference contrast (AVEC-DIC) microscopy: A new method capable of analyzing microtubule-related movement in the reticulopodial network of Allogromia laticollaris. *Cell Motil.* 1: 291-302.

Allen R. D., Travis J. L., Aleen N. S. and Yilmaz H. 1981b. Video-enhanced Contrast Polarization (AVEC-POL) Microscopy: A New Method Applied to the detection of Birefringence in the Motile Reticulopodial Network of Allogromia laticollaris. *Cell Motil.* 1:275-289.

Allen R. D., Tasaki I., Brady S. T. and Gilgert S. 1982. Fast axonal transport in squid giant axon. *Science* 218: 1127-1128.

Allen R. D., Weiss D. G., Hayden J. H., Brown D. T., Fujiwake H. and Simpson M. 1985. Gliding movement of and bidirectional organelle transport along single native microtubules from squid axoplasm: Evidence for an active role of microtubules in cytoplasmic transport. *J. Cell Biol.* 100: 1736-1752.

Armstrong R., Toews A., Ray R. B. and Morell P. 1985. Retrograde axonal transport of endogenous phospholipids in cat sciatic nerve. *J. Neurosci.* 5: 965-969.

Armstrong R., Toews A. D. and Morell P. 1987. Axonal transport through nodes of ranvier. *Brain Res.* 412: 196-199.

Bargmann W. 1966. Neurosecretion. *Int. Rev. Cytol.* 19: 183-202.

Bennett G., Digiamgerardino L., Koenig H. L. and Droz B. 1973. Axonal migration of protein and glycoprotein to nerve endings. II. Radioautographic analysis of the renewal of glycoproteins in never endings of chicken ciliary gangling after intracerebral injection of [^{3}H]fucose and [^{3}H]glucosamine. *Brain Res.* 60: 129-146.

Berlinrood M., Mcgree-Russell M. and Allen R. D. 1972. Patterns of particle movements in nerve fibers *in vitro*. An analysis by photokymography and microscopy. *J. Cell. Sci.* 11: 875-886.

Berry R. W. 1980. Evidence for multiple somatic pools of individually axonally transported proteins. *J. Cell Biol.* 87: 379-385.

Bisby. M. A. 1976. Orthograde and retrograde axonal transport of labeled protein in motoneurons. *Exp. Neural.* 50: 628-640.

Bisby. M. A. 1978. Fast axonal transport of labeled protein in sensory axons. *Exp. Neuro.* 61: 281-300.

Bisby M. A. 1985. Retrograde axonal transport of phospholipid in rat sciatic nerve. *J. Neurochem.* 45: 1941-1947.

Bisby M. A. 1987. Does recycling have functions other than disposal?. In *Axonal Transport*. Smith R. S. and Bisby M. A., eds., New York, Alan R. Liss, pp. 365-383.

Bisby M. A. and Bulger V.T. 1977. Reversal of axonal transport at a nerve crush. *J. Neurochem.* 29: 313-320.

Black M. M. and Lasek R. J. 1979. Axonal transport of actin: slow component b is the principal source of actin for the axon. *Brain Res.* 171: 401-413.

Black M. M. and Lasek R. J. 1980. Slow components of axonal transport: two cytoskeletal networks. *J. Cell Biol.* 86: 616-623.

Blobel G. 1982. Regulation of intracellular Protein Traffic. *Harvey Lect.* 76: 125-147.

Bradley W. G. and Williams M. H. 1973. Axoplasmic flow in axonal neuropathies. I. Axoplasmic flow in cats with toxic neuropathies. *Brain Res.* 96: 235-246.

Brady S. T. 1985. A novel brain ATP_{ase} with properties expected for the fast axonal transport motor. *Nature* 317: 73-75.

Brady S. T., Lasek K. J. and Allen R D. 1982. Fast axonal transport in extruded axoplasm from squid giant axon. *Science* 218: 1129-1131.

Brady S. T., Lasek K. J. and Allen R D. 1985. Videomicroscopy of fast axonal transport in extruded axoplasm: A new model for study of molecular mechanisms. *Cell Motil.* 5: 81-101.

Bray J. J., Kon C. M., and Breckenridge B. M. 1971. Reversed polarity of rapid axonal transport in chicken motoneurons. *Brain Res.* 33: 560-564.

Breuer A. C., Christian M., Henkart M. and Nelson P. G. 1975. Computer analysis of organelle translocation in primary neuronal cultures and continuous cell lines. *J. Cell Biol.* 65: 562-576.

Brimijoin S. and Helland L. 1976. Rapid retrograde transport of dopamine-β–hydroxylase as examined by the stop-flow technique. *Brain Res.* 102: 217-228.

Brimijoin S., Rosonsen R. and Olsen J. 1979. Comparison of the temperature-dependence of rapid axonal transport and microtubules in nerves of the rabbit and bullfrog. *J. Physiol. (Lond.)* 287: 303-314.

Brimijoin S. and Wiermaa M. J. 1977a. Rapid axonal transport of tyrosine hydroxylase in rabbit sciatic nerve. *Brain Res.* 121: 77-96.

Brimijoin S. and Wiermaa M. J. 1977b. Direct comparison of the rapid axonal transport of norepinephrine and dopamine-β-hydroxylase activity. *J. Neurobiol.* 8: 239-250.

Brimijoin S. and Wiermaa M. J. 1978. Rapid orthograde and retrograde axonal transport of acetylcholinesterase as characterized by the stop-flow technique. *J. Physiol. (Lond.)* 285: 129-142.

Brimijoin S. Lundberg J. M., Brodin E., Hökfelt T., and Nilsson G. 1980. Axonal transport of substance P in the vagus and sciatic nerves of the guinea pig. *Brain Res.* 191: 443-457.

Broadwell R. D. and Brightman M. W. 1979. Cytochemistry of undamaged neurons transporting exogenous protein *in vivo*. *J. Comp. Neurol.* 185: 31-74.

Bulger V. T. and Bisby M. A. 1978. Reversal of axonal transport in regenerating nerve. *J. Neurochem.* 31: 1411-1418.

Burdwood W. 1965. Bidirectional particle movement in neurons. *J. Cell Biol.* 27: 115A.

Burgess L. and Kelly R. 1987. Constitutive and regulated secretion of proteins. *Ann. Rev. Cell Biol.* 3: 243-294.

Cancalon P. 1979. Subcellular and polypeptide distributions of slowly transported proteins in the garfish olfactory nerve. *Brain Res.* 161: 115-130.

Cancalon P. and Beidler L. M. 1975. Distribution along the axon and into various subcellular fractions of molecules labeled with [^{3}H]leucine and rapidly transported in the garfish olfactory nerve. *Brain Res.* 89: 225-244.

Cancalon P. and Beidler L. M. 1977. Differences in the composition of the polypeptides deposited in the axon and the nerve terminals by fast axonal transport in the garfish olfactory nerve. *Brain Res.* 121: 215-227.

Carslaw H. S. and Jaegar J. C. 1959. *Conduction of Heat in Solids.* Oxford, Clarendon, 2nd edition.

Carton H. C. and Appel S. H. 1973. The contribution of axoplasmic flow in optic nerve and protein synthesis within the optic tectum to synaptic membrane proteins of the chick optic tectum. *J. Neurochem.* 20: 1707-1717.

Chan H. Smith R. S., and Snyder R. E. 1989. The junction between the parent and daughter axons in regenerating myelinated nerve: properties of structure and rapid axonal transport. *J. Comp. Neurol.* 283: 391-404.

Chretien M., Pater G., Souyri F. and Droz B. 1981. Acryl-amided-induced neuropathy and impairment of axonal transport of proteins. *Brain Res.* 205: 15-28.

Crank J. 1957. *The Mathematics of Diffusion.* Oxford, Clarendon.

Cooper P. D. and Smith R. S. 1974. The movement of optically detectable organelles in myelinated axons of *Xenopus laevis*. *J. Physiol.* 242: 77-79.

Dalström A. 1965. Observations on the accumulation of noradrenaline in the proximal and distal parts of peripheral adrenergic nerves after compression. *J. Anat.* 4: 677-689.

Dahlström A. and Haggendal J. 1966. Studies on the transport and life-span of amine storage granules in a peripheral adrenergic neuron system. *Acta Physiol. Scand.* 67: 278-288.

Dahlström A. and Haggendal J. 1967. Studies on the transport and life-span of amine storage granules in the adrenergic neuron system of the rabbit sciatic nerve. *Acta Physiol. Scand.* 69: 153-157.

Droz B., Koenig H. L. and Digiamberardino L. 1973. Axonal migration of protein and glycoprotein to nerve endings. I. Radioautographic analysis of the renewal of protein in nerve endings of chicken ciliary ganglion after intracerebral injection of [^{3}H]lysine. *Brain Res.* 60: 93-127.

Droz B. and Koenig H. L. 1970. Localization of protein metabolism in neurons. In *Protein Metabolism of the nervous System.* Lajtha, ed., New York, Plenum Press, pp. 93-108.

Droz B. and Leblond C. P. 1962. Migration of proteins along the axons of the sciatic nerve. *Science* 137: 1047-1048.

Droz B. and Leblond C. P. 1963. Axonal migration of proteins in the central nervous system and peripheral nerves as shown by radioautography. *J. Com. Neuro.* 121: 325-346.

Edström A. and Hanson M. 1973. Retrograde axonal transport of proteins *in vitro* in frog sciatic nerve. *Brain Res.* 61: 311-320.

Edström A. and Mattsson H. Rapid axonal transport in vitro in the sciatic system of the frog of fucose-, glucosamine- and sulphate- containing material. *J. Neurochem.* 19: 1717-1729.

Fahim M. A. Lasek R. J., Brady S. T., and Hodge A. J. 1985. AVEC-DIC and electron microscopic analyses of axonally transported particles in cold-blocked squid giant axons. *J. Neurocytol.* 14: 689-704.

Farquhar M. G. 1985. Progress in unraveling pathways of Golgi traffic. *Ann. Rev. Cell Biol.* 1: 447-88.

Fishman J. B. and Fine R. E. 1991. A trans Golgi-derived exocytic coated vesicle can contain both newly synthesized cholinesterase and internalized transferrin. *Cell* 48: 157-173.

Forman D. S. 1982. Microscopic Methods for the observation of axonal transport in living axons. In *Axoplasmic Transport*. Weiss D. G., ed., Basel, Springer-Verlag, pp. 424-428.

Forman D. S. 1987. Axonal transport of mitochondria. In *Axonal Transport*. Smith R. S. and Bisby M. A., eds., New York, Alan R. Liss, pp. 155-164.

Forman D. S., Grafstein D. S. B. and McEwen B. S. 1972. Rapid axonal transport of [^{3}H]fucosyl glycoproteins in the goldfish optic system. *Brain Res.* 48: 327-342.

Forman D. S., Padjen A. L. and Siggns G. R. 1977. Axonal transport of organelles visualized by light microscopy: cinemicrographic and computer analysis. *Brain Res.* 136: 197-213.

Friede R. D. 1959. Transport of oxidative enzymes in nerve fibers, a histochemic investigation of the regenerative cycle in neurons. *Exp. Neurol.* 1: 441-466.

Frizell M. and Sjöstrand J. 1974. retrograde axonal transport of rapidly migrating proteins in the vagus and hypoglossal nerves of the rabbit. *J. Neurochem.* 23: 651-657.

Gilbert S. P. and Sloboda R. D. 1984. Bidirectional transport of fluorescently labeled vesicles introduced into extruded axoplasm of the squid *Loligo peali*. *J. Cell Biol.* 99: 445-452.

Gilbert S. P. and Sloboda R. D. 1989. A squid dynein isoform promotes axoplasmic vesicle translocation. *J. Cell Biol.* 109: 2379-2394.

Goldberg S. and Kotani M. 1967. The projection of optic nerve fiber in the frog *Rana catesbeiana* as studied by radioautography. *Anat. Rec.* 158: 325-332.

Goodrum J. F. and Morell P. 1982. Axonal transport, deception, and metabolic turnover of glycoproteins in the rat optic pathway. *J. Neurochem.* 38: 690-704.

Grafstein B. 1967. Transport of protein by goldfish optic nerve fibers. *Science* 157: 196-198.

Grafstein B. and Forman D. S. 1980. Intracellular transport in neurons. *Physiol. Rev.* 60: 1167-1283.

Grafstein B., Miller J. A., Ledeen R. W., Haley J., and Specht S. C. 1975. Axonal transport of phospholipid in goldfish optic system. *Exp. Neurol.* 46: 261-281.

Griffin J. W., Price D. L., Drachman D. B. and Morrish J. 1981. Incorporation of axonally transported glycoproteins into axolemma during nerve regeneration. *J. Cell Biol.* 88: 205-214.

Gross G. W. 1973. The effect of temperature on the axoplasmic transport in C-fibers. *Brain Res.* 56: 339-363.

Gross G. W. and Beidler L. M. 1973. Fast axonal transport in the C-fibers of goldfish olfactory nerve. *J. Neurobiol.* 4: 413-428.

Gross G. W. and Beidler L. M. 1975. A quantitative analysis of isotope transport velocities in the C-fibers of the garfish olfactory nerve. *J. Neurobiol.* 6: 213-232.

Gurgess T. L. and Kelly R. B. 1987. Constitutive and regulated secretion of proteins. *Ann. Rev.* 3: 243-293.

Haley J. E. and Ledeen R. W. 1979. Incorporation of axonally transported substances into myelin lipids. *J. Neurochem.* 32z: 727-742.

Hammerschlag R. 1980. The role of calcium in the initiation of fast axonal transport. *Fed. Proc.* 39: 2809-2814.

Hammerschlag R. 1982. Multiple roles of calcium in the initiation of fast axonal transport. In *Axoplasmic Transport.* Weiss D.G., ed., Basel, Springer-Verlag, pp. 279-286.

Hammerschlag R. 1983/84. How do neuronal proteins know where they are going? Speculations on the role of molecular address markers. *Dev. Neurosci.* 6: 2-17.

Hammerschlag R. and Stone G. C. 1982. Metalloendoprotease inhibitors block fast axonal transport. *Trans. Amer. Soc. Neurochem.* 17-163.

Hammerschlag R. and Stone G. C. 1987. Further studies on the initiation of fast axonal transport. In *Axonal Transport.* Smith R. S. and Bisby M. A. eds., New York, Alan R. Liss, pp. 37-51.

Hammond G. R. and Smith R. S. 1977. Inhibition of the rapid movement of optically detectable axonal particles by colchicine and vinblastine. *Brain Res.* 128: 227-242.

Hanson M. and Edström A. 1977. Fast axonal transport: effect of antimitotic drugs and inhibitors of energy metabolism on the rate and amount of transported protein in frog sciatic nerve. *J. Neurobiol.* 8: 97-108.

Harry G. J., Goodrum J. F., Bouldin T. W., Toews A. D., and Morell P. 1989. Acrylamide-Induced increases in deposition of axonally transported glycoproteins in rat sciatic nerve. *J. Neurochem.* 52: 1240-1247.

Hässig R., Tavitian B., Pappalardo F. and Di Giamberardino L. 1991. Axonal transport reversal of acetylcholinesterase molecular forms in transected nerve. *J. Neurochem.* 57: 1913-1920.

Hayden J. and Allen R. D. 1984. Detection of single microtubules in living cells: Particle transport can occur in both directions along the same microtubule. *J. Cell Biol.* 99: 1785-93.

Hebb C. O. and Waites M. H. 1956. Cholin acetylase in antero- and retro-grade degeneration of a cholinergic nerve. *J. Physiol. (Lond.)* 132: 667-671.

Helenius A. and Simons K. 1975. Solubilitation of membranes by detergents. *Biochem. Biophys. Acta* 415: 29-79.

Hendrickson A. E. 1972. Electron microscopic distributions of axoplasmic transport. *J. Comp. Neurol.* 144: 381-398.

Hendry I. A. 1977. The effect of the retrograde axonal transport of nerve growth factor on the morphology of adrenergic neurons. *Brain Res.* 134: 213-223.

Hendry I. A., Stach R. and Hurrup K. 1974. Characteristics of the retrograde axonal transport system for nerve growth factor in the sympathetic nervous system. *Brain Res.* 82: 117-128.

Hirokawa N., Ptister K. K., Yorituji H., Wagner M. C., Brady S. T. and Bloom G. S. 1989. Submolecular domains of bovine brain kinesin identified by electron microscopy and monoclonal antibody decoration. *Cell* 56: 867-878.

Hoffman P. N. and Lasek R. J. 1975. The slow component of axonal transport. Identification of major structural polypeptides of the axon and their generality among mammalian neurons. J. *Cell Biol.* 66: 351-366.

Hollenbeck P. J. 1988. Kinesin: its properties and possible functions. *Protoplasm* 145:145-152.

Hollenbeck P. J. 1989. The distribution, abundance and subcellular localization of kinesin. *J. Cell Biol.* 108: 2335-2342.

Holtzman E. 1977. The origin and fate of secretory packages especially synaptic vesicles. *Neurosci.* 2: 327-355.

Hörtnagl H., Hörtnagl H. and Winkler H. 1969. Bovine splenic nerve: characterization of noradrenaline-containing vesicles and other cell organelles by density gradient centrifugation. *J. Physiol. (Lond.)* 205:103-114.

Inoué S. 1981. Video image processing greatly enhances contrast quality, and speed in polarization-based microscopy. *J. Cell Biol.* 89: 346.

Inoué S. 1986. *Video Microscopy*. New York, Plenum, pp. 405-406.

Johnson E. M., Andres R. Y. and Bradshaw R. A. 1978. Characterization of the retrograde transport of nerve growth factor (NGF) using high specific activity [^{125}I]NGF. *Brain Res.* 150: 319-331.

Johnson E. M., Rich K. M. and Yip H. K. 1986. The role of NGF in sensory neurons *in vivo*. *Trends Neurosci.* 9: 33-37.

Karlsson J. O. and Sjöstrand J. 1971. Electrophoretic characterization of rapidly transported proteins in axons of retinal ganglion cells. *Fed. Europ. Biochem. Soc. Lett.* 16: 329332.

Kelly R. B. 1985. Pathways of protein secretion in eukaryotes. *Science* 230: 25-32.

Koonce M. P. and Schliwa M. 1985. Bidirectional organelle transport can occur in cell processes that contain single microtubules. *J. Cell Biol.* 100: 322-326.

Kendal W. S., Koles Z. J. and Smith R. S. 1983. Oscillatory motion of intra-axonal organelles of *Xenopus laevis* following inhibition of their rapid transport. *J. Physiol. (Lond.)* 345: 501-513.

Kirkpatrick J. B., Bray J. J. and Palmer S. M. 1972. Visualization of axoplasmic flow by Normarski microscopy: comparison to rapid flow of radioactive proteins. *Brain Res.* 43: 1-10.

Koles Z. J., McLeod K. D. and Smith R. S. 1982. A study of the motion of organelles which undergo retrograde and anterograde rapid axonal transported in *Xenopus*. *J. Physiol.* 328:469-484.

Kristensson K. 1977. Retrograde axonal transport of horseradish peroxidase. Uptake at mouse neuromuscular junctions following systemic injection. *Acta Neuropathol.* 38: 143-147.

Kristensson K. and Olsson Y. 1971a. Uptake and retrograde axonal transport of peroxidase in hypoglossal neurons. Electron microscopical localization in neuronal perikaryon. *Acta Neuropathol.* 19: 1-9.

Kristensson K. and Olsson Y. 1971b. Uptake of exogenous proteins in mouse olfactory cell. *Acta Neuropathol.* 19: 145-154.

Lagercrantz H. 1976. On the composition and function of large dense cored vesicles in sympathetic nerves. *Neurosci.* 1: 81-92.

Lasek R. 1968a. Axoplasmic transport in cat dorsal root ganglion cells: as studied with [^{3}H]-L-leucine. *Brain Res.* 7: 360-377.

Lasek R. J. 1968b. Axoplasmic transport of labeled proteins in rat ventral motoneurons. *Brain Res.* 21: 41-51.

Lasek R. J. and Brady S. T. 1985. Attachment of transported vesicles to microtubules in axoplasm is facilitated by AMP-PNP. *Nature* 316: 645-647.

Laudron P. M. 1984. Axonal transport of receptors: coexistence with neurotransmitter and recycling. *Biochem. Pharm.* 33: 897-903.

Lavail J. H. and Lavail M. M. 1974. The retrograde intraaxonal transport of horseradish peroxidase in the chick visual system: a light and electron microscopic study. *J. Comp. Neurol.* 157: 303-358.

Lavail J. H. and Lavail M. M. 1975. The retrograde intraaxonal transport of horseradish peroxidase in retinal ganglion cells of the chicks. *Brain Res.* 85: 273-280.

Lentz T. L. 1972. Distribution of ^{3}H-leucine during axoplasmic transport within regenerating neurons as determined by electron-microscope autoradiography. *J. Cell Biol.* 52: 719-732.

Levy C., Scherman D., and Laduron P. M. 1990. Axonal transport of synaptic vesicles and muscarinic receptors: effect of protein synthesis inhibitors. *J. Neurochem.* 54: 880-885.

Lindsey J. D., Hammerschlag R. and Ellisman, M. H. 1981. An increase in smooth endoplasmic reticulum and a decrease in Golgi apparatus occur with ionic conditions that block initiation of fast axonal transport. *Brain Res.* 205: 275-287.

Longo F. M. and Hammerschlag R. 1980. Relation of somal lipid synthesis to the fast axonal transport of protein and lipid. *Brain Res.* 193: 471-485.

Lorenz T. and Willard M. 1978. Subcellular fractionation of intraaxonally transported polypeptides in the rabbit visual system. *Natl. Acad. Sci. USA.* 75: 505-509.

Lubinska L. and Niemierko S. 1971. Velocity and intensity of bidirectional migration of acetylcholinesterase in transected nerves. *Brain Res.* 27: 329-342.

Lubinska L., Niemierko S., Oderfeld B. and Szwarc L. 1964. Behavior of acetylcholinesterase in isolated nerve segments. *J. Neurochem.* 11: 493-503.

Martz D., Garner J., and Lasek R. J. 1989. Protein changes during anterograde-to-retrograde conversion of axonally transported vesicles. *Brain Res.* 476: 199-203.

Matsumoto T. 1920. The granules, vacuoles and mitochondria in the sympathetic nerve-fibers cultivated *in vitro*. *Bull. Johns Hopkins Hosp.* 31: 91-93.

Matsumoto D. E. and Scalia F. 1981. Long-term survival of centrally projection axons in the optic nerve of the frog following destruction of the retina. *J. Comp. Neurol.* 202: 135-155.

McEwen B. C. and Grafstein B. 1968. Fast and slow components in axonal transport of protein. J. *Cell Biol.* 38: 494-508.

Meyer M. R. and Bittner G. D. 1978. Histological studies of tropic dependencies in crayfish giant axons. *Brain Res.* 143: 195-211.

Miani N. 1960. Proximo-distal movement along the axon of protein synthesized in the perikaryon of regenerating neuron. *Nature* 189: 541.

Miani N. 1962. Evidence of a proximo-distal movement along the axon of phospholipid synthesized in the nerve-cell body. *Nature* 193: 887-888.

Montal M. 1986. Functional reconstitution of membrane proteins in planar lipid bilayer membranes. In *Techniques of the Analysis of Membrane Proteins.* Ragan C. I. and Cherry R. J. eds., London, Chapman & Hall, pp. 97-128.

Morin P., Liu N., Johnson R. J., Leeman S. E., and Fine R. E. 1991. Isolation and characterization of rapid transport vesicle subtypes from rabbit optic nerve. *J. Neurochem.* 56: 415-427.

Muñoz-Martínez E. J., Núñez R., and Sanderson A. 1981. Axonal transport: a quantitative study of retained and transported protein fraction in the cat. *J. Neurobiol.* 12: 15-26.

Nagatsu I., Kondo Y., Kato T. and Nagatsu T. 1976. Retrograde axoplasmic transport of inactive dopamine beta-hydroxylase in sciatic nerve. *Brain Res.* 116: 277-285.

Neighbors B. W., Williams R. C. and McIntosh J. R. 1988. Localization of kinesin in cultured cells. *J. Cell Biol.* 106: 1193-1204.

Ochs S. 1972. Fast transport of materials in mammalian nerve fibers. *Science* 176: 252-260.

Ochs S. 1974. Energy metabolism and supply of ~p to the fast axoplasmic transport mechanism in nerve. *Fed. Proc.* 33: 1049-1057.

Ochs S. 1975. Retention and redistribution of proteins in mammalian nerve fibers by axoplasmic transport. *J. Physiol. (Lond.)* 253: 459-475.

Ochs S. 1982. *Axoplasmic Transport and Its Relation to Other Nerve Functions.* New York, Wiley-Interscience.

Ochs S. and Smith C. 1975. Low temperature slowing and cold-block of fast axoplasmic transport in mammalian nerves *in vitro*. *J. Neurobiol.* 6: 85-102.

Ochs S., Johnson J. and NG M.-H. 1967. Protein incorporation and axoplasmic flow in motoneuron fibers following intra-cord injection of labeled leucine. *J. Neurochem.* 14: 317-331.

Paravicini U., Stoeckel K. and Thoenen H. 1975. Biological importance of retrograde axonal transport of nerve growth factor in adrenergic neurons. *Brain Res.* 84: 279-291.

Palade G. 1975. Intracellular aspects of the process of protein synthesis. *Science* 189: 347-358.

Partlow L. M., Ross C. D. and Thoenen H. 1972. Transport of axonal enzymes in surviving segments of frog sciatic nerve. *J. Gen. Physiol.* 60: 388-405.

Pfeffer S. R. and Rothman J. E. 1987. Biosynthetic protein transport and sorting by the endoplasmic reticulum and Golgi. *Ann. Rev. Biochem.* 56: 829-852.

Pfister K., Wagner M. C., Stenoien D. L., Brady S. T. and Bloom G. S. 1989. Monoclonal antibodies to kinesin heavy and light chains stain vesicle-like structures, but not microtubules, in cultured cells. *J. Cell Biol.* 108: 1453-1463.

Rothman J. E. 1985. The compartmental organization of the Golgi apparatus. *Sci. Am.* 253: 74-89.

Sabri M. I. and Ochs S. 1972. Characterization of fast and slow transported proteins in dorsal root and sciatic nerve of cat. *J. Neurobiol.* 4: 145-165.

Sahenk Z. and Lasek R. J. 1988. Inhibition of proteolysis blocks anterograde-retrograde conversion of axonally transported vesicles. *Brain Res.* 460: 199-203.

Sahenk Z. and Mendell J. R. 1980. Axoplasmic transport in zine pyridinethione neuropathy: evidence for an abnormality in distal turn around. *Brain Res.* 186: 343-353.

Sahenk Z. and Mendell J. R. 1981. Acylamide and 2,5-hexanedione neuropathies: abnormal bidirectional transport rate in distal axons. *Brain Res.* 219: 397-405.

Schliwa M. 1989. Head and tail. *Cell* 56: 719-720.

Schliwa M. 1984. Mechanism of intracellular organelle transport. In *Cell Muscle Motility*. Shaw J. W. ed., New York, Plenum, vol. 5, pp. 1-81.

Schmidt R. E., Yu M. J. C. and McDougal D. B. 1980. Turnaround of axoplasmic transport of selected particle-specific enzymes at an injury in control and diisopropylphosphorofluoridate-treated rats. *J. Neurochem.* 35: 641-652.

Schnapp B. J., Vale R. D., Sheetz M. P. and Reese T S. 1985. Single microtubules from squid axoplasm support bidirectional movement of organelles. *Cell* 40: 455-62.

Schnapp B. J. and Reese T. S. 1989. Dynein is the motor for retrograde axonal transport of organelles. *Proc. Natl. Acad. Sci. USA.* 86: 1548-1552.

Schonbach J., Schonbach C. and Cuénod M. 1971. Rapid phase of axoplasmic flow and synaptic protein: an electron microscopical autoradiographic study. *J. Comp. Neurol.* 141: 485-498.

Schonbach J., Schonbach C. and Cuénod M. 1973. Distribution of transported proteins in the slow phase of axoplasmic flow. An electron microscopical autoradiographic study. *J. Comp. Neurol.* 152: 1-16.

Schroer T. A., Brady S. T.and Kelly R. B. 1985. Fast axonal transport of foreign synaptic vesicles in squid axoplasm. J. *Cell Biol.* 101: 568-572.

Schroer T. A., Schnapp B. J., Reese T. S. and Sheetz M. P. 1988. The role of kinesin and other soluble factors in organelle movement along microtubules. *J. Cell Biol.* 107: 1785-1792.

Schroer T. A., Steuer E. R. and Sheetz M. P. 1989. Cytoplasmic dynein is a minus end-directed motor for membranous organelles. *Cell* 56: 937-946.

Schwartz J. H. 1979. Axonal transport: components, mechanisms, and specificity. *Ann. Rev. Neurosci.* 2: 467-504.

Scott F. H. 1905. On the metabolism and action of nerve cells. *Brain* 28: 506-526.

Sherbany A. A., Ambron R. T. and Schwartz J. H. 1979. Membrane glycolipids: regional synthesis and axonal transport in a single identified neuron of *Aplysia californica*. *Science* 203: 78-81.

Scholey J. M., Porter M. E., Grissom P. M. and McLntosh J. R. 1985. Identification of kinesin in sea urchin eggs, and evidence for its localization in the mitotic spindle. *Nature* 318: 483-486.

Singer P. A., Mehler S. and Fernandez H. L. 1982. Blockade of retrograde axonal transport delays the onset of metabolic and morphologic changes induced by axotomy. *J. Neurosci.* 2: 1299-1306.

Smith R. S. 1971. Centripetal movement of particles in myelinated axons. *Cytobios*. 3: 259-262.

Smith R.S. 1972. Detection of organelles in myelinated nerve fibers by dark-field microscopy. *Can. J. Physiol. Pharmacol.* 50: 467-469.

Smith R. S. 1980. The short term accumulation of axonally transported organelles in the region of localized lesions of single myelinated axons. *J. Neurocytol.* 9: 39-65.

Smith R. S. 1987. Control of the direction of rapid axonal transport in the vertebrates. In *Axonal Transport*. Smith R. S. and Bisby M. A., eds., New York, Alan R. Liss, pp. 139-154.

Smith R. S. 1988. Studies on the mechanism of the reversal of rapid axonal transport in myelinated axons of *Xenopus laevis*. *Cell Motil. Cytoskel.* 10: 296-308.

Smith R. S. 1989. Real-time imaging of axonally transported subresolution organelles in vertebrate myelinated axons. *J. Neurosci. Meth.* 26: 203-209.

Smith R. S. and Bisby M. A. 1987. *Axonal Transport*. New York, Alan. R. Liss.

Smith R. S. and Koles Z. J. 1976. Mean velocity of optically detected intraaxonal particles measured by a cross-correlation method. *Can. J. Physiol. Pharmacol.* 54: 859-869.

Smith R. S. and Snyder R. E. 1991. Reversal of rapid axonal transport at a lesion: leupeptin inhibits reversed protein transport, but does not inhibit reversed organelle transport. *Brain Res.* 552: 215-227.

Smith R. S., Chan H. and Snyder R. E. 1991. Brefeldin A inhibits fast axonal protein transport and disassembles Golgi apparatus but does not diminish anterograde axonal vesicle transport. *Neurosci. Abst.* 17: 59.

Snider M. D. and Roger O. C. 1986. Membrane traffic in animal cells: Cellular glycoproteins return to the site of Golgi mannosidase I. *J. Cell Biol.* 103: 265-275.

Snyder R. E. 1984. The design and construction of a multiple proportional counter used to study axonal transport. *J. Neurosci. Meth.* 11: 79-88.

Snyder R. E. 1986a. The kinematics of turnaround and retrograde axonal transport in frog sciatic nerve. *J. Neurobiol.* 17: 637-647.

Snyder R. E. 1986b. A radiolabeled pulse for the simultaneous study of anterograde and retrograde axonal transport. *J. Neurosci. Meth.* 17: 109-119.

Snyder R. E. 1989. Loss of material from the retrograde axonal transport system in frog sciatic nerve. *J. Neurobiol.* 20: 81-94.

Snyder R. E. and Smith R. S. 1982. Application of position-sensitive detectors to the study of the axonal transport of β-emitting isotopes. In *Axoplasmic Transpot.* Weiss D. G., ed., Basel, Springer-Verlag, pp. 442.

Snyder R. E. and Smith R. S. 1984. Physical methods for the study of the dynamics of axonal transport. *CRC Crit. Revs. Biomed. Eng.* 10: 89-123.

Snyder R. E. and Smith R. S. 1990. Evidence for the recycling of axonally transported organelles. *Neurosci. Abst.* 16: 49.

Snyder R. E., Chen X. and Smith R. S. 1990. Protein loss from axonal transport occurs without diminution of vesicle traffic. *NeuroRep.* 1: 259-262.

Steinman R. M., Mellman I. K., Muller W. A. and Cohn Z. A. 1983. Endocytosis and the recycling of plasma membrane. *J. Cell Biol.* 96: 1-27.

Stoeckel K. G., Guroff G., Schwab M. and Thoenen H. 1976. The significance of retrograde axonal transport for the accumulation of systemically administered nerve growth factor (NGF) in the rat superior cervical ganglion. *Brain Res.* 109: 271-284.

Stoeckel K. G., Schwab M. and Thoenen H. 1975. Specificity of retrograde transport of nerve growth factor (NGF) in sensory neurons: a biochemical and morphological study. *Brain Res.* 89: 1-14.

Stone G. C. and Hammerschlag R. 1987. Molecular mechanisms involved in sorting of fast-transported proteins. In *Axonal Transport.* Smith R. S. and Bisby M. A., eds., New York, Alan R. Liss, pp. 15-36.

Stone G. C. Hammerschlag R. and Bobinski J. A. 1984a. Involvement of coated vesicles in the initiation of fast axonal transport. *Brain Res.* 291: 219-288.

Stone G. C., Hammerschlag R. and Bobinski J. A. 1984b. Fast axonal transport of tyrosine sulfate-containing proteins: preferential routing of sulfoproteins toward nerve terminals. *Cell. Mol. Neurobiol.* 4: 249-262.

Stone G. C., Hammerschlag R. and Bobinski J. A. 1987. Complex compartmentation of tyrosine sulfate-containing proteins undergoing fast axonal transport. *J. Neurochem.* 48: 1736-1744.

Stoorvogel W., Geuze H. J., Griffith J. M. and Strous G. J. 1988. The pathways of endocytosed transferrin and secretory protein are connected in the trans-Golgi reticulum. *J. Cell Biol.* 106: 1821-1829.

Tartakoff A. Vassalli P. 1978. Comparative studies of intracellular transport of secretory proteins. *J. Cell Biol.* 79: 694-707.

Thilo L. 1985. Quantification of endocytosis-derived membrane traffic. 822: 243-266.

Toews A. D., Armstrong R., Holshek J., Gould R. M. and Morell P. 1987. Unloading and transfer of axonally transported lipids. In *Axonal Transport.* Smith R. S. and Bisby M. A., eds., New York, Alan R. Liss, pp. 327-346.

Toews A. D., Saunders B. F. and Morell P. 1982. Axonal transport and metabolism of glycoproteins in rat sciatic nerve. *J. Neurochem.* 39: 1348-1355.

Tsukita S. and Ishikawa H. 1980. The movement of membranous organelles in axons. Electron microscopic identification of anterogradely and retrogradely transported organelles. *J. Cell Biol.* 84: 513-530.

Vale R. D., Schnapp B. J., Reese T, S. and Sheetz M. P. 1985a. Movement of organelles along filaments dissociated from the axoplasm of the squid giant axon.. *Cell* 40:449-454.

Vale R. D., Schnapp B. J., Reese T, S. and Sheetz M. P. 1985b. Organelle, bead and microtubule translocations promoted by soluble factors from the squid giant axon. *Cell* 40:559-69.

Vale R. D., Reese T, S. and Sheetz M. P. 1985c. Identification of a novel force-generating protein, kinesin, involved in microtubule-based motility. *Cell* 42: 39-50.

Vale R. D., Schnapp B. J., Mitchison T., Steuer E., Reese T. S. and Sueetz M. P. 1985d. Different axoplasmic proteins generate movement in opposite directions along microtubules *in vitro*. *Cell* 43: 623-32.

Vale R. D., Schnapp B. J., Reese T, S. and Sheetz M. P. 1985e. Purification and structure of a novel microtubule translocator (kinesin) from squid and bovine neural tissue. *J. Cell Biol.* 101: 37a.

Vale R. D.. 1987. Intracellular transport using microtubule-based motors. *Ann. Rev. Cell Biol.* 3:347-78.

Vallee R. B. and Bloom G. S. 1991. Mechanisms of fast and slow axonal Transport. *Ann. Rev. Neurosci.* 14: 59-92.

Verner K. and Schatz G. 1988. Protein translocation across membranes. Science 239: 1307-1313.

Viancour T. A. 1990. Organelle flux in intact and transected crayfish giant axons. *Brain Res.* 535: 245-254.

Viancour T. A., Sheller K. A., Bittner G. D. and Seshan K. R. 1988. Protein transport between crayfish lateral giant axons. Brain Res. 439: 211-221.

Waller A. V. 1852. A new method for the study of the nervous system. *Lond. J. Med.* 43: 609-625.

Walter P. and Lingappa V. R. 1986. Mechanisms of protein translocation across the endoplasmic reticulum membrane. *Ann. Rev. Cell Biol.* 2: 499-516.

Watson W. E. 1968. Observation on the nucleolar and total cell body nucleic acid of injured nerve cells. *J. Physiol. (Lond.)* 196: 655-630.

Weiss D. G. 1982. *Axoplasmic Transport*. Basel, Springer-Verlag.

Weiss D. G., Krygier-Brevart V., Gross, G. W. and Kreutzberg G. W. 1978. Rapid axoplasmic transport in the olfactory nerve of the pike. II. Analysis of transported proteins by gel electrophoresis. *Brain Res.* 139: 77-87.

Weiss P. and Hiscoe H. B. 1948. Experiments on the mechanism of nerve growth. *J. Exp. Zool.* 107: 315-395.

Wickner W. T. and Lodish H. 1985. Multiple mechanisms of protein insertion into and across membranes. *Science* 230: 400-406.

Willard M., Cowan W. M. and Vagelos P. R. 1974. The polypeptide composition of intraaxonally transported proteins: evidence for four transport velocities. *Proc. Natl. Acad. Sci. USA.* 71: 2183-2187.

Wooten G. F. 1973. Subcellular distribution and rapid axonal transport of dopamine-β-hydroxylase. *Brain Res.* 137: 37-52.

Zarbin M. A., Palacios J. M., Wamsley J. K. and Kuhar M. T. 1983. Axonal transport of beta-adrenergic receptors: Antero- and retrogradely transported receptors differ in agonist affinity and nucleotide sensitivity. *Molec. Pharmcol.* 24: 341-348.